Self-powered and self-sensing devices based on human motion

Zhihui Lai [a,b], Junchen Xu [a,b], Chris R. Bowen [c], Shengxi Zhou [d,*]

[a] Shenzhen Key Laboratory of High Performance Nontraditional Manufacturing, College of Mechatronics and Control Engineering, Shenzhen University, Shenzhen 518060, China.
[b] Guangdong Key Laboratory of Electromagnetic Control and Intelligent Robots, College of Mechatronics and Control Engineering, Shenzhen University, Shenzhen 518060, China.
[c] Department of Mechanical Engineering, University of Bath, Bath BA2 7AK, UK.
[d] School of Aeronautics, Northwestern Polytechnical University, Xi'an 710072, China.
[*] Corresponding author: zhoushengxi@nwpu.edu.cn (Shengxi Zhou)

Abstract. The emergence of human motion-based energy harvesters is a reflection of the need to develop future energy supplies for small-scale human motion-based self-powered and self-sensing devices. Such systems have widespread application in modern society, which includes health monitoring, medical care, wearable devices, wireless sensor nodes, and outdoor rescue. This paper overviews the state-of-the-art and recent progress in human motion-based self-powered and self-sensing devices, where we classify the range of available energy sources, the energy conversion mechanisms, relevant materials, and novel device architectures to harvest human motion energy. The range of human motion energy sources is classified into three categories based on how they act as excitation sources for energy harvesting. The commonly used energy conversion mechanisms are then overviewed in detail, which include electromagnetic, piezoelectric, electrostatic (dielectric elastomer generator and triboelectric nanogenerator), and the range of potential electroactive materials are discussed. In addition, the harvesting structures, operating mechanisms, and performance of human motion-based energy harvesters are overviewed, discussed and characterized based on the range of available human motion energy sources. Furthermore, the application of self-powered devices in delivering power to implantable medical devices, wearable devices and other low-powered electronics are comprehensively reviewed. The state-of-the-art and future advances in human motion based self-sensing devices are then reviewed and related to their application in human activity recognition, health monitoring and human-machine interactions. Finally, key developments are summarized and discussed, and the potential research directions and critical challenges are presented to highlight future opportunities.

1. Introduction

World-wide, the supply of energy is a cornerstone of the development of human society. The creation of energy sources that help protect our environment is also an issue of concern for the whole world. Historically, the range of energy sources utilized by humans have developed initially from traditional fossil fuels (firewood, coal, and oil) and progressed to renewable forms of energy (wind, hydropower, nuclear, wave, tidal, biomass, vibrational, and human body energy). Additional energy conversion mechanisms, including solar energy conversion[1-4], thermoelectric conversion[5], and electromechanical conversion (based on electromagnetic induction, piezoelectric, and electrostatic effects) have been employed to utilize ambient forms of energy. These energy sources can be used in a wide range of applications, including *large-scale* manufacturing, engineering, farming, transportation, and medical treatment to *small-scale* power supplies for lighting, entertainment, low-power consumer electronics and wearable devices. Today, the development of small-scale wireless electronic devices, such as wireless sensor nodes [6], wearable and implantable devices [7], and bioinspired sensors [8], has led to a significant demand for independent, distributed, autonomous, and high-performance power supplies.

To date, chemical batteries are widely used to power small-scale wireless electronic devices; however, they cannot satisfy the requirements of delivering a continuous power supply while being lightweight, comfortable, and small-scale for future wireless electronic devices. In particular, the use of bulky and heavy batteries is unsuitable in portable applications such as outdoor activities and personnel (e.g. rescue or ambulance); in addition, batteries are a potential source of pollution during their manufacture and disposal. The lifetime of the batteries is limited due to their low energy storage density, thus resulting in an inconvenience and potential danger when replacing batteries, especially for implantable biomedical devices and other wireless medical and rehabilitation devices. Moreover, many battery systems are unable to operate at low or high temperature, thus limiting their applications in hostile environments, which is common for the outdoor exploration devices for the travellers and the outdoor rescue devices.

In recent decades, the rapid development of advanced energy harvesting (EH) technologies and relevant functional materials has led to the creation of small-scale energy harvesters [9-13]. The energy harvesters have been designed to scavenge energy, especially undesired sources of energy. Although such energy sources can typically produce small-scale levels of power, ranging from μW level to mW level, these energy harvesters can act as a portable energy supply that is not reliant on the large-scale power grid or battery supplies during operation. Thus, they are of interest for portable power supplies for creating autonomous low-powered wireless electronic devices.

Hence, energy harvesting technologies that scavenge energy from green and sustainable energy sources has significant potential in powering wireless electronic devices. Potential energy sources include many environmental forms of energy, which include wind, waves, tidal motion, mechanical vibrations, mechanical rotations, environmental noise, and human body related energy [14]. Among these energy sources, the human body is of importance as it can be harvested *actively* (i.e., energy is harvested from intentional human activities, such as hand shaking and palm clapping) or *passively* (i.e., energy is harvested from unintentional activities or dissipated energy sources, such as breathing and swing motion during walking). Of particular interest, when it is difficult to harvest energy from the external environment, is the possibility to obtain energy from our own body so that energy is always available.

It has been reported that the energy stored in an average-sized person's fat is as much as a 100-kg battery [15]. Therefore, the human body can act as an energy source for many portable self-powered and self-sensing devices. Moreover, during a normal active day a person dissipates a significant amount of energy, typically ~ 2000 kcal, while sleeping, walking, running, sitting, talking and breathing, with an estimated average power of 1000 W [16, 17]. Therefore, both active and passive harvesting of energy from the human body (especially for dissipated energy), can provide a new solution for sustainable energy and provide power for a range of low-powered wearable or implantable electronics [18]. As a result, the development of human body-based energy harvesters is of particular importance, especially in emergency situations; for example, a simple hand torch powered by human motion can be extremely important to provide lighting, especially when no external power supplies are available.

Power can be readily generated from a range of human body-related sources [19], see Fig. 1, such as temperature differences [20-22], heat dissipation [23, 24], blood pressure [25], human sweat [26, 27], and human motion which includes the movement of human body, swing motion, and joint rotation. Therefore, human body energy sources can be generalized into *human-motion-based* energy and *non-human-motion-based* energy, with the former attracting the most attention in the literature. For example, in 1770, the French scientist

Abraham-Louis Perrelet designed a fully autonomous self-winding pedometer watch that generated energy from the movement of a human arm [28]. This represents one of the earliest recorded small-scale human motion-based energy harvesters. It should be noted that some extended human body motions, such as as the strike of walking stick as it impacts the floor, can be also converted into electricity provide activity monitoring, tracing, and accident alert [29]; however, they are not strictly defined as human motion in this review.

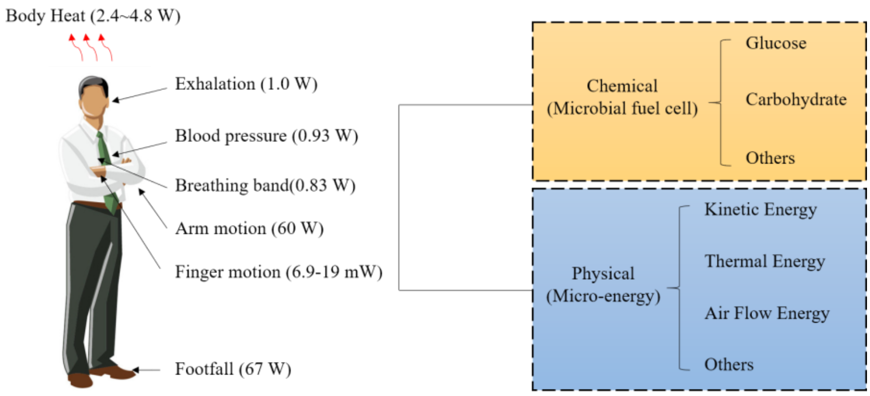

Fig. 1 Range of energy sources from the human body.

In most cases, energy from the human body can be transformed into electrical energy using a range of energy conversion mechanisms. For example, thermoelectric energy harvesting is based on the Seebeck effect [20-22, 30, 31], thermo-osmotic [32] or thermomagnetic generator [33] and is able to harvest energy from the temperature difference between the human body and ambient environment; pyroelectric energy harvesting is based on the change of spontaneous polarization of a pyroelectric material and can generate electricity from temperature fluctuations [24, 34-36]; biofuel cells can harvest energy from biofluids such as human sweat [26]; and specific electromechanical conversion mechanisms [25, 37] such as electromagnetic, piezoelectric, and electrostatic energy harvesting technologies can harvest energy from human motion. These are shown in Fig. 2. The generated electrical energy can be stored or further utilized to provide power for low-powered electronics. In other studies, energy from the human body can be transformed into other non-electrical energy forms of energy. One example is the mechanical watch, where for centuries mechanical winding mechanisms have been used to convert arm shaking or swing motion into potential energy, which was stored to power a watch. Other examples can be reported recently: hydraulic energy can be generated from human walking which is induced by backpack motion and can support the operation of a hydraulic exoskeleton for a load carrying mission [38], and the energy from leg swings can be stored as elastic potential energy in flat spiral springs and subsequently released to assist in walking for patients with lower limb dyskinesia through exoskeletons [39]. While these harvested energies are useful in specific applications, they cannot be readily used as an electrical power source, thus their applications are relatively limited.

As a result, human motion is an energy source which provides the possibility for creating energy harvesters that produce electrical energy as a result of our own body motion, rather than from the ambient environment. Human motion-based energy harvesters have wide applications in our daily life, ranging from health monitoring, activity recognition, human-machine interactions, to field survival [40, 41]. As an example, bioinspired sensors are a new form of sensor that utilizes existing technologies and processes to simulate structures and materials in nature [8], which has attracted significant interest recent decades [42-44]. While bioinspired sensors often exhibit a low-power consumption [45], they require a power supply to support their function. Xue *et al*. concluded in their review paper [8] that there are two approaches to address the power supply: (1) bioinspired sensors can be combined with energy harvesting technologies, which can convert energy from ambient environment into electricity. (2) bioinspired sensors based on triboelectric nanogenerators and piezoelectric nanogenerators can directly convert the detection signal (such as vibration, and pressure) into a sensing signal without the need for a an external power supply. Inspired by this approach, the electricity harvested from human motion can be used for two main portable devices namely *self-powered* devices and *self-sensing* devices.

The adjective of being *self-powered*, according to the *Marrian-Webster* Dictionary, means having its own power or propelling force [46]. In recent years, small-scale self-powered devices which generate electricity from vibrations, rotational motion, and wind have attracted significant attention [47]. The development of human motion-based energy harvesting technologies and associated human motion-based self-powered devices make them highly portable, so that they can be applied to a wide range of applications, as summarised in Fig. 2. The applications of self-powered devices include powering implantable biomedical devices, wearable devices and other low-power electronics.

Correspondingly, the concept of *self-sensing* is a new term that refers to the ability of a structural material to sense by itself without sensor incorporation [48]. While this definition originated with a reference to self-sensing concrete, it can be extended to a range of other smart materials that are able to act as self-powered sensors. Therefore, self-sensing devices are initially self-powered and are then sensitive to a specific physical quantity such as force, temperature, or motion. Thus, human motion-based self-sensing devices are able to power themselves by utilizing human motion energy and can be applied in human activity monitoring, healthcare monitoring, human-machine interaction and bioinspired sensor systems [49-51], whose applications include both healthcare and human-machine interaction [8]. These applications provide new prospects in the development of human motion-based self-sensing devices, as seen in Fig. 2. In summary, in this review paper, *self-powered* devices refer to self-powered devices which do not have sensing abilities, while self-sensing devices refer in the self-powered devices possessing specific sensing ability.

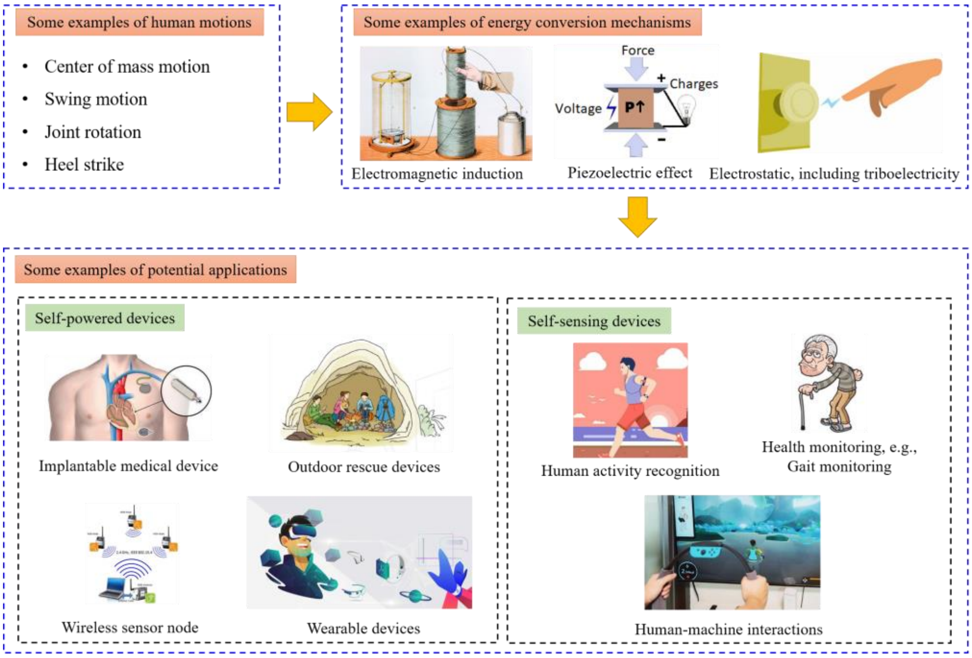

Fig. 2 Energy sources and energy conversion mechanisms for human motion-based energy harvesting and its application in a range of applications; including powering low-powered electronics and self sensing.

In recent decades, relevant review papers on human body-based energy harvesting have been published [put all the references here 52-60], For example, Zhang *et al*. summarized human activity-induced energy harvesting based on ferroelectrics and ferroelectric biomaterials [52]. The review paper of Proto *et al*. focused on the development of nanogenerators based on piezoelectric, triboelectric and thermoelectric physical effects to harvest energy from body-based biomechanical and thermal energies [53]. Huang *et al*. reviewed the functional materials, fiber fabrication techniques and device design strategies to form fiber-based energy conversion devices for human-body energy harvesting [54]. Zhou *et al*. overviewed the mechanical and biochemical energy from human activities, and the working principles, design approaches, wearing style, and materials to produce energy harvesters were compared and analyzed [40], while Zou *et al*. foucussed on the thermal, chemical and mechanical energy contained in the human body, and the application of harvesting for smart bioelectronic system [55]. Shi *et al*. examined walking based energy harvesting to scavenge energy from body vibrations, inertial elements, and foot pressures [56]. Mitcheson *et al.* summarized the energy harvesters based on human motion, and discussed the trends, applications and future developments [28]. Khalid *et al*. reported on the piezoelectric, electromagnetic and triboelectric energy harvesting technologies to scavenge biomechanical energy from walking, stretching, and limb movement [57]. Dagdeviren *et al.* summarized harvesting from living subjects (including the energy in chemical, thermal and mechanical forms) for self-powered electronics [58], while Invernizzi *et al*. addressed the main physical and physico-chemical processes that lead to energy generation from human motion [59]. In the review paper of Cai *et al.*, the principles, development, and applications of human motion (including center of mass motion, joints motion, foot strike and limb swing motion) excited energy harvesters were reviewed [60].

Commented [CB1]: I have removed some sentence - reads like a list - you do not need lots for all.

However, to the best of the authors' knowledge, no previous work has reviewed the human motion-based self-powered and self-sensing devices. For an improved understanding of this research topic, a comprehensive review is required that summarizes the classifications of available human motions, the range of available energy conversion mechanisms, the available materials, device structures, performance and ultimately the applications.

In this review, the progress, challenges and potential opportunities of human motion-based self-powered and self-sensing devices are comprehensively reviewed and critically discussed. The remainder of the review is organized as follows: Section 2 classifies the available human motion forms of energy based on how they operate as excitation sources. The commonly used energy conversion mechanisms and materials are carefully introduced in Section 3. In Section 4, the state-of-the-art advances of the human motion-based energy harvesters are comprehensively reviewed, discussed and characterized by introducing their device structures, operating mechanisms and performance based on a range of human motion forms of energy. The application of human motion-based self-powered and self-sensing devices are then summarized and categorized in Section 5, and the application challenges are discussed. Finally, conclusions, challenges and prospects are addressed in Section 6.

2. Classification of energy sources from human motion

Energy conversion mechanisms, materials and structures for self-powered and self-sensing devices highly depend on the nature and properties of the range of potential human motions. Therefore, it is necessary to classify the range of energy sources from human motion which can be harvested, along with their motion characteristics. Cai *et al*. [60] classified human forms of motion into centre of mass (COM), joint, foot strike and limb swing motion. According to Zhou *et al*. [40], the mechanical energy generated by human motion includes energy produced from arm joint movement, ankle joint movement, centre of mass motion, knee joint movement, heel strike and limb swing. However, these classification methods have primarily considered the *origin* of the energy sources, but they do not clearly classify the human motion energy according to their typical properties. Hence, in this review, human motion forms of energy are classified into three categories based on how they operate as a *source of excitation* for human motion-based energy harvesters, as shown in Table 1: This includes **Category I** – Human motion that operates as an external base excitation; **Category II** – Human body movement that operates as a direct form of excitation that leads to deformation; and **Category III** – Human body movement that leads to a slowly varying pressure or small displacement. The specific properties and representative examples of these three categories are shown in Table 1, which should be considered in the design of energy harvesters.

Table 1 Classification, definition, properties and representative examples of human motion energies.

Category and definition	Properties	Representative examples

Category I: Human motion that operates as an external base excitation	For macroscopic motion: ■ Operate as vbrational or rotational base excitation ■ Human motion with high amplitude (mm or cm level) ■ Low frequency (typically < 10 Hz) For microscopic motion: ■ Operate as vbrational or rotational base excitation ■ Small level of amplitude ■ High frequency	1. Walking or running related motions (unintentional motion): ■ Centre of mass motion ■ Swing motion ■ Joint rotation 2. Macroscopic motion not related to walking or running (intentional motions): ■ Human joint movement ■ Arm / hand shaking 3. Micro-physiological motion ■ Heart beat ■ Vibration of vocal cords
Category II: Human body movement that operates as a direct deforming form of excitation	■ Random and intermittent ■ Harvesters that deform along with this type of human motion	■ Compression / stretching / twisting excitations ■ Bending motion of a finger, wrist, arm, elbow, knee and thigh
Category III: Human body movements that lead to a slowly varying pressure or small displacement motion	■ Microscopic motion ■ Slowly-varying pressure or small-displacement motion (μm level)	■ Touching, tapping, pressing, sliding or hammering of finger, hand, toe and heel ■ Foot pressure during walking or running ■ Breathing ■ Blood pressure variation

(1) Human motion that operates as an external base excitation (Category I). For energy harvesters such as energy-harvesting backpacks [61], they are able to harvest energy from the continuous vibrational or rotational excitation induced by human motion. Under these circumstances, human motion operates as an external form of base excitation for the energy harvester. This category of human motion provides an external vibrational or rotational excitation, which acts as a base excitation for the energy harvester. In most cases they are macroscopic motions which are visible to the naked eye with a magnitude at the mm or cm level, while in the other cases, such as heartbeat, the motions can be smaller.

Examples of these motions are related to walking or running, including the walking/running induced centre of mass motion, swing motion, joint rotation and other energy sources. A complete gait cycle of a person can be divided into two main stages: stance and swing [62], as shown in Fig. 3Fig. 3. During each cycle, the centre of mass of a person moves up and down, thereby producing a vertical vibrational excitation, which can be harvested by an energy harvester mounted on the waistline [63], backpack [64-66] or other body parts. The swing motion of arms [67-69], wrists [70], lower-limbs [71], thighs [72], legs [73-76] and feet [77, 78] during the swing stage

Formatted: 06 C Heading, Font: +Body (Calibri), 11 pt, Font color: Auto, (Asian) Chinese (China) of waking acts as an external base excitation and can be harvested. This form of motion is the primary energy source for many human motion-based harvesters. Moreover, when a person walks or runs, the rotation of joints [59], such as the knee-joint [15, 79], can be transformed into electricity. Other walking or running related energy sources include the impact/strike energy of the leg and the heel [73, 77], which are suitable for harvesting using shoe (including sole or insole)-mounted generators.

It should be noted that since the frequencies of human walking and running motion are relatively low [77], the frequencies of the related motions are also low; typically < 10 Hz [80]. Thus, to harvest energy from these forms of motion to deliver a self-powered and self-sensing device, energy harvesters should be designed and explored to scavenge low-frequency motions with wide-frequency characteristics, or can provide frequency up-conversion technologies, frequency tuning technologies, or non-resonant technologies [80-87]. Moreover, the irregular motion associated with human walking or running is difficult to harvest due to their high amplitude (>1 g) and random (time-varying) characteristics [67, 88], which should be considered in the design of a human motion-based energy harvester.

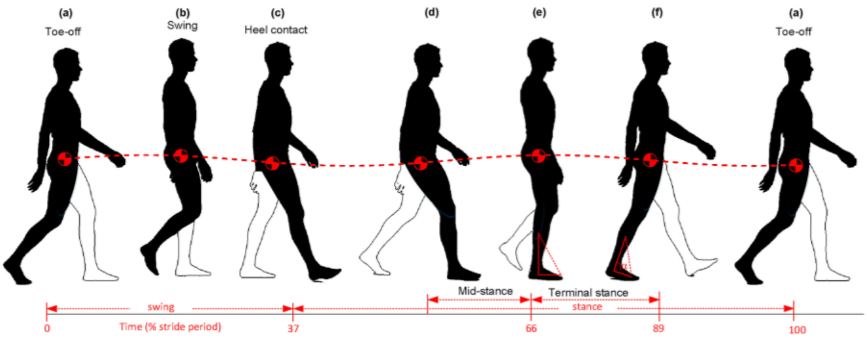

Fig. 3 A typical gait cycle during walking, an example of Category I energy source [62].

The other range of human motions that operate as an external form of base excitation are not related to walking or running. These motions involve intentional actions from human body [68, 89-91], such as human joint movement (e.g., bending of a finger or arm), arm/hand shaking, or regular hammering by the hand. The frequencies of these human motions are also low, but they can be controlled by human, which is beneficial in the design of an active human motion-based energy harvester, which has significant potential in emergency conditions where there is no external power supply.

In addition to macroscopic human motion, the internal organs of a human, such as the heart, vascular wall, and vocal cords can provide an external excitation for *in vivo* energy harvesters [92]. It should be noted that the energy from the heartbeat, pulse, and vibration of the vascular wall and vocal cords can be several orders of magnitude lower than macroscopic motions; nevertheless the micro-scale physiological movement is a promising energy source for human motion-based energy harvesters powering ultra-low-powered implantable medical devices (IMDs).

(2) Human body movement that operates as a direct form of excitation (Category II). Energy harvesters based on flexible and stretchable materials are able to move and deform in line with the movement of the human body. For these harvesters, the human motion acts as a direct form of excitation which leads to excitation, which means that the active part of the harvester deforms with the human motion. Examples include compression/stretching/twisting excitations [93], the bending motion [94-101] of a finger, wrist, arm, elbow, knee and thigh, and other motions such as reciprocal abdominal motions resulting from the human breathing [102], and the motion of left ventricle in closed chest environment [103].

It can be found that in many cases the motion of a joint can act as a direct form of excitation by deformation for self-powered or self-sensing devices. However, since joint rotations of the elbow, ankle, knee, shoulder and other body parts can often be random and intermittent, the obtained electrical signals are typically irregular with varying magnitude [98], and this should be considered in the design and development of such energy harvesters. Moreover, as the energy harvesters should deform along with the human motion, flexible materials such as stretchable piezoelectric materials, textiles and dielectric elastomers should be selected to design energy harvesters aiming to exploit this type of human motion.

(3) Human body movements that lead to a slowly varying pressure or small displacement motion (Category III). The slowly varying pressure from finger touching, foot standing, and blood pressure, can provide positive work that can be transformed into electrical energy. In most cases, the slowly varying pressure results in a small displacement or motion (μm level), which can be used to stimulate an energy harvester. Hence, this categoty of human motions are always microscopic, and the slowly-varying pressure or small-displacement motion is directly applied to the harvesters.

The most common source of such human motion is touching, tapping, pressing, sliding or hammering of the finger [99, 104-107], hand [99, 104, 106, 108], toe [99] and heel [107]. Another important source of energy is foot pressure

[109-116] during walking or running, which may result in friction forces [117, 118] that can be harvested. Moreover, slowly varying pressure or small displacement motion can originate for palm clapping [119, 120], the continual contact-separation processes between elastomer materials and human skin [121], breathing[122] and blood pressure variation [25]. It can be found that both active and passive harvesters can be designed to harvest energy from human body movements that lead to slowly varying pressures or small displacement motions.

3. Energy conversion mechanisms and materials for human motion-based self-powered and self-sensing devices

A variety of forms of human motion energy can be harvested for self-powered and self-sensing devices through a range of energy conversion mechanisms. The characteristics of the range of electromechanical energy conversion technologies, can match the available energy forms, and can lead to different design methodologies and a range of energy harvesting structures. Therefore, energy conversion mechanisms suitable for small-scale human motion-based self-powered and self-sensing devices will be introduced in this subsection, along with the potential energy conversion materials.

3.1. Electromagnetic induction

In 1821, the phenomenon of *electromagnetic* (EM) induction was discovered by Faraday. He established Faraday's law, and invented an electric generator (Faraday's wheel) in 1831 [123]. It was found that when the magnetic flux Φ_B through a looped electrical conductor varies with time t, a voltage V, which relates to the induced electromotive force (*emf*, f_{em}), will be formed, thus generating electrical energy [124], as shown in Fig. 4. If the circuit is closed with a load resistance, R, an induced current of $I = V / R$ along the circuit will be obtained. The *emf* is related to the rate of change of Φ_B and can be expressed as $f_{em} = -d\Phi_B/dt$. According to the energy conservation principle, it is apparent that the system generates electrical energy that is equal to the physical work done against this force, ignoring any heat production.

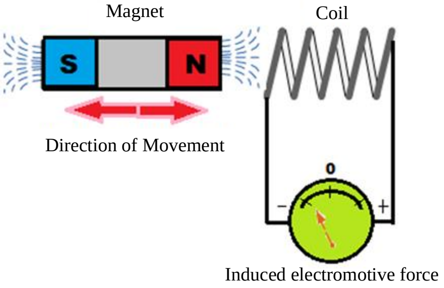

Fig. 4 Schematic of the electromagnetic induction effect.

According to the mechanism of electromagnetic induction, electricity can be generated when an external mechanical excitation is applied to vary the magnetic field across a coil. After Faraday's wheel, this electromechanical conversion mechanism led to the design of a range of electromagnetic generators (EMGs) which are able to transform fossil-fuel energy, water power and wind energy into electricity using a steam, water and wind turbine, respectively. At the small-scale level, many electromagnetic generators have been proposed to harvest a range of energy forms, including energy from human motion [61, 62, 68, 69, 115, 125-127].

It is well known that the magnetic flux $\Phi_B = B \cdot S$, where B is the magnetic induction and S is the area perpendicular to B. Hence, for the purpose of creating a time-varying magnetic flux, two main forms of electromagnetic generators are envisaged. The first type of electromagnetic generators is achieved by moving a coil while fixing the magnet, and this type of electromagnetic generator (a coil) consists of N turns of a coil which are excited to cut the magnetic induction lines of a constant magnetic field B. The same result can be achieved by moving a permanent magnet nearby a stationary or fixed coil, thus leading to another type of electromagnetic generator.

The main components of a vibrational or rotational electromagnetic generator are therefore its permanent magnets and coils, which influence the performance of electromagnetic generators. Permanent magnets are a class of materials which can generate a stable magnetic field autonomously. The magnetization M, which is defined as the magnetic dipole moment per unit volume, is a key material property parameter to evaluate the strength of a magnet. This can be calculated for $M = \chi_m \cdot H$, where H is the magnetic field strength and χ_m is the magnetic susceptibility. The materials of the permanent magnets can be classified into four classes based on their magnetic properties: *diamagnetic*, *paramagnetic*, *ferromagnetic* and *ferrimagnetic* materials. Diamagnetism and paramagnetism can be induced when an external magnetic field B_{ext} is applied to a material with $\chi_m < 0$ and $\chi_m > 0$, respectively, thus creating an attracting force. These two materials can only retain magnetization when a magnetic field is applied, which means that they do not have permanent magnetic properties, and are therefore not important for energy harvesting. In comparison, ferromagnetic and ferrimagnetic materials can be used to generate a permanent magnetic field due to the alignment of the electron spin moments of the component atoms/molecules. If the local magnetic moments in the materials are parallel, the materials provide a strong contribution to the magnetization and are called *ferromagnetic* materials. Conversely, those materials, in which the nearest neighbouring atoms (with different moments) present antiparallel alignment, thus reducing magnetization, are called *ferrimagnetic* materials. In Table 2, the important characteristic parameters of the most common magnetic materials are presented. A particular case of ferrimagnetic materials are anti-ferromagnetic materials, whose magnetization is zero; this type of material is unsuitable for energy harvesting.

Table 2 Material properties of some commonly used bulk magnets [59]. BH_{max} indicates the maximum volumetric energy density; H_c is the coercive force; the Curie temperature means the critical temperature for the magnets to lose their permanent magnetic properties. Among these magnetic materials, AlNiCo and $SmCo_5$ are ferromagnetic, ferrites are generally ferrimagnetic, and NdFeB can behave both as a ferro- and as a ferrimagnet.

Material	BH_{max} [kJ m^{-3}]	H_c [kA m^{-1}]	Curie temperature [℃]	Advantage	Disadvantage
Ferrites	10-40	100-300	450	Low cost, corrosion resistance	Low mechanical strength, low energy product
AlNiCo	10-88	275	700-860	Corrosion and heat resistance	Low coercive force and energy product
$SmCo_5$	120-200	600-2000	700	High energy product, heat resistance	High cost, low mechanical strength
NdFeB	200-440	750-2000	310-400	Very high energy product and coercive force	Low working temperature, low corrosion resistance

The coil is the other main component of an electromagnetic generator. For an electromagnetic generator to transform the energy of human motion into electricity, its size should be sufficiently small to allow the device to be portable or wearable. Two approaches are possible to achieve this goal: the use of micro wire-wound coils or micro-fabricated coils. For the micro-wound coils, the wire diameter is decreased and the increase in resistance per unit length further reduces the efficiency of the electromagnetic generator. Compared to the micro-wound coils, micro-fabricated coils can be readily fabricated into a small size and complex geometry, and have therefore attracted significant attention for energy harvesting [59].

It should be noted that electromagnetic generators are recommended for macroscale devices, which can be readily fabricated using high performance bulk magnets and multi-turn coils. Moreover, the generated voltage of small-scale electromagnetic generators is relatively low (typically < 1 V [59]), however the current produced is relatively high. For wearable or portable human motion-based self-powered and self-sensing devices of small size, their energy harvesting performance is limited. Moreover, since electromagnetic generators use vibrational magnets or coils, small-scale generators are most suitable in harvesting energy from human motion that operates as an external base excitation (Category I).

3.2. Piezoelectric effect

The piezoelectric (PE) effect was first discovered in 1880 by French physicists Pierre Curie and Jacques Curie [128]. They found that specific inorganic crystals, polymers, and biological matters (such as bone, DNA and various proteins) can be polarized electrically when subjected to an applied mechanical stress. The polarization charges can be generated on both surfaces of a piezoelectric crystal, thus generating a voltage difference between the two surfaces, as shown in Fig. 5. This is the so-called *direct piezoelectric effect*. A year later, from the principles of thermodynamics, Gabriel Lippmann mathematically deduced the *converse, or inverse, piezoelectric effect* [129], which indicates that a piezoelectric material deforms when it is subjected to an electric field. One can see that the direct piezoelectric effect can be used for both sensing and energy harvesting, where the applied mechanical stress or strain generates surface charges or an electrical signal (an electric field under open circuit conditions) on the piezoelectric material. In recent decades, piezoelectric generators (PEGs) have shown their advantages of simple configuration, large energy conversion efficiency, and the ease of integration into more complex systems [130], thus resulting in the rapid development of piezoelectric generators. The phenomenon of the piezoelectric effect is attributed to the unique elemental structure of specific crystal lattices. In their crystalline ionic structure, a balanced equilibrium exists between the positive and negative charges, which is neutralized along the virtual polar axis. When these crystalline structures are subjected to a mechanical excitation (stress, vibration or strain), this equilibrium can be disturbed, leading to an irregular arrangement of the dipoles and producing an electrical charge [131, 132]. Thus, the positive and negative charges are separated with the destroy of the molecule's neutrality, and surface charges can be collected via electrodes under short circuit conditions, or result in a potential difference between the surfaces under open circuit conditions. The number and strength of the electric dipoles of the piezoelectric material is a factor that affects the material's behaviour and performance. Additional details about the influence of mechanical excitations on the molecular and atomic structure of piezoelectric materials can be found in Refs. [59, 133].

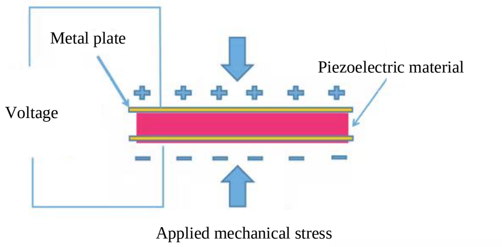

Fig. 5 Schematic of the direct piezoelectric effect.

Commented [CB2]: Add a polarisation direction P

From a macrocosmic point of view, the direct and converse piezoelectric effects are governed by the following piezoelectric constitutive equations, which show the relationship between the mechanical stress/strain and the electric field/charge density:

$$\begin{bmatrix} Converse \\ Direct \end{bmatrix} = \begin{bmatrix} S \\ D \end{bmatrix} = \begin{bmatrix} s^E & d^t \\ d & \varepsilon^T \end{bmatrix} \begin{bmatrix} T \\ E \end{bmatrix} \quad (1)$$

Here, s^E is the compliance under a constant electrical field; ε^T is the dielectric permittivity under a constant stress; d and d^t are respectively the matrices for direct and converse piezoelectric effect, where the superscript t represents the transpose.

For a piezoelectric element with area A, thickness h, and piezoelectric charge constant $d = d_{33}$ along the h direction, it can be approximately regarded as a parallel plate capacitor, whose capacitance $C = \varepsilon_0 \varepsilon_r A / h$, where ε_0 and ε_r are the vacuum permittivity and the relative permittivity of the material, respectively. When the element is applied with a stress σ (or a force $F = \sigma A$), the accumulated charge Q on the electrode, the induced voltage V over the element, and the total generated electrical energy W can be obtained, as follows:

$$Q = d \cdot \sigma \cdot A \quad (2)$$

$$V = \frac{Q}{C} = \frac{d\sigma A}{\varepsilon_0 \varepsilon_r A / h} = g \cdot \sigma \cdot h = \frac{gFh}{A} \quad (3)$$

$$W = \frac{1}{2} QV = \frac{1}{2} dg\sigma^2 \cdot Volume = \frac{1}{2} \frac{dgF^2 h}{A} \quad (4)$$

where d is a constant and $g = d / (\varepsilon_0 \varepsilon_r)$ is called the piezoelectric voltage coefficient. $Volume = A \cdot h$ indicates the constant volume of the element.

Approximately 200 different piezoelectric materials have shown their potential in energy harvesting applications [134]. These materials can be categorized into four major groups, including single crystals [132, 135], ceramics [132], polymers and polymer composites/nanocomposites [133]. The piezoelectric properties partly determine the energy harvesting performance of piezoelectric generators. Among these materials, single crystals have the highest piezoelectric coefficient ($d_{33} = 2200$ pCN^{-1}, $k_{33} = 93\%$) [136], which is beneficial for their applications in many electromechanical sectors such as sonar transducers, accelerometers, actuators, and medical ultrasonic devices. The piezoelectric ceramics such as barium titanate ($BaTiO_3$), lead-zirconate-titanate (PZT), potassium niobite ($KNbO_3$) are polycrystalline materials which have relatively high piezoelectric properties. The PZT-based ceramics are the most important and widely used piezoceramics in energy harvesting/storage field, although they are lead-based materials. Piezoelectric polymers such as polylactic acid (PLA), polyvinylidene fluoride (PVDF), co-polymers, cellulose and derivatives are a type of carbon-based materials with long polymer chains. Due to their mechanical flexibility compared to signal crystals and ceramics [132] they can withstand larger strains, providing them with potential for applications that require large bending or twisting; these materials are suitable for applications such as ultrasonic transducers, audio transducers, medical transducers, display devices, and sensors. The piezoelectric polymer composites and nanocomposites (polyvinylidene fluoride-zinc oxide (PVDF-ZnO), cellulose $BaTiO_3$, polyimides-PZT) have been specially developed to modulate and enhance the properties of the above materials [137].

The most commonly employed piezoelectric materials for energy harvesting include SiO_2 (quartz), AlN, BaTiO3 (BT), poly(vinylidene fluoride) (PVDF), PZT, PMN-PT ($Pb[Mg_{1/3}Nb_{2/3}]$), PZN-PT ($Pb[Zn_{1/3}Nb_{2/3}]O_3$-$PbTiO_3$), and a range of composite systems. In Table 3, the properties of key piezoelectric materials are summarized [138-141]. The most important materials for energy harvesting from human motion are PVDF polymer and PZT ceramic due to their optimal piezoelectric performance, and more details on these materials and their manufacturing approaches can be found in Refs. [[59, 133, 141]].

It is noted that the choice of a piezoelectric material also depends on the functionality of the application sector, design flexibility, application frequency, and available volume [133].

Table 3 Piezoelectric materials and their properties [138-141].

	BaTiO3	PZT-4	PZT-5A	PZT-5H	PZT-8	PVDF	PMN-33%PT	PZN6%PT
d_{31} (10^{-12} C/N)	-78	-123	-171	-275	-97	-23	-920	-1400
d_{33}	149	289	374	593	225	33	2200	2400
d_{15}		496	584	741	330			
g_{31} (10^{-3} Vm/N)	5	-11.1	-11.4	-9.1	-11	216	-17.1	24.3
g_{33}	14.1	26.1	24.8	19.7	25.4	330	44	41.7
g_{15}		39.4	38.2	26.8	28.9			
k_{33}	0.48	0.7	0.71	0.75	0.64	0.15	0.93	0.9
Mechanical Q_M	300	500	75	65	1000	3-10	69	
Dielectric loss		0.4%		2%	0.4%		0.42%	
Curie temperature (℃)	115	328	365	193	300	100	145	100

There are many structural configurations available for piezoelectric generators, such as bimorph/unimorph cantilever beam, circular diaphragm, cymbal type and stack type configurations [133, 142]. Among these device configurations, the cantilever beam type configuration [133, 143], including bimorph cantilever and unimorph cantilever, consists of one or two piezoelectric layers and a non-piezoelectric layer. One end of these layers is fixed, allowing the structure to operate in its flexural mode. The cantilever beam type is one of the most commonly used energy harvesting structures, in particular for vibrational harvesting. The circular diaphragm configuration is another piezoelectric generator structure, which is based on a thin disk-shaped piezoelectric layer that is attached to a metal gasket which is fixed between two clamping rings. The circular diaphragm configuration is suitable to harvest energy from slowly varying, periodic pressure, and vibrations. The cymbal and stack type configurations have been proposed for vibrational energy harvesting. The cymbal type consists of a piezoelectric layer placed between two metal end caps on both sides and is of interest for applications that lead to high impact forces. The piezoelectric stack consists of multiple piezoelectric layers stacked over each other. Additional details regarding these four configurations of piezoelectric generators can be found in Refs. [133, 142, 144], and a comparative analysis of the major advantages and disadvantages are summarized in Table 4. Piezoelectric generators should therefore be designed by considering the application perspective and operation mode.

Table 4 Major advantages and disadvantages of different structural configurations of piezoelectric generators [132, 133, 145].

Type of configuration	Features/advantages	Disadvantages
Unimorph/bimorph cantilever beam	■ Simple structure ■ Low fabrication cost ■ Low resonance frequency ■ Power output is proportional to proof mass ■ High mechanical quality factor ■ Compatible with pressure mode operation	■ Inability to resist high impact force
Circular diaphragm	■ Compatible with pressure mode operation	■ Stiffer than a cantilever of same size ■ High resonance frequencies
Cymbal type	■ High energy output ■ Withstand high impact force	■ Limited to applications demanding high-magnitude vibration sources
Stacked type	■ Withstand high mechanical load ■ Suitable for pressure mode operation ■ Higher output from d_{33} mode	■ High stiffness

According to the properties of the energy harvesting configurations described here, specific piezoelectric generators are suitable to harvest almost every type of human motion, including human motion as an external base excitation (Category I), human body movement acting as a direct form of deformation (Category II), and slowly varying pressures or small displacements (Category III). We note that piezoelectric generators are suitable to develop microsystems since their high power density, simple structure, ease of fabrication and low number of peripheral components. Moreover, piezoelectric generators can generate high output voltage, but low current, which results from the high resistance/impedance of the materials and should be considered in the design of human motion-based piezoelectric generators.

3.3. Electrostatic effect in dielectric elastomer generators

In the energy harvesting field, *electrostatic* (ES) or capacitive energy harvesting is based on the variable capacitor, whose charging capacitance depends on the level of external excitation or deformation [146]. The plates of the initially charged capacitor are separated when an external force or vibration is applied, thus converting mechanical energy into electricity. As a result, mechanical forces from the movement of the source are employed to undertake work against the attraction of the charged plates of the electrostatic generator (ESG); hence, a variable capacitor is formed and the electrical energy stored in the capacitor can be enhanced [147].

Traditional electrostatic generators using a parallel plate capacitor are not as popular and widely reported as piezoelectric generators or electromagnetic generators due to their low energy density, which results from the limited variance in capacitance. In recent decades, electrostatic generators based on dielectric elastomers acting as the variable capacitor [148] have provided a considerably enhanced capacitance variance under external large strains, thereby attracting significant attention.

Dielectric elastomers (DEs) are a type of hyperelastic soft materials in the form of thin films. Dielectric elastomer-based electromechanical transducers can operate as actuators, sensors and harvesters. When the dielectric elastomer material is subjected to an electric field, it decreases its thickness and increases its area due to the Maxwell stress caused by the opposite charges stored on the compliant electrodes (work as anode and cathode, respectively), which are coated on both faces of the dielectric elastomer film. In these cases, the dielectric elastomers are acting as *actuators* or *artificial muscles*, when the thin dielectric elastomer membrane is squeezed by the Maxwell pressure caused from electrostatic effect [149-154]. For example, a soft robot based on this material has been developed to work in the Mariana Trench [155]. For dielectric elastomer sensors, their variation of capacitance can be used to measure, or sense, a stretch or an applied force [156]. Moreover, dielectric elastomer materials can be also used for energy harvesting based on their mechanical-to-electrical energy conversion mechanism. This is the so-called dielectric elastomer generator (DEG), which are considered as a promising form of harvester due to the following advantages: 1) their cyclic working principle can matches well with an alternating or time-varying mechanical energy; 2) they have relatively high energy densities, with a theoretical energy density of 3 J/g [157] and experimental values of up to 0.78 J/g [158]; 3) the energy conversion mechanism of dielectric elastomer generators is based on the deformation-recovery process of the dielectric elastomer material, therefore, theoretically the convertible energy density of dielectric elastomer generators is independent of the operating frequency; 4) the raw materials are low cost; 5) they are light weight, architecturally simple, with few or no moving rigid parts, and provide silent operation. Moreover, the layout and operation principle of dielectric elastomer generators can be adapted to different dimensional ranges [159], enabling a diversity of applications including human motion energy harvesting.

The operation principle of dielectric elastomer generators is relatively simple, which was first studied by Pelrine *et al*. in 2001 [148]. As shown in Fig. 6, a dielectric elastomer generator mainly consists of a deformable dielectric elastomer membrane (DEM) coated with compliant electrodes to form a variable capacitor [160]. When the dielectric elastomer membrane is under an electric field and is mechanically stretched, it will recover to its initial state when the external force or excitation is removed. Therefore, charges on the electrodes produce an increased voltage due to the work done against the electric field pressure, leading to an increase in the electrostatic potential energy of the charges. Three main energy harvesting cycles possible for dielectric elastomer generators, include *constant charge* mode, *constant voltage* mode and *constant electric field* mode [161]. The generated energies using these three energy harvesting cycles are $U_0 2\ln(1/\alpha)$, $U_0(1-\alpha^2)$ and $U_0(1-\alpha^2)$, respectively [162], where α indicates the contraction ratio [161] and U_0 defines the specific energy. More details of these energy harvesting cycles can be found in Refs. [[163]].

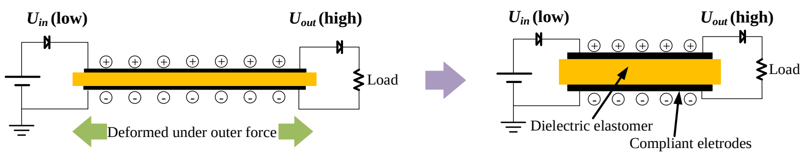

Fig. 6 Schematic of the working principle of a dielectric elastomer generator[164].

Commented [CB3]: "Deformed under external force"
Not outer force

Is left with force and right no force? Not clear.

Commented [CB4R3]: What is purple arrow?

The group members of Prof. Zhigang Suo at Harvard University have made relevant contributions in this field. They established a thermodynamic model to analyze the mechanical-to-electrical energy conversion process of a dielectric elastomer generator, and introduced a work-conjugate plot to determine the maximum energy that can be converted from a mechanical strain [165]. They revealed that the planes of the working-conjugate coordinates are determined by the modes of failure of the dielectric elastomer material, including electrical breakdown, electromechanical instability, loss of tension, and rupture by stretch. This work-conjugate plot is a useful tool for the design of the practical energy harvesting cycle of a dielectric elastomer generator [158, 162, 166-168]. It should be pointed out that most dielectric elastomer generators can only increase the amount of power of the priming charges supplied by an electrical energy source, which is normally provided by an external power supply. Thus, they cannot achieve autonomous power generation. However, the energy source could be eventually replaced since the charges may be transferred to the load or even dissipated, which restricts the application of dielectric elastomer generators in self-powered or self-sensing devices. One potential solution for this issue was proposed by Anderson *et al.*, who reported on a self-priming dielectric elastomer generator system [169-173] that can utilize the generated energy to replenish the charge losses, meaning that the external energy source is no longer necessary. Thus, the self-powered and self-sensing dielectric elastomer generator devices can be further designed to expand the applications of dielectric elastomer generators.

The properties of dielectric elastomer materials play a key role in energy harvesting performance, which include the relative permittivity (dielectric constant), the breakdown (BD) strength, and the Young's modulus. Since the discovery of the dielectric elastomer materials in 1990s, many materials have been studied for dielectric elastomer generators, including: 1) acrylic elastomers, in particular, commercially available acrylics from 3M (VHB tapes), which are widely used to build laboratory demonstrators [158, 170, 174, 175]; 2) natural or synthetic (e.g., styrene-based) rubbers [157, 176]; and 3) silicone elastomer (polydimethylsiloxane) (PDMS) [177, 178]. Acrylic VHB tape has been widely used for the demonstration of dielectric elastomer generators since it can be easily adhered to substrates and can be coated with commercial conductive grease/paste, thus making the manufacture of dielectric elastomer generator prototypes particularly convenient. Moreover, the low Young's modulus of the acrylic materials allows them to achieve high strains and large elongation compared to other elastomers. These materials possess a relatively high relative permittivity and breakdown strength, which can be further improved with pre-strain [179]. However, acrylic elastomers have high electromechanical losses and have limited reliability under periodic excitations [180]. They are also temperature and humidity-sensitive materials, and present a slow response actuation when they are subjected to an input voltage. Natural rubbers, which are soft elastomers with the advantage of a low Young's modulus, high elongation at break, and high breakdown strength, but a low relative permittivity, have been indicated as a promising dielectric elastomer material for energy harvesting due to its large breakdown strength [157, 181]. Similar properties can be also observed in the styrene-based synthetic rubbers, whose application in dielectric elastomer generators have been rarely explored to date [182]. Silicones are considered as a candidate for future of dielectric elastomer generators since they can be manufactured through different techniques [183, 184] and offer the possibility for improvement in their electromechanical properties through physicochemical modification of their components [185]. Moreover, the high reliability and long-term stability of silicones make them attractive for harvesting. The drawbacks of these materials include their low relative permittivity, which can be addressed through a range of approaches [185]. The material properties of three representative commercial elastomers can be found in Table 5, which is obtained by Chen *et al*. [182] and other researchers [186, 187]. The listed materials include: 1) acrylic VHB 4905 by 3M, which is a commercialized tape; 2) natural rubber Oppo Band Green 8003 by Oppo, which is mostly used as an exercise band; 3) Elastosil silicone by Wacker Chemie AG, which was developed as a general-purpose raw material, but recently the high-tolerance thin films have been developed for dielectric elastomer applications specially. More details about the pre-mentioned materials and other DE materials can be found in Ref. [[188]].

Table 5 Electromechanical properties of three representative commercial dielectric elastomer materials [189].

	Acrylic VHB 4905	Oppo Band Green rubber	Elastosil silicone
Shear modulus (kPa)	17	620	308
Relative permittivity	4.14	2.74	2.85
BD strength	70-180	100-300	75-195
Conductivity	1-5	0.1-0.4	5×10^{-4}-5×10^{-2}
Mechanical loss (loss)	12-17	4-23	2-4

The compliant electrodes are another important material for assembling a dielectric elastomer generator. For the fabrication of laboratory prototypes, carbon-loaded grease is widely used, which can be simply painted on dielectric elastomer membranes, especially the acrylic dielectric elastomer materials [158, 170, 175, 190]. However, the carbon-loaded grease is not stable and durable for practical applications. Other candidates suitable for real applications are conductive elastomer layers doped with conductive fillers [183], and sputtered micrometer-thin metal films [191].

The deformability of the dielectric elastomer materials makes it possible to design many different topologies, thus providing significant flexibility in the design of practical dielectric elastomer generator models. An overview of some relevant dielectric elastomer generator topologies was summarized by *Moretti* et al. [189]. The simplest dielectric elastomer generator topology is the planar topology, and the dielectric elastomer membranes are stretched by loads applied at the electrode perimeter and is suitable for equibiaxial (or equal-biaxial) stretching [181, 192] and pure-shear stretching (strip-biaxial extension) [193] conditions. The diamond dielectric elastomer generator (or parallelogram dielectric elastomer generator) [176], conical dielectric elastomer generator [112, 194-196], ball-contact/impact type dielectric elastomer generator [113, 164, 197, 198] and circular diaphragm dielectric elastomer generator are other practical topologies [175]. These topologies can lead to various dielectric elastomer generator structures for harvesting energy from vibrations, wind and human motion. In particular, dielectric elastomer generators are flexible, independent of frequency, have various architectures, and are suitable to harvest energy from almost every type of human motions, including human motion as an external base excitation (Category I), human body movement acting as a direct form of excitation by deformation (Category II), and slowly varying pressures or small displacement motions (Category III).

3.4. Electrostatic effect in triboelectric nanogenerators

Triboelectricity is a well-known electrostatic phenomenon. It appears commonly in our daily life when two distinct materials with different electrostatic properties physically contact with each other: when the two materials contact with each other, one material is charged positively and the other one is charged negatively. The following separation will produce a net potential difference between two materials. It is noted that the charge exchange mechanism between the contacted materials is not yet fully understood [199-201]. In many cases such as xerography, self-cleaning wrapping materials, adhesion of clean rooms, explosions in fuel storage tanks, triboelectricity is considered as an unwanted or even adverse phenomenon which may cause damage. When triboelectricity occurs, the opposite charges are produced on the electrodes based on electrostatic induction, thus, a potential difference will be generated on the surfaces of the two materials when they are separated by an external mechanical force. This processes also result in an electron flow between the electrodes and generate an alternating current (AC) output [202, 203]. This is particularly interesting when the system is at a nano-level, leading to the triboelectric (TE) nanogenerator (TENG) with high power densities, which was first reported by Wang *et al.* in 2012 [204]. Subsequently, researchers have paid significant attention to the TENG since it can convert mechanical energy into electricity with unique advantages such as ease of fabrication, numerous available materials and configurations [205-209]. To date, the power density per unit area and unit volume of TENGs have reached 500 W/m^2 and 15 mW/m^3, respectively, and an instantaneous conversion efficiency up to 70% was reported, which can reach 85% under low-frequency excitations [210, 211].

It should be pointed out that the two material layers that separated during external excitations of a TENG can be regarded as a capacitor with varying capacitance. Therefore, the TENG is a type of novel electrostatic generator whose underlying fundamental mode of operation is based on Maxwell's displacement current [212]. Following the detailed summary from Wang *et al.* [167, 171], there are four different operation modes for TENGs [206, 213], which include: (a) the vertical contact-separation (C-S) mode; (b) the lateral sliding (LS) mode; (c) the single-electrode (SE) mode; (d) the free standing triboelectric-layer (FT) mode, as shown in Fig. 7. The contact-separation mode shown in Fig. 7(a) is one of the most straightforward layouts of a TENG. When two dielectric films, which are backed with an electrode, make contact with each other frictionally, oppositely charged surfaces can be created due to their distinct electron affinity. When an external force is applied upon one of the two surfaces, they will be separated and a potential difference can be created between the deposited electrodes, thereby producing a current across an appropriate load to balance the potential difference [204]. Hence, a regular external excitation can result in a regular contact and separation of the two films, and the induced electrons will flow back and forth to generate an AC output in the external circuit [214, 215]. In the lateral sliding mode (Fig. 7(b)), the charge densities of the top and bottom layers are equal and opposite since they have opposite triboelectric polarities and are in full contact with each other initially. When an external force is applied, the top layer will slide outward relative to the bottom layer. Thus, their contact area decreases, and the charges separate. A potential difference is then generated, which drives the electrons to flow from the bottom electrode to the top electrode until the top layer slides out completely. Similarly, a reverse motion can generate a reverse electron flow until electrostatic equilibrium is achieved [206, 216]. Fig. 7(c) illustrates the single-electrode mode, whose opposite contact layer can move freely without connection, thus it is free to move. A ground electrode and a moveable contrasting layer can be used to assemble such a single-electrode mode. A potential difference is produced during the periodic contact-separation processes of the moveable layer, thus leading an electron flow between the electrode and ground [217-219]. This mode can work in both lateral sliding and vertical contact-separation modes. Finally, the free standing triboelectric-layer mode shown in Fig. 7(d) can operate in non-contact mode, in which two symmetric electrodes are under the dielectric layer with a small gap. Considering the movable layer is initially charged in the triboelectric process, the dielectric layer moving close to, and away, from the electrodes will generate an asymmetric charge distribution, leading to the electron flow from one electrode to the other and producing an AC current output [220, 221].

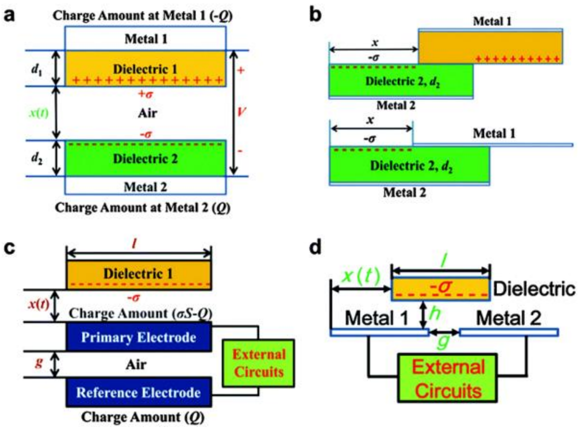

Fig. 7 The operation modes of the TENG [210]: (a) Traditional vertical contact-separation mode; (b) Lateral-sliding mode; (c) Single-electrode mode and (d) Freestanding triboelectric-layer mode.

It should be noted that most materials cannot be charged equally. In fact, their ability to bear a certain amount of charge differ. Furthermore, the performance of a material to attract or release the electrons is decided by the nature of the used material. As a point of reference, a "Triboelectric series" (TE series) shown in Fig. 8 have been empirically defined [59]. This series lists materials from those that tend to be positively charged, to those that tend to be negatively charged. Materials located far from each other in the triboelectric series will exchange a larger amount of charges compared to those close to each other, therefore, the triboelectric series is a useful tool for the prediction of the sign and the extent of the charge separation.

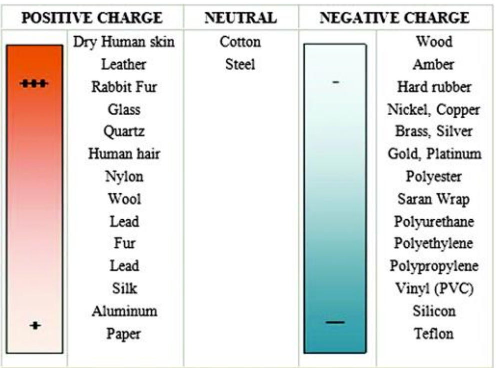

POSITIVE CHARGE	NEUTRAL	NEGATIVE CHARGE
Dry Human skin	Cotton	Wood
Leather	Steel	Amber
Rabbit Fur		Hard rubber
Glass		Nickel, Copper
Quartz		Brass, Silver
Human hair		Gold, Platinum
Nylon		Polyester
Wool		Saran Wrap
Lead		Polyurethane
Fur		Polyethylene
Lead		Polypropylene
Silk		Vinyl (PVC)
Aluminum		Silicon
Paper		Teflon

Fig. 8 The triboelectric series [59].

As stated previously, TENGs have four operation modes suitable for various applications, and the range of available materials is abundant. Therefore, TENGs have attracted significant attention in energy harvesting for applications in pacemakers, cell modulation, nerve stimulation, wound healing, tissue repairing, neural prosthesis, drug delivery, hair regeneration, gene delivery, microbial disinfection, healthcare monitoring and as a biodegradable energy source [222]. Moreover, TENGs can be designed to harvest a range of energy sources from human motion, including human motion operating as an external base excitation (Category I), human body movement acting as a direct form of excitation by deformation (Category II) and slowly varying pressures or small displacement motions (Category III).

3.5 Summary of energy sources, conversion mechanisms and materials

The design of human motion-based energy harvesters is highly dependent on the energy conversion mechanisms and adopted materials, which have been discussed in this section. The four main energy conversion mechanisms that can convert energy from human motion into electrical energy are introduced. The corresponding main energy harvesters are electromagnetic generators, piezoelectric generators, dielectric elastomer generators and TENGs, among which the latter two types of harvesters are both electrostatic generators. Moreover, the relevant materials for these energy harvesters and the main properties were introduced in detail. We also summarised the suitable energy sources for different types of harvesters, which can provide a guideline for the design of optimized human motion-based energy harvesters. Based on introduction and discussion, the features/advantages and disadvantages of these four types of generators for harvesting human motion energies are summarized in Table 6, and the relevant materials and degree of applicability for different catergories of human motion energy sources are presented. This table provides a reference for the design (including the energy conversion mechanism, material and structure) of energy harvesters for a ranage different human motions.

Table 6 Main properties, advantages and disadvantages of electromagnetic generators, piezoelectric generators, dielectric elastomer generators and TENGs in harvesting human motion, along with the relevant materials and degree of applicability for different categories of human motion energy sources.

Type of generator	Main properties / advantages	Main disadvantages	Recommended materials	Degree of applicablity for different categories of human motions*		
				I	II	III
Electromagnetic generator	■ Recommended for macroscale devices ■ Relatively low voltage (typically < 1 V) ■ Relatively high current	■ Limited energy harvesting performance for small-size harvesters ■ Low efficiency at low frequency	Permanent magnets: ferromagnetic materials like AlNiCo and $SmCo_5$, ferrimagnetic materials such as ferrites Coils: micro-fabricated coils	High	-	Low
Piezoelectric generator	■ Four types of structural configurations suitable for different energy sources ■ Suitable for microsystems ■ High output voltage	■ Low current ■ Relatively low energy density	PVDF polymer and PZT ceramic	High	High	High
Dielectric elastomer generator	■ Working principle matches different types of mechanical energy ■ High energy density, which is independent of the operating frequency ■ Low-cost raw materials ■ Adapted to different dimensional ranges ■ Soft materials	■ Cannot achieve autonomous power generation with a traditional dielectric elastomer generator	Dielectric elastomer membrane: acrylic elastomers, natural or synthetic rubbers and silicone elastomer Compliant electrodes: carbon-loaded grease, conductive elastomer layers and sputtered micrometer-thin metal films	Medium	Medium	Medium
TENG	■ Four operation modes suitable for various applications scenarios ■ Abundant range of materials ■ High power density ■ High conversion efficiency	■ Low current at high voltage ■ Limited durability	Selected from the triboelectric series	Medium	Medium	High

* Category I indicates human motion operating as an external base excitation; Category II indicates human body movement acting as a direct form of excitation by deformation; Category III indicates slowly varying pressures or small displacement motions.

It should be noted that other electromechanical conversion mechanisms exist, such as the magnetostriction [223], piezoelectrochemical[224], and reverse electrowetting [225-228]. These are not reviewed in this paper since their application in human motion-based energy harvesters are still under investigation, but are worthy of investigation.

4. Human motion-based energy harvesters

Human motion-based energy harvesters can produce electrical energy when subjected to a variety of human motions, which can power a range of wearable or portable devices, thereby leading to potential self-powered and self-sensing devices operating with different mechanisms, device structures, performance and application areas. As stated in Section 2, the energy associated with human motion is classified into three categories, see Table 1. The range of available energy sources determines the range of possible energy harvester schemes. Therefore, energy harvesters which have potential to form integrated self-powered and self-sensing devices are reviewed in this section from the perspective of sources of human motion. This provides a reference for the improved design of self-powered and self-sensing devices based on each form of human motion.

4.1. Energy harvesters based on human motion as an external base excitation (Category I)

As introduced in Section 2, the human motions of Category I includes the walking/running-related motions and non-walking/running-related motions. The relevant energy harvesters are always mounted onto a human's body. The energy harvesters based on walking/running-related motions harvest energy *passively*, therefore, they have potential to harvest energy during a person's normal walking or running cycle; meanwhile, those energy harvesters based on the non-walking/running-related motions are suitable to generate energy *actively*.

4.1.1. Walking or running-related motion to provide an external base excitation. For walking or running-related motion that operates as an external base excitation, they involve the centre of mass lifting/lowering, swing motion, and joint rotation. All of these motions have low frequency features, commonly less than 10 Hz. Therefore, relevant energy harvesters using broadband technologies, frequency up-conversion strategies or non-frequency-related technologies, such as the twinkling phenomenon [229], mechanical impact [230-233], magnetic plucking mechanisms [79], and other mechanisms [234-237], can be adopted to convert energy associated with low-frequency, random and irregular human body motion can be converted into electrical energy.

The continuous centre of mass lifting and lowering during walking or running can act as a source of vertical base excitation for energy harvesters that are mounted onto, for example, a person's back or waistline. In the work of Rome *et al*. in 2005 [64], they recognized that the vertical movement of a heavy load during walking represents a significant mechanical energy source that can be converted into electrical energy, potentially at a substantial level. A walking person can be regarded as an inverted pendulum [238, 239]: one foot is placed down and then the body vaults over it, causing the hip to move up and down by a distance of 4 to 7 cm [240]. Thus, for a load carried by a person in a backpack, it will move up and down with the same vertical distance because it is fixed to the body. This concept leads to a type of classical harvester – the backpack-type harvesters, which can generate electrical energy when they are carried on a person's back, as shown in Fig. 9(a-c). The first backpack-type harvester [64, 241] is shown in Fig. 9(a), which was termed the suspended-load backpack. In this device, the load is mounted on a plate is suspended by springs, which are then connected to a pact frame that is fixed to the body. During walking, the load is constrained by a bushing that is connected to vertical rods, therefore, the load can only move up and down freely. A geared direct current (DC) motor attached to the backpack frame acts as a generator which can convert the mechanical energy of the load into electrical energy through a gear system. Another backpack-type device was reported by Xie *et al*. in 2015 [242], as shown in Fig. 9(b). This device consists of a container holding the energy harvester and another container carrying an external load. The framework of the harvester assembled in the device container can move with the backpack when worn by a person. The carrying load in the suspended container can serve as an oscillating mass, since it can oscillate relatively to the framework. Thus, the generator can convert the relative mechanical motion between the oscillating mass and the framework into electrical energy using a frequency-tuneable mechanism. A recently reported wearable energy harvesting backpack can be found in Fig. 9(c), which was reported by Cao, *et al.* [243]. In the backpack, a carried mass was suspended by two tension springs fixed to the top frame. The vertical motion of the suspended mass during walking will drive the electromagnetic motor to convert vibrational energy into electrical energy through a rack-pinion mechanism, which converts the vertical oscillation of the carried mass into rotational motion. It was concluded that the backpack-type harvesters were designed to transform the energy associated with the load/mass motion resulting from the human's walking. The research group led by Prof. Lei Zuo in Virginia Tech also improved the energy harvesting performance of the backpack-type harvesters to provide a broader bandwidth by introducing mechanical motion rectification [244, 245]. Feenstra *et al*. also proposed another backpack-type energy harvesters employing a mechanically amplified piezoelectric stack [246].

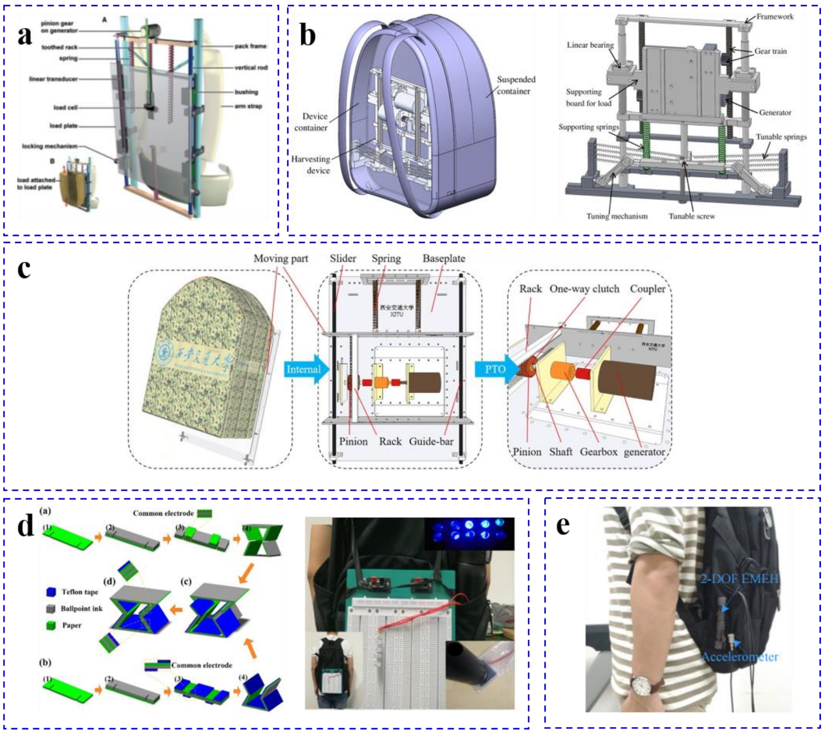

Fig. 9 Backpack-type self-powered devices that can harvest energy from centre of mass lifting and lowering motion during a person's walking or running: (a) Suspended-load backpack with a pack frame fixed to the body [64]; (b) backpack-type energy harvester and the frequency-tuneable backpack-based harvester prototype [242]; (c) overview and internal view of energy harvesting backpack, and details of the power takeoff [243]; (d) preparation mechanism of the fabricated X-shaped paper TENG (XP-TENG) which can be placed in a backpack to harvest energy [65]; (e) a two-degree-of-freedom electromagnetic generator vertically placed in a backpack [66].

Additional energy harvesters based on the centre of mass lifting and lowering include energy harvesters mounted on a backpack, as shown in Fig. 9(d) and (e). A novel X-shaped paper TENG (XP-TENG) proposed by Xia *et al*. [65] is shown in Fig. 9(d), with its preparation mechanism presented from (a) to (d). This XP-TENG can convert human motion energy into electrical energy when it is packaged and installed at the bottom of a backpack. The XP-TENG forms from a ballpoint ink layer that is painted by a brush pen and consists of Teflon tape that serves as the triboelectric pairs, and paper that is the supporting component. The generated electricity can illuminate 10 blue commercial light emitting diodes (LEDs). Another example proposed by Fan *et al*. [66] is shown in Fig. 9(e), where a nonlinear two-degree-of-freedom (2-DOF) electromagnetic generator is presented. It involves a 1-DOF electromagnetic generator that is levitated magnetically in a cylinder housing, thereby acquiring some advantages including tunable operating frequency, improved power output, and extended operating bandwidth. The device can achieve a maximum output power of 1.22 mW when it is installed vertically in a backpack that worn by a human on a treadmill moving with a constant speed of 9 km/h. Additional energy harvesters which can be mounted on a backpack and can be used to harvest centre of mass lifting/lowing motion energy can be found in Ref. [83, 247, 248].

In addition to backpack-type harvesters and energy harvesters mounted on a backpack, additional device types can be used to harvest energy associated with centre of mass lifting/lowering motion. One interesting example is a pendulum excited piezoelectric generator attached at the waistline [63], which involves a compliant piezoelectric unimorph that can convert kinetic energy from walking and jogging into electrical energy. It should be noted that the movement of the waist during a person's walking or running comprises several components, which include constant velocity translation, and the superimposed and complex curvilinear motion with components in both axes of constant motion and in the vertical direction. All these energy sources from human motion can be harvested by the proposed devices.

The swing motion of the arms, lower-limbs and legs during walking and running is another type of energy source that can be harvested. Most energy harvesters are designed for harvesting energy from a variety of rotational or swing motions, as shown in Fig. 10(a)-(j), They can be used to harvest energy from the swing motion of a person during walking or running when they are placed upon arms, lower-limbs, and legs. For example, Fig. 10(a) shows an electromagnetic generator with a hollow tube and two magnets fixed to both ends [73]. An inside magnetic stack, which is subjected to the nonlinear repulsive force of the end magnets, can move inside the tube freely with the system, thus generating a current in the coils that are wrapped around the outside of the tube. Fig. 10(b) shows a piezoelectric generator [74], where two piezoelectric cantilever beams can harvest energy directly from vibration along the tibial axis, and they can also generate electrical energy from their vibrations via magnetism when a ferromagnetic ball (located in a sleeve) is subjected to the excitation produced by the leg swing. Fig. 10(c) shows another piezoelectric generator, whose main components are a ridged cylinder and a piezoelectric bimorph. Under a certain excitation, the cylinder will slide freely on a shaft and the ridge will impact the tip of the bimorph, which will further vibrate at its resonant frequency after it separates with the ridge. Thus, electrical energy can be obtained via the direct piezoelectric effect. All these designs were demonstrated to be capable of harvesting energy from the swing motion of legs. Moreover, the rope-driven rotor based rotational energy harvester [67] shown in Fig. 10(d) and the cycloid-inspired wearable electromagnetic generator [68] shown in Fig. 10(e) can harvest energy from an arm swing. Fig. 10(f) shows a transverse mechanical impact driven frequency up-converted piezoelectric and electromagnetic hybrid energy harvester that can harvest energy from human-limb motion [71]. Fig. 10(g) shows a hip-mounted electromagnetic generator to harvest energy from the thigh swings during walking [72]. A liquid metal magnetohydrodynamics generator shown in Fig. 10(h) has shown its potential for energy harvesting when actuated by wrist swings during brisk walking [70]. A multi-coil topology harvester [77] presented in Fig. 10(i) and a nonlinear piezoelectric generator consisting of a piezoelectric cantilever beam that magnetically couples to a ferromagnetic ball and a crossbeam [78], as shown in Fig. 10(j), can harvest energy from foot swings when mounted on a shoe. These architectures can harvest energy from both human-based motion and other swing or rotation motion. Following this idea, additional swing or rotation-motivated energy harvesters can be used to harvest energy from human swing motions when mounted on the human body. The vibro-impact dielectric elastomer generator [113, 164, 197, 198] shown in Fig. 10(k) can generate energy when the inner ball impacts either dielectric elasomer membranes on both ends under the external excitation applied on the outer cylinder. However, specific energy harvesters have been designed for the human motion-based swing energy harvesting. One example can be found in Fig. 10(l), which shows a wearable electromagnetic generator with a flat-type magnets and coils. Energy can be generated in the swing motion of the arm during walking. Although this study focused on the manufacture and assessment of two types of conductive yarns which could be used as coils and could be easily integrated into outdoor garments, this concept provided a novel design for human swing motion-based energy harvesters.

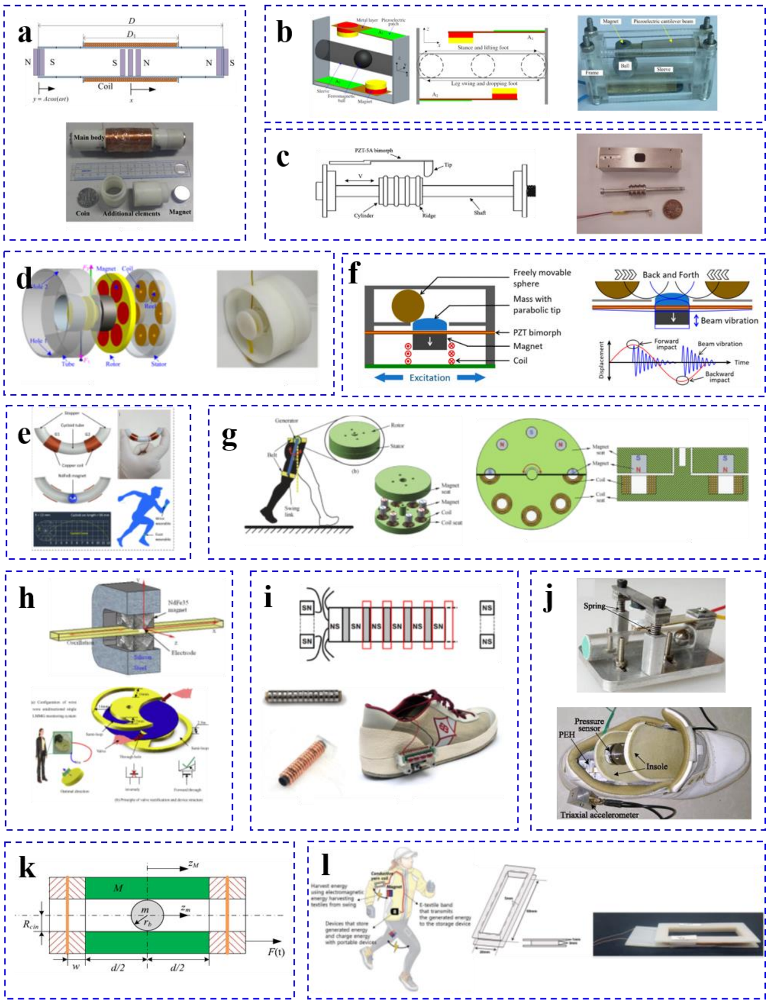

Fig. 10 Energy harvesters based on the swing motions during a person's walking or running. (a) Schematic/prototype of magnetic-spring based harvester [73]; (b) configuration of the piezoelectric generator [74]; (c) Schematic drawing/prototype of the impact-driven piezoelectric generator [76]; (d) rotational energy harvester based on a rope-driven rotor [67]; (e) schematic structure and the operation mechanism of the cycloid-shaped electromagnetic generator [68]; (f) transverse-impact driven frequency up-converted hybrid energy harvester and its operation mechanism [71]; (g) hip-mounted generator [72]; (h) a single unit liquid metal magnetohydrodynamics generator (LMMG) and the configuration of a unidirectional flow passage *in vivo* [70]; (i) harvester attached externally to a shoe with magnet stack [77]; (j) piezoelectric generator and its application when embedded into a shoe [78]; (k) schematic of the vibro-impact dielectric elastomer generator [113, 164, 197, 198]; (l) concept for integrated energy harvester design and an example of fabricated conductive yarn coil [69].

The rotations of the joints of a person during walking or running can also operate as the base excitation source for energy harvesters. The most common joint rotation motion includes the motion of the ankle, knee, elbow and shoulder. Some representative architectures can be found in Fig. 11 and Fig. 11(a) shows a biomechanical energy harvester reported in 2008 that generates electrical energy during human walking when it is mounted at the knee [15]. Using the orthopaedic knee brace of the harvester, the motion of the knee can drive a gear train through a one-way clutch. When the speeds are suitable, the motion associated with knee extension can be transmitted, which can be further converted into electrical energy via a DC brushless motor. It should be pointed out that this device assists muscles with negative work. Another approach is shown in Fig. 11(b), which is a piezoelectric knee-joint energy harvester that can harvest knee-joint motion energy during walking when installed on the leg [79]. In this device, an inner hub is fixed to the shank, while an outer ring is fixed to the thigh. They will rotate relatively to each other under the knee motions during walking. As a result, piezoelectric beams with secondary magnets are plucked by the primary magnets fixed on the outer ring through the magnetic force, thus producing electricity through the piezoelectric effect.

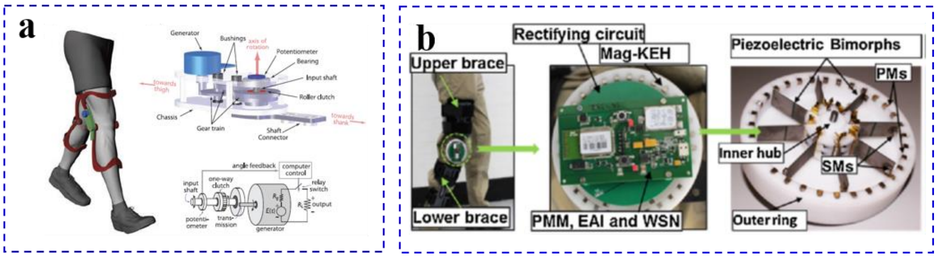

Fig. 11 Energy harvesters based on the rotation of joints during walking or running. (a) biomechanical energy harvester that can generate electricity during walking [15]; (b) wireless sensing system powered by the knee-joint piezoelectric generator [79].

Energy harvesters can be designed based on other walking or running-related motions, such as the impact/strike of the leg, the heel and the foot during walking or running. Energy harvesters mounted vertically upon the leg, the heel and the foot can be excited by continuous impacts during walking, which predominately originate from strikes between the shoe and the ground. For example, the device reported by Wang *et al.* [73] (Fig. 10(a)) can be vertically attached to a human's lower-limb, thereby producing electrical energy from strikes. Ylli *et al.* [77] proposed another shock-excited harvester based on the acceleration excitation source relating to the acceleration pulses upon heel-strike. Moreover, the biomechanical energy in human motion control processes, which is hard to classified into the three catergries, can be harvested through a hybridized electromagnetic-triboelectric nanogenerator proposed by Liu *et al* [249].

4.1.2. Additional macroscopic motion operating as an external base excitation. In addition to walking or running-related motions, macroscopic motion that does not relate to walking or running can also operate as a continuous base excitation source for energy harvesters. As previously introduced in Section 2, this type of motion includes the intended actions from the human body, such as human joint movement, arm/hand shaking, hammering by hand, and bending by arm. Considering that this type of motion is produced by a person intentionally, the relevant energy harvesters can be operated based on a person's subjective demand, making them useful in emergency situations when an urgent power supply is needed. Moreover, since the frequency and amplitude of the excitation depend on the person, the energy harvester design can be more diverse compared to the human walking or running-related energy harvesters. It should be noted that such energy harvesters are similar to those excited by human walking or running-related centre of mass lifting/lowering and swing motions since they are excited by external excitations. Their most important difference is the optimal frequency – for human walking or running-related energy harvesters, and they should be capable of operating effectively under the walking or running frequency, which is typically as low as less than 10 Hz; for the energy harvesters excited by the person's intentional motions, their optimal operating frequency can be higher. Hence, these two types of harvesters can be replaceable by tuning their optimal operating frequency.

In Fig. 12, examples of energy harvesters excited by human motions which are not related to walking or running are presented. Fig. 12(a) shows an AA-sized electromagnetic generator [89], which consists of a 3D-printed tube that is fully wrapped with coils and a cylindrical permanent magnet that is able to move freely inside the tube. The structure of this device is similar to the pre-introduced electromagnetic generator shown in Fig. 10(a). This device has can generate an average output power up to 63.9 mW with a power density of 9.42 mW/cm^3 when it is driven by a hand shaking at 5 Hz. Moreover, this generator can be installed on the ankle and excited by the human walking-induced swing motion with the frequency of 1 Hz, thus producing a power of 4.2 mW and a power density of 0.62 mW/cm^3. In Fig. 12(b), Salauddin *et al.* present a human-induced vibration driven hybrid electromagnetic-triboelectric generator [90] including a Halbach magnet array, nanostructured polytetrafluoroethylene (PTFE), Al nano-grass, and magnetic springs. This energy harvester can be installed on a smart mobile to produce an output power of 5.8 mW during handshaking. In addition, this harvester can also harvest energy from the centre of mass lifting/lowering motions when it is embedded in a mobile phone and then mounted in a backpack, thereby producing the slightly lower output powers of 2.6 mW and 3.4 mW from human walking and slow running, respectively. A fully-enclosed hybrid electromagnetic-triboelectric nanogenerator, which involves a magnetic ball moving freely inside a hollow circular tube [91], is shown in Fig. 12(c). This hybrid generator can effectively harvest energy from irregular low-frequency (< 5 Hz) natural human wrist motions (such as swing, waving, and shaking) via both a rolling electrostatic effect and electromagnetic induction. Moreover, the cycloid inspired wearable electromagnetic generator proposed by Maharjan *et al*. [68] (Fig. 10(e)) can harvest energy from the motion of hand-shaking and custom arm swing motions.

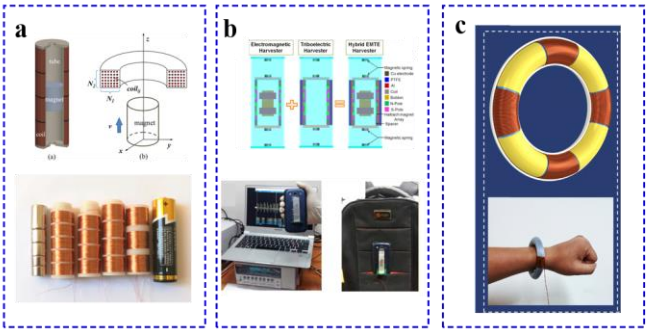

Fig. 12 Energy harvesters excited by the human motion not related to walking or running. (a) Structure and assembled prototypes of the human motion harvester [89]; (b) hybrid electromagnetic-triboelectric generator and its application in energy harvesting from handshaking, walking and slow running [90]; (c) schematic and photograph of a circular-shaped hybrid electromagnetic-triboelectric nanogenerator [91].

Moreover, as stated in Section 2, micro-physiological motion, such as the heartbeat, vibrations of the vascular wall and vocal cords, are a promising energy source that can operate as an external base excitation. While these harvesters can only produce a low-magnitude of energy, they have potential to power ultra-low-powered implantable medical devices (IMDs), which act as a significant role in the disease treatment and health monitoring of humans. To date, many micro-physiological movement-based energy harvesters have been proposed and studied, most of which are used to power implantable medical devices. Additional features such as structural size, durability and biocompatibility should be considered in the design of such energy harvesters. These energy harvesters are presented in Section 5.1.1, in which the implantable medical devices are also introduced.

4.2. Energy harvesters based on human body movement acting as a direct form of excitation for deformation (Category II)

Specific human body movements, such as the bending motion based on joint rotation [250], can directly stretch or deform an energy harvester, thus acting as a direct form of excitation by deformation. These energy harvesters have flexible and stretchable materials which can be attached to the human body and can be deformed and recovered following the movement of human body. According to our introduction on materials in Section 3, some piezoelectric, triboelectric and dielectric materials have the properties of stretchability, therefore, these energy harvesters are most based on the piezoelectric and electrostatic mechanisms.

In Fig. 13, examples of classical energy harvesters excited by the direct deformation and movement of human body are presented. Fig. 13(a) shows a wearable energy harvester with a polydimethylsiloxane (PDMS) elastomer film [94], a magnet and a flexible substrate of a nickel cantilever beam, which has a lead zirconate titanate (PZT) piezoelectric ceramic film bonded to its surface. The beam resonates under the coaction of the magnetized nickel cantilever and the fixed magnet when the PDMS substrate is stretched out and rebounds regularly, which will result from the continuous joint rotation when this device is installed on a human joint and both ends of the substrate are adhered to the two sides of the joint. Thus, a continuous releasing/pull-in motion of the joint will be converted into electrical energy. While the operating mechanism of this device is complex, in contrast Fig. 13(b)-(h) shows simple energy harvesters with the joint rotation-based bending motions working as a source of direct form of deformation. These devices are based on stretchable flexible smart electronics or smart materials, which can be easily fixed on the surfaces of joints such as the finger, the elbow and the knee, thereby producing electrical energy according to their own mechanical-electro conversion mechanisms when they are stretched following rotation of the joint. These smart electronics or smart materials include: 1) TENGs, such as an all-rubber-based thread-shaped TENG [95] (Fig. 13(b)), a stretchable triboelectric textile [96] (Fig. 13(c)), and a single waterproof and fabric-based multifunctional TENG [97] (Fig. 13(d)); 2) flexible piezoelectric generators [98-100] (Fig. 13(e-g)); 3) dielectric elastomer generators [101] (Fig. 13(h)). Moreover, Fig. 13(i) shows an interesting modified pant belt which can harvest energy from a human's breathing motion [102]. The belt consists of an array of polyvinylidene fluoride (PVDF) piezoelectric films and an energy harvesting circuit. When this belt is worn, the internal pressure of human body, which may change during a person's normal respiration, will be applied to the device. Kinetic energy will be converted into electrical energy through the integrated piezoelectric film. Fig. 13(j) shows a piezoelectric mechanical energy harvesting device that can be used in closed chest environments [103], which is composed of an array of microscopic piezoelectric ribbons that are integrated on a thin polyimide substrate. Thus, electrical energy can be produced when the device is deformed during the motion of the left ventricle. Although this device is relatively immature, it shows an application potential in biological environments to support implantable wireless electronic devices, such as the pacemaker, due to its biocompatibility.

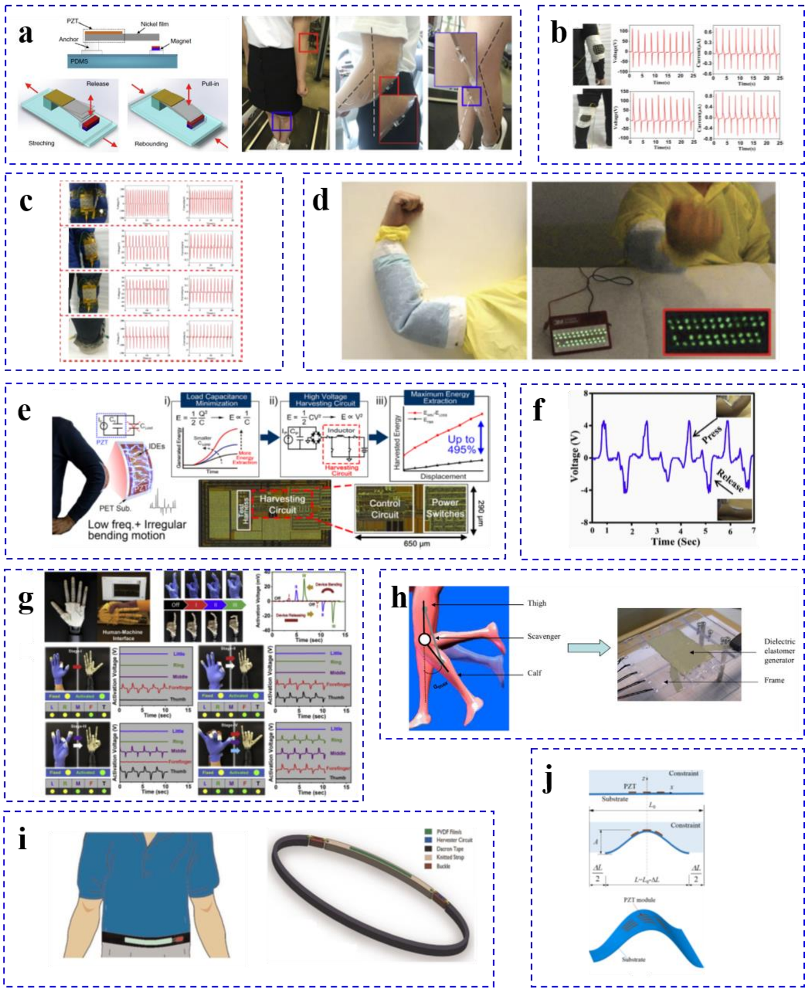

Fig. 13 Energy harvesters excited by the direct deformation and movement of the human body. (a) Structure, operation mechanism and applications of the wearable energy harvester with a magnet and a micromachined nickel cantilever [94]; (b) self-powered smart textile that can harvest energy when fixed on the elbow and the knee [95]; (c) stretchable triboelectric textile that can harvest energy when fixed under the arm, at the elbow joint, at the knee joint and under the foot [96]; (d) waterproof and fabric-based multifunctional TENG harvesting human-motion energy through a garment [97]; (e) flexible piezoelectric generator used in wearable application [98]; its driving mechanism (i - iii) and chip micrograph are presented; (f) voltage response of a flexible and self-powered piezoelectric nanogenerator (PENG) due to arm bending [99]; (g) intelligent human-robotic interface based on the interaction between human and 3D printing robotic hands [100]; (h) dielectric human kinetic energy harvester [101]; (i) pants belt with an integrated energy harvester that can generate energy from abdominal passive motion [102]; (j) piezoelectric generator for left ventricle motion in closed chest environment [103].

4.3. Energy harvesters based on slowly varying pressures or small displacement motion (Category III)

The final type of human motion-based energy source results from slowly varying pressures such as the finger touching, foot standing, and blood pressure. It should be noted that in most cases the energy is harvested through the small displacement motions that result from a slowly varying pressure, but these displacement motions are relatively small (μm level), which do not act as continuous excitations. In these cases, the flexible and stretchable materials are recommended.

In Fig. 14, examples of energy harvesters based on the slowly varying pressure or small displacement motion are introduced. Fig. 14(a) shows a dielectric and dielectric materials-based TENG (DD-TENG) [104], which can continuously generate energy through the continuous contraction and separation between the dielectric materials. The DD-TENG can be further developed into a pouch-type DD-TENG device through a simple sealing and pinning process [104]. When this device is touched by the fingers and the hand, it can harvest mechanical energy. Moreover, it can be used to harvest the energy of human motion during walking and running by simply installing onto a luggage or bag and hanging it on the shoulders, thus acting as a wearable device. Although the main purpose of the design is to reduce the effect of relative humidity on the output energy of a TENG, it provides a commonly-used pouch-type structure with a TENG inside to harvest energy from slowly varying pressure of a person. Similar TENG-based devices, which are capable of harvesting slowly varying pressure-induced energy from finger touching and finger tapping can be found in Fig. 14(b-d), where a crepe cellulose paper and nitrocellulose membrane-based TENG [105], a human body constituted TENG [106], a stretchable and shape-adaptable liquid-based single-electrode TENG [108] (this device can also harvest energy from different types of body motions such as the bending/releasing of the knee, elbow and wrist when it is worn in various parts of human body) are presented. In addition to TENGs, piezoelectric generators using stretchable and flexible materials can utilize a similar pattern. For example, Fig. 14(e) shows a fabricated piezoelectric nanogenerator comprising of a NiO@SiO_2/PVDF nanocomposite [107], which can produce energy through the piezoelectric effect under finger pressing, toe pressure, heel pressure and wrist bending. A ZnO nanorod patterned textile based sandwich structured-piezoelectric nanogenerator [119] is shown in Fig. 14(f) which can generate energy from palm pressing and foot stepping. The piezoelectric generator reported by Mondal *et al*. [99] can be used to harvest energy from finger tapping and toe pressing. The above-mentioned slowly varying pressure-based TENGs and piezoelectric generators have simple structures, and their related work was focused on the material properties that can enhance the energy harvesting performance. Moreover, Fig. 14(g) shows the reported bio-based TENGs using human fingernails [120], which serve as highly triboelectric materials. Energy harvesting gloves are further designed based on the TENGs and Teflon pasted on a copper foil. When the fingers move back and forth, they are in contact with the Teflon layer and form five single-electrode TENGs, thereby generating electrical energy. Fig. 14(h) shows an interesting human skin and polydimethylsiloxane (PDMS) interaction based TENG [121], in which electrical energy is produced by continuous contact-separation processes between PDMS and the human skin when it is positioned over the human wrist. In Fig. 14(i), an arterial blood pressure-based piezoelectric generator is presented [25]. The proposed harvester is a piezoelectric bimorph with a circular and curved shape that fits into the blood vessel and undergoes bending motion because of bold pressure variation, thereby generating electrical energy. This harvester shows significant application potential since it provides a novel solution to power the implantable micro-sensors in the human brain.

The pressure produced during walking can be used to generate electrical energy, thereby leading to a range of interesting device designs – the sole/insole-mounted energy harvesters, which can harvest energy from the pressure of the foot. Some typical architectures can be found in Fig. 15 and Fig. 15(a) shows an in-shoe magnetic harvester that can convert human foot strike energy into electricity [109]. Footstep motion can be transmitted to the upper moving board and can then be amplified by two sets of trapezoidal sliders; the linear footstep motion is further converted to a rotational motion through a gear train; the rotational motion then drives the generator to produce electrical energy; the harvester involves horizontal and vertical springs that can provide a restoring force. Xie *et al*. pointed out that the allowed vertical displacement of the shoe heel is extremely small (approx. 1 cm [251]), and the frequency of the foot strike is relatively low, which should be considered in the design of displacement-based energy harvesters. Fig. 15(b)-(e) shows some TENG devices [110, 114, 117, 118], which can be attached into an insole for harvesting energy from the walking-based press, or the friction between the foot and the shoe, or that between the sole and the floor. It can be found that the structures of many TENGs are simple, and they can be easily attached into shoes without changing their original shapes and hindering human footsteps during walking. Hence, TENGs have potential advantages for sole/insole-mounted energy harvesting documents. Moreover, Fig. 15(f) shows a pressure-type generator which can harvest human motion energy during stepping. This device consists of a base, a pressure device, a transmission structure, and a small brushless DC motor. The detailed operating mechanism can be seen in Ref. [[115]]. Inspired by this device, a similar contact-type dielectric elastomer generator proposed by Zhang *et al*. [112] can be used to harvest pressure energy when it is assembled into a shoe. Electrical energy can be generated through the deformation-recovery processes under intermittent pressures from the foot.

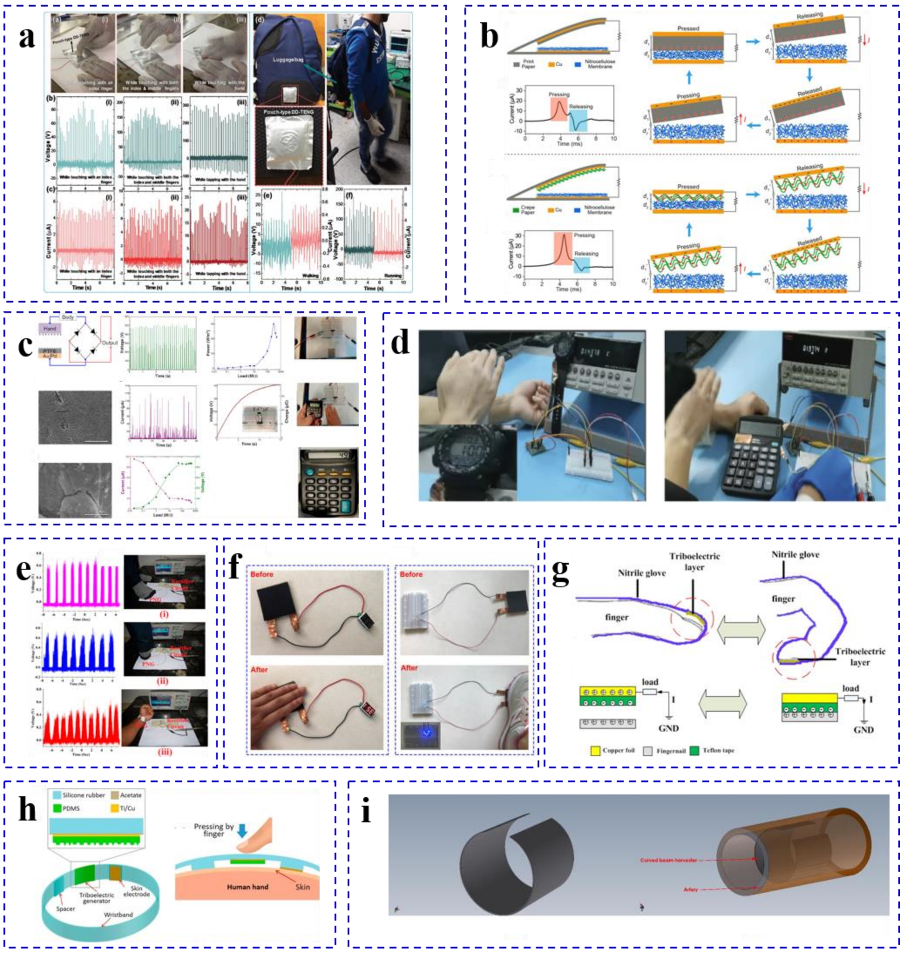

Fig. 14 Energy harvesters excited by the slowly varying pressure or small displacement motion. (a) the photographic a), output voltage b) and output current c) of a pouch-type dielectric and dielectric materials-based TENG device under various human activities while touching with an index finger (i), both the index and middle fingers (ii) and the hand (iii), respectively; relevant figures when it is located on a luggage/laptop is plotted in d-f) [104]; (b) working principle of the paper-based TENG[105]; (c) human body constituted TENG which can generate electricity when the right hand is used to pat the polytetrafluoroethylene (PTFE) film and the left hand is connected to a rectifier [106]; (d) liquid-based single-electrode TENG to power portable electronic products

when it is tapped by hand [108]; (e) piezoelectric power generation by piezoelectric nanogenerator due to toe pressure, heel pressure and wrist bending [107]; (f) ZnO nanorods patterned textile based piezoelectric nanogenerator which can power a miniature display screen by palm pressing and light several light emitting diodes (LEDs) by foot stepping [119]; (g) operation mechanism of fingernail single electrode mode TENG glove under the states of finger extending and finger bending [120]; (h) wrist-band coupled TEG and the contact and separation actions using finger-tip [121]; (i) curved beam harvester inside the artery [25].

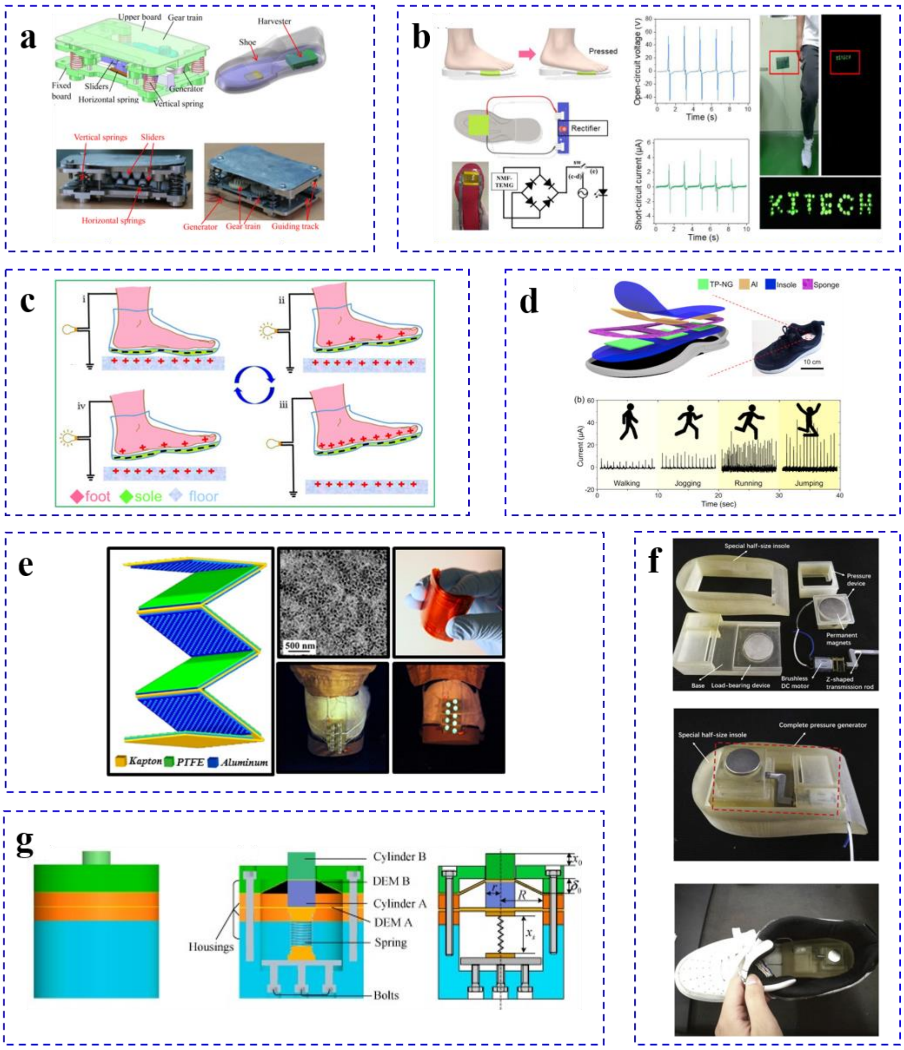

Fig. 15 Sole/insole-mounted energy harvesters related to the human walking or running. (a) model of the in-show energy harvester and schematic when assembled in the heel area of a shoe [109]; (b) operation mechanism and circuit configuration for an energy-harvesting insole which can power 57 light emitting diodes (LEDs) under walking [117]; (c) operation of the TENG when walking [118]; (d) hybrid triboelectric-piezoelectric nanogenerators (TP-NGs) embedded in a shoe insole, where the TP-NGs are

located at the forefoot, arch, and heel positions [110]; (e) flexible multi-layered TENG with five layers of units and its application in lighting the commercial LED bulbs during walking [114]; (f) pressure-type generator and its application when installed into a shoe [115]; (g) contact-type dielectric elastomer generator which can generate electricity when installed into a shoe [112].

4.4. Summary of human motion-based energy harvesters

The development of human motion-based energy harvesters can be designed to integrate self-powered and self-sensing devices with a variety of mechanisms, structures, performance and application prospects. The state-of-the-art advances in human motion-based energy harvesters have been comprehensively reviewed in this section.

From the perspective of the human motion sources, human motion-based energy harvesters can harvest energy from a range of human motion via different energy conversion mechanisms and materials (Section 3). For energy harvesters based on the human motion acting as an external base excitation (Category I), they can harvest energy passively or actively. In general, walking or running-related motion is suitable for passive energy harvesters, in which frequency up-conversion strategies should be taken into account due to the low-frequency of the relevant motions including the centre of mass lifting/lowing, swing motions, joint rotation and other walking or running-related motion. In addition to walking or running, additional macroscopic motions are suitable for active energy harvesters and can operate based on a person's subjective demand, making them highly useful in emergency situations when a power supply is urgently needed. Continuous excitations can also involve some micro-physiological movements such as the heartbeat, the pulse, the vibration of the vascular wall and the vocal cords, which is a promising energy source for human motion-based energy harvesters to power ultra-low-powered implantable devices.

For energy harvesters based on the human body movement operating as a direct form of excitation for deformation (Category II), flexible and stretchable materials are necessary to allow them to be attached to the human body and be deformed/recovered following the movement of the human body. In addition, for energy harvesters based on a slowly varying pressure or small displacement motion (Category III), flexible and stretchable materials are also recommended. Among these energy harvesters, promising sole/insole-mounted energy harvesters can be designed to harvest energy from the pressure of the foot.

Moreover, the energy conversion mechanisms for human motion-based energy harvesters, along with their energy sources from human motion, energy harvesting performance and applications, are summarized in Table 7, which provide an overall understanding of the progress of human motion-based energy harvesters. It can be found that as we analyzed, electromagnetic generators are suitable to harvest energy from Category I and III sources, but they are less suitable to harvest human motion energy of Category II due to the limited flexibility and stretchability of electromagnetic generators. In contrast, piezoelectric generators, dielectric elastomer generators and TENGs can harvest all categories of human motion energies, indicating their feasibility in their design for a range of human motions. Hence, for a given energy source from human motion, the appropriate energy conversion mechanisms can be chosen accordingly.

The power and power density of human motion-based energy harvesters reported in literature are presented in Table 7. It is noted that the same method to calculate the output power is not used; where some paper report the average power, while some reported the peak power. Hence, it is difficult to fully evaluate and compare the energy performances of the proposed harvesters. Nevertheless, we can still learn the levels of output power and power density. It is also noted that for most harvesters, the power density was calculated from the output power per unit volume (W/m^3), while for some harvesters, especially the TENGs based systems, which produce streatchable and deformable thin harvesters, their power densities were calculated as output power per unit area (W/m^2). Moreover, there are limited reports on the energy conversion efficiency of the harvester, which are typically reletavely low, indicating that the output power of the human motion-based energy harvesters can be further improved by enhancing the energy conversion efficiency of the harvesters with repsect to the harvesitng structure and active material employed. With regard to the application areas, it can be seen that there are limited examples where the pratical applications of the human motion-based energy harvesters in powering low-powered electronics or provding self sensing functionality, while most work to date simply introduces the potential applications of the harvesters, which have not been realized physically. Hence, more effort is needed to be made to make the harvesters practicable in real operation environmenst.

Table 7 Energy conversion mechanism, human motion energy source, energy harvesting performance and application case of human motion-based energy harvesters in the literature.

Energy conversion mechanism	Applicable human motion source	Performance		Application case	Ref.	Year
		Power/power density	Efficiency			
Electromagnetic	Category I	7.4 W	30%-40%	Unspecified	L. C. Rome et al [64]	2005
		0.3 -2.46 mW	-	Unspecified	C. R. Saha et al. [83]	2008

5 W	< 63%	Unspecified	J. M. Donelan et al. [15]	2008
3.61 μW	> 45%	Unspecified	D. Jia et al. [70]	2009
1.44 mW/~0.03-0.5 $mWcm^{-3}$	-	Unspecified	B. J. Bowers et al [84]	2009
0.35-0.5 mW	-	Unspecified	S. E. Jo et al [252]	2012
4.1 μW	-	Unspecified	S. Ju et al [88]	2013
44.1-99.3 μW	21%	Unspecified	D. Dai et al [72]	2014
92 μW	10%	Powering sensorized total human knee prosthesis	V. Luciano et al [253]	2014
71-342 μW	-	Unspecified	D. F. Berdy et al [247]	2015
0.84 mW/40 μWcm^{-3} (swing harvester), 4.13 mW/86 μWcm^{-3} (shock harvester)	-	Unspecified	K. Ylli et al [77]	2015
0.32 mW (average), 1.89 mW (maximum)	30.98%	Unspecified	J. Yeo et al [254]	2015
0.833 mW	-	Powering a non-contact temperature measurement system	D. Alghisi et al [255]	2015
4.52-42.7 mW/0.19-0.91 $mWcm^{-3}$	-	Unspecified	K. Ylli et al [75]	2016
-	-	-	J. Jun et al [256]	2016
0.3-0.47 mW	-	Unspecified	J. Seo et al [257]	2016
203 μW (hand shaking), 32 μW (walking) and 78 μW (running)/52 μWcm^{-3}	-	Unspecified	M A Halim et al [258]	2016
4.95 mW (worn at the arm during a run), 6.57 mW (hand shaking)/730 μWcm^{-3}	-	Unspecified	M Geisler et al [259]	2017
1.1 mW (walking), 2.28 mW (running)	-	Unspecified	S. Wu et al [19]	2017
Up to 6.01 mW (vertically attached), up to 10.66 mW (transversely attached)	-	Unspecified	W Wang et al [73]	2017
4.8 mW/228.6 μWcm^{-3}	-	Charging a NiMH battery and supply an acceleration and temperature wireless sensor node	M Geisler et al [260]	2017
-	-	Unspecified	H. Lee et al [69]	2018
63.9 mW/9.42 $mWcm^{-3}$ (hand shaking), 4.2 mW/0.62 $mWcm^{-3}$ (worn on ankle during walking)	-	Unspecified	X Zhao et al [89]	2018
20 mW/0.82 $mWcm^{-3}$	-	Unspecified	P Gui et al [126]	2018
2 mW	42%	Unspecified	P Chen et al [261]	2018
10.4 mW	-	Unspecified	H Liu et al [262]	2018
1.09-1.22 mW	-	Powering a hygrothermograph	K Fan et al [66]	2019
8.8 mW/0.73 $mWcm^{-3}$	7.7%	Powering a sports stopwatch	P. Maharjan et al [68]	2019
1-440 μW	-	Powering a LoRaWAN sensor node	V. Nico et al [127]	2019
Without ferrofluid: 10.15 mW (walking) and32.53 mW (running); with ferrofluid: 17.72 mW (walking) and 54.61 mW (running)/1.45 $mWcm^{-3}$	-	Unspecified	C Li. et al [263]	2019
0.074-0.090 mW/0.95-1.16 μW/g	-	Unspecified	L. C. Zhao et al [264]	2019
6.11 W	-	Unspecified	L. Huang et al [61]	2020

		0.45 mW/20.9 μWcm^{-3} (human jogging), 0.65 mW/30.2 μWcm^{-3} (arm swing)	-	Unspecified	K. Fan et al. [67]	2020
		3.48-4.04 W	-	Unspecified	Z. Hou et al [243]	2021
		~0.3 W/3 W/kg	-	Unspecified	M Liu et al [62]	2021
	Category II	-		-	-	-
	Category III	0.81-1.39 W/9.7 mWcm^{-3}	~57%	Unspecified	L. Xie et al [109]	2015
		97 mW/1.17 mWcm^{-3}	-	Unspecified	F. Deng et al [115]	2019
		32.2 mW (peak value) and 7.7 mW (RMS power)/72.2 μWcm^{-3}	-	Powering a hygrothermograph and 70 LEDs	Y. Zhang et al [265]	2020
Piezoelectric	Category I	-	-	Unspecified	L. Mateu et al [116]	2005
		~0.4 mW	-	Unspecified	J Feenstra et al [246]	2008
		600 μW/10 μWcm^{-3}	25%	Unspecified	M. Renaud et al [266]	2008
		Up to 2.1 mW/3.8-13 μWcm^{-3}	8%	Unspecified	P.Pillatsch et al [81]	2012
		8 μW (hybrid harvester), 3 μW (bistable harvester)	-	Powering pacemakers	M. A. Karami et al [92]	2012
		51 μW	-	Unspecified	S. Wei et al [76]	2013
		43 μW/23.2 μWcm^{-3}	-	Unspecified	P. Pillatsch et al [267]	2014
		3.7 μW/7.4 μWcm^{-3}	-	Unspecified	M. Wahbah et al [268]	2014
		0.29 mW	1.71%	Unspecified	R. Shukla et al [63]	2015
		Up to 16 mW	-	Powering a custom wireless temperature sensor module	D. Alghisi et al [269]	2015
		3.21 Mw, 18.73 μW and 23.2 μW for linear, monostable and bistable harvesters	-	Unspecified	J. Cao et al [270]	2015
		52.8 mWm^{-2}	-	Self sensing for human body biological signals such as coughing action and arterial pulses	N. Wu et al [271]	2015
		Over 100 μW	-	Unspecified	P. Pillatsch et al [272]	2016
		-	-	Unspecified	K. Fan et al [74]	2017
		0.03-0.35 mW	-	Unspecified	K. Fan et al [78]	2017
		0.175 mW/7.6 μWcm^{-3}	-	Unspecified	M. A. Halim et al [80]	2017
		~1.9-~4.5 mW	80%	Powering a wireless sensor node	Y. Kuang et al [79]	2017
		30.55 μW	-	Unspecified	W. Wang et al [273]	2017
		-	-	Self sensing for human-activity-related multimodal stimuli such as pressure, strain, sound, temperature and light illumination	Y. Chen et al [274]	2017
		0.136-0.457 μW	-	Unspecified	K. Li et al [94]	2018
		-	-	Self sensing for human activity recognition	S. Khalifa et al [275]	2018
		Up to 2.779 mW	-	Unspecified	I. Izadgoshasb et al [276]	2018
		17.47 μW	-	Unspecified	W. Wang et al [277]	2018
		0.96-86.12 μW		Unspecified	I. Izadgoshasb et al [278]	2019
		1.6 mW	-	Unspecified	F. Gao et al [279]	2019
		402 mWm^{-2}	-	Self sensing for biomechanical strain	I. Choudhry et al [280]	2020
		15.41 mW/1049.01 μWcm^{-3}		Powering low-powered electronics such as watch and screen	B. Wang et al [281]	2021
	Category II	1.5 mW	-	Unspecified	H. Abdi et al [102]	2014
		0.4-0.6 μW	-	Self sensing for human motion such as wrist bending and torsion	Y. K. Fuh et al [250]	2015

		31.9 μW	-	Interface as a machine controller	G. D. Pasquale et al [282]	2015
		0.03-0.073 μW	-	Unspecified	Y. Zhang et al [103]	2016
		Of the order of 0.1 μW on the hip and ankle and 1 μW on the knee	-	-	Y. Cha et al [283]	2017
		685 Wm^{-3}	13.86%	Powering low-powered electronics, and self sensing for pressue and form a health-data glove for healthcare monitoring	B. Dutta et al [107]	2018
		-	-	Unspecified	M. B. Khan et al [98]	2019
		4.24 mW	-	Powering low-powered electronics, and self-sensing for bending and vibration	S. Mondal et al [99]	2020
		2 pW	-	Be a drive unit of the synchronous human-robot interface	P. K. Yang et al [100]	2020
		402 mWm^{-2}	-	Self sensing for biomechanical strain	I. Choudhry et al [280]	2020
	Category III	-	-	Unspecified	L. Mateu et al [116]	2005
		18.6 mW (slow walking) and 27.5 mW (fast walking)	-	Unspecified	L. Xie et al [284]	2014
		5.75-8.92 mW	-	Form a self-powered pedometer	H. Kalantarian et al [285]	2016
		0.03-0.35 mW	-	Unspecified	K. Fan et al [78]	2017
		11.7 μW (Carotid artery) and 203.4 μW (Aorta)	-	Powering embedded micro sensors in human brain	A. Nanda et al [25]	2017
		685 Wm^{-3}	13.86%	Self sensing for low level pressure and form a hand-data glove for healthcare monitoring	B. Dutta et al [107]	2018
		-	-	Unspecified	W. Cao et al [286]	2018
		-	-	Unspecified	Z. He et al [287]	2018
		1.136 W	-	Unspecified	S. M. Hossain et al [288]	2018
		-	-	Unspecified	Z. Zhang et al [119]	2019
		12.8 mW	-	Unspecified	F. Qian et al [289]	2019
		4.24 mW	-	Powering low-powered electronics, and self-sensing for pressing	S. Mondal et al [99]	2020
		402 mWm^{-2}	-	Self sensing for biomechanical strain	I. Choudhry et al [280]	2020
Electrostatic: dielectric	Category I	2.1 $mWcm^{-3}$	-	Unspecified	C. Jean-Mistral et al [101]	2012
	Category II	-	-	Reducing knee joint torque deviation	H. Lai et al [290]	2019
	Category III	120 mW	-	Unspecified	V. Goudar et al [111]	2014
		22.94 mW		Unspecified	C. Zhang et al [112]	2020
Electrostatic: triboelectric	Category I	30.7 Wm^{-2}	~10.62%	Unspecified	W. Yang et al [248]	2013
		60 μW	-	Unspecified	Y. Lu et al [291]	2014
		0.5 mW	-	Unspecified	J. Chen et al [292]	2016
		4.88-13.5 mW/542.22 μWcm^{-2}	-	Unspecified	K. Xia et al [65]	2018
		-	-	Self sensing for physical activity recognition	H. Huang et al [293]	2018
		5.28 μW	-	Unspecified	H. J. Hwang et al [294]	2019
		0.377 μJ from each cardiac motion cycle/110 mWm^{-2}	-	Powering cardiac pacemaker	H. Ouyang et al [295]	2019
	Category II	0.892 $mWcm^{-2}$	-	Driving portable electronics such as	Z. Tian et al [296]	2017

				competition timer, digital clock and electronic calculator		
		0.88 Wm^{-3}	20%	Real-time human-interactive sensing	K. Dong et al [93]	2018
		1 mW	-	Powering a calculator	X. Hou et al [96]	2018
		16 mWm^{-3}	-	Self-powered human-system interfaces	Y. C. Lai et al [97]	2019
		163.3 μW	-	Unspecified	J. Zhu et al [95]	2019
		2.0 Wm^{-2}	-	Driving portable electronic products such as calculator, and self sensing for motion counter	L. Wang et al [108]	2021
	Category III	9.8 $mWcm^{-2}$ and 10.24 $mWcm^{-3}$	-	Unspecified	P. Bai et al [114]	2013
		6.7 Wm^{-2}	-	Unspecified	S. Wang et al [221]	2014
		7.33 mW/0.626 Wm^{-2}	-	Unspecified	Y. Kang et al [297]	2015
		370.8 μWcm^{-2}	-	Powering low-powered electronics such as pedometer	M. S. U. Rasel ea al [121]	2017
		4.8113 mW(clapping motion) and 7.5248 μW(slow walking)/46.6 μWcm^{-2}	24.94%	Unspecified	X. Li et al [298]	2017
		0.88 Wm^{-3}	20%	Real-time human-interactive sensing	K. Dong et al [93]	2018
		30 Wm^{-2}	-	Motion sensor and signal sender	R. Zhang et al [106]	2018
		72 μW	-	Driving a watch	H. Zhang et al [41]	2018
		44.6 mWm^{-2}		Powereing commercial electronic devices such as calculator and sigtal thermometer, and monitoring human motions such as walking, running and jumping	Z. Zhang et al [299]	
		18.15-25.35 Wm^{-2}	-	Unspecified	A. R. Mule et al [104]	2019
		16.1 Wm^{-2}	-	Self sensing for press and human-machine interfacing	S. Chen et al [105]	2019
		1.8 mW/2 Wm^{-2}	-	Self sensing for temperature and press	L. Wang et al [300]	2019
		36 μW	-	Self-powered physiological monitor	X. Cui et al [118]	2019
		6.2 μW	-	Unspecified	Khushboo et al [301]	2019
		48.8 μW/122 mWm^{-2}	-	Self sensing for distinguishing different people	J. Fu et al [120]	2020
		0.9 μWcm^{-2}	-	Unspecified	H. J. Oh et al [117]	2020
		2.0 Wm^{-2}	-	Driving portable electronic products such as calculator, and self sensing for motion counter	L. Wang et al [108]	2021
		11.7 μW/8.87 μWcm^{-3}	-	Self sensing for weight and pressure	J. Fu et al [302]	2021
Hybrid	Category I	(EM/TE) 5.8 mW (handshaking), 2.6 mW (waking) and 3.4 mW (slow running)/up to 344 Wm^{-3}	-	Charging low-powered electronics such as humidity/temperature meter	M. Salauddin et al [90]	2018

	(EM/TE) 8.8 mW	7.7%	Driving low-powered electronics such as sports stopwatch, wristwatch, digital humidity temperature meter	P. Maharjan et al [68]	2019
	(EM/PE) 93 μW by PE transducer) and 61 μW by EM transducer)/8 μWcm^{-3}	-	Unspecified	M. A. Halim et al [71]	2019
	(EM/TE) 3.25 Wm^{-2} by TENG and 79.9 Wm^{-2} by EM generator	-	Unspecified	C. Hou et al [303]	2019
	(PE/TE) 2.4 W/13.94-22.004 μWcm^{-3}	-	Demonstrative rehabilitation, human-machine interfacing and sports monitoring	S. Gao et al [304]	2021
	(EM/TE) 0.43 W (average) and 0.55 W (peak value)/1.26 $mWcm^{-3}$	-	Powering low-powered electronics such as pedometer, Bluetooth module, and recodering motion	L. Liu et al [249]	2021
Category II	-	-	-	-	-
Category III	(PE/TE) 52-127 μW		Powering a wireless pressure sensor network and self-detection of human body motion	D. W. Lee et al [110]	2020

5. Application status and challenges

With the help of the energy harvesters introduced in Section 4, human motion-based self-powered and self-sensing devices can be further developed for different applications. In this section, the state-of-the-art advances in human motion-based self-powered and self-sensing devices are comprehensively reviewed from the perspective of the end applications, and challenges are further discussed.

5.1. Human motion-based self-powered devices

The proposed human motion-based energy harvesters can be applied in a range of applications as self-powered devices. Their suitability is determined by the structure, size, output power, mechanical flexibility, and biocompatibility. It is noted that self-powered devices have their own power or propelling force, according to *Merriam-Webster* dictionary [46], hence, the combination and integration of conventional electronics and energy harvesting technologies can lead to a generalized self-powered device. It can be seen from Table 7~~Table 7~~ that some of the proposed devices have been specifically designed to power themselves and used in specific applications. However, some devices reported in the literature have only reported their energy harvesting performance, and in these cases the devices have the potential to power other electronic

Formatted: 06 C Heading, Font: +Body (Calibri), 11 pt, Font color: Auto devices. In this section, the applications of human motion-based self-powered devices, including the harvesters having potential to form a self-powered device, are introduced.

5.1.1. Powering implantable medical devices. Implantable medical devices (IMDs) usually refer to microsystems which are placed inside the body of a patient who suffers from severe or chronic diseases such as diabetes, colon cancer and heart disease [17]. Common implantable medical devices include pacemakers, cochlear implants, visual prostheses, neural recording microsystems, deep brain stimulators, implantable cardiac defibrillators, coronary stents, hip implants, interocular lenses, and implantable insulin pumps. Some implantable devices, such as pacemakers, require an external power supply, and one of the most challenging issues is to power these devices durably, stably and safely. At present, most of implantable devices are powered by chemical batteries and when the batteries are exhausted they need to be replaced or taken out, which brings additional pain and danger for the patients [305]. Hence, researchers have attempted to solve this issue by improving the power supply system for these devices. One possible solution is to power implantable devices by extracting energy from their operation environments, in particular from human body motion.

To design reliable human motion-based micro energy harvesters (MEHs) for biomedical applications, a number of important factors need to be taken into account. For example, most implantable devices are directly used inside a human body, thus, micro energy harvesters must be anti-infection. They should have considerable stability and durability; their size should also be small (in general under 1 cm^3 in volume [306]) to avoid any unnecessary impact on human body. Micro energy harvesters should have good biocompatibility to integrate with currently available in vivo implantable medical devices. Moreover, when designing a micro energy harvester, it is of importance to comprehensively explore the characteristics of the energy sources to be harvested, such as the frequency and amplitude of the expected motion. In addition, implantable medical devices should also be considered in the design of the energy harvesters. For implantable devices with a need for long-term operation, such as the pacemakers, the energy harvesters should exhibit high stability and a long lifespan. However, for applications related to short-term transient electronics for implantable medical devices, which are integrated with living tissue and used for diagnostic and/or therapeutic purposes during certain physiological processes [307, 308], the energy harvester should be degradable and resorbable in the body; as a result there is no need for a medical operation to remove the device and adverse long-term effects are avoided. Hence, biodegradable energy harvesters fabricated with abosrbale organic and inorganic materials have been proposed [309].

To date, many human motion-based energy harvesters have been proposed to power implantable medical devices. Implantable cardiac pacemakers are good examples, which have unique challenges in terms of a high level of safety and reliability, as shown in Fig. 16. The required power of modern pacemakers has been significantly reduced to be less than one microwatt in recent years [305, 310]. Since batteries take up approximately 2/3 of the size of a typical pacemaker, utilizing an energy harvester to power a pacemaker can not only expand the lifetime of the pacemaker but also makes it possible to significantly reduce its size. To achieve this goal, Karami *et al*. designed mono-stable and bi-stable energy harvesters in 2012, using vibrations from heartbeats, which were converted into electrical energy that can continuously recharge the batteries of pacemakers [92]. The results showed that a bistable energy harvester can produce a satisfactory power level (more than 3 μw) regardless of the heart rate, which ranges from 7 beats per minute to 700 beats per minute. Recently, a self-powered pacemaker charged by the heart's own movement has been proposed by researchers from Stanford University [311]. The pacemaker is able to harvest the energy associated with the relative motion between a magnet and a conductor due to the contraction of the heart muscle via electromagnetic induction. The power generated by this energy harvester can be as high as 160 μw, which can be stored to power the pacemaker when the heart has disease. Ouyang *et al*. proposed an implanted symbiotic pacemaker based on an implantable triboelectric that is capable of harvesting energy from cardiac motion [295]. This pacemaker successfully corrected sinus arrhythmia and prevented deterioration with an open circuit voltage up to 65. 2 V and an energy of 0.495 μJ per cardiac motion cycle, which is higher than the required endocardial pacing threshold energy (0.377 μJ). Moreover, the arterial blood pressure-based piezoelectric generator [25] shown in Fig. 14(i) is designed to power embedded micro sensors in the human brain to measure neural and physiological data. When the harvester is implanted into the carotid artery, the harvested power for slower pulse rates approaches 30 μw. Additional *in vivo* examples of energy harvesting from animals can be found in the review paper of Dagdeviren *et al*. [58], which provides novel concepts that have potential for applications in the human body in the near future.

It can be found that in designing this type of energy harvester, their light weight, small size, anti-infection property, stability, durability, biocompatibility and absorbability should be taken into account [16], and the harvester must not impede the normal operation of internal organs. In solving these issues, self-powered devices have significant potential to power implantable biomedical devices, and benefit our health. Additional examples about the implantable energy harvesters can be found in the review of Jiang *et al*. [312], where harvesters which can harvest energy from not only human motion energy (organ motion such as heartbeat and respiration), but also chemical energy from the redox reaction of glucose.

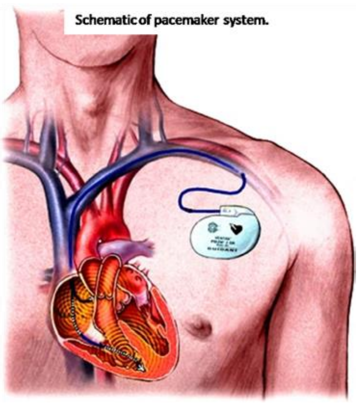

Fig. 16 Self-powered devices for implantable biomedical devices [313].

5.1.2. Powering wearable devices. Wearable devices represent electronic components and software controlled products that can be incorporated into clothing or can be worn on the body like accessories [314]. Today, a variety of wearable devices have been developed, which include electronic skin (e-skin) [315-318], biomedical monitors [95, 108], bionic-robots [319-321], human-interactive interfaces [93, 99, 322-324], military [325, 326], and consumer electronics (smart glasses [327-330], smartwatches [331-336]). Wearable devices have shown their capabilities in providing human health-related information and human-machine interactions. Therefore, wearable devices are becoming increasingly more popular as research areas in both academia and industry since they are considered to have an ability to enable a paradigm shift in the digital world.

To date, most wearable devices are powered by batteries. However, with the developments of modern and future wearable devices, they raise new requirements such as a need to be lightweight, conformal and seamless, which cannot be satisfied by the current rigid and bulky batteries, especially in the applications such as outdoor activities, harsh industrial scenarios and service personnel (ambulance, rescue and military). Moreover, the chemical used in existing batteries also leads to environmental pollution problems. Hence, power generation technologies that harvest energy from green and sustainable energy sources have a potential in powering wearable devices. In the review paper by Gao *et al.* [18], the state of the art in wearable power generation methodologies, including electromagnetic wave energy harvesting, photovoltaic energy conversion, thermoelectric energy generation, fuel cell chemical energy conversion and mechanical harvesting, were comprehensively introduced and summarized. Among these technologies, human motion-based energy harvesters provide a potential solution to power wearable devices. To date, human motion-based energy harvesters for wearable devices can be divided into *integrated* harvesters and *independent* harvesters.

Integrated harvesters indicate that the energy harvesting component is a key part of a wearable device[281]. This is commonly seen in self-powered e-skins and textile-type harvesters [292, 337]. E-skin is a type of flexible and stretchable skin-type electronics that is capable of transducing a mechanical signal into an electrical signal, which has applications in wearable electronic devices, health control, healthcare monitoring and artificial intelligence [338-340]. A complete e-skin device includes the power supply, a variety of skin-like sensors and actuators, and pathways for signal extraction and processing [341]. The long-term continuous power supply for e-skins is a challenge, which can be potentially solved by harvesting energy from ambient environment, especially from the human body including the physical motion and its thermal emission. Hence, human motion-based self-powered e-skins, which are mostly based on piezoelectric and triboelectric generators, have begun to emerge [342-344]. One example can be found is a self-powered, wireless-control, neural-stimulating e-skin with a TENG driven by human motion [345]. Since e-skins often work as a sensor, their detailed introduction is presented in the section of human motion-based self-sensing devices (Section 5). The textile-type human motion-based energy harvester is another type of integrated harvester. The integration of comfortable, soft and breathable wearable electronics integrated into textiles or clothes has been widely used in many fields, which brings significant convenience and advantages to our daily life. For wearable applications, the ubiquitous and stable energy associated with human motion is the ideal energy source for wearable electronics, thus leading to a type of sustainable self-powered multi-functional electronic device [346, 347], such as highly stretchable TENGs [95-97], wearable pouch-type TENGs [104], flexible piezoelectric nanogenerators [119], wearable electromagnetic harvesting textiles [69], are suitable in these applications. Additional examples of textile-type harvesters can be found in Refs. [296, 298, 324, 348]. It can be seen that integrated human motion-based self-powered devices are mostly made of flexible and stretchable materials since their mechanical properties match the human body.

In comparison, independent human motion-based energy harvesters can provide energy for wearable devices, including consumer electronics such as smart watches and smart glasses, which provide a convenience for our daily life. Specific energy harvesters have been proposed to power such devices, instead of batteries, thereby providing a potential solution to significantly improve their endurance time. For example, human motion-based energy harvesters have demonstrated their application potential in powering a commercial wrist watch [68, 91]. However, since independent energy harvesters operate as an *external* power supply they can increase the size of the wearable devices and make their structure more complex. Therefore, integrated energy harvesters should be further developed in the future work to design complete self-powered consumer electronics.

5.1.3. Powering other low-powered electronics. In addition to implantable biomedical devices and wearable devices, which are in demand for self-powered applications, other low-powered electronics can be powered by human motion-based energy harvesters. For example, harvesters have shown their application in powering portable devices: a scientific calculator can be powered by an air-cushion TENG [299], a human body constituted TENG [106], a double-layer-stacked triboelectric textile [296] and a stretchable triboelectric textile [96] excited by human movement; a timer can be powered by a human body constituted TENG [106] and a double-layer-stacked triboelectric textile [296]; a double-layer-stacked triboelectric textile can be used to power a digital clock [296]. Some harvesters can be used to power a wireless sensor[261] such as a digital thermometer [299], temperature sensor [91, 269], an insole pressure network [110] and a wireless sensor node [72, 79, 83, 102, 259, 260]. Many human motion-based energy harvesters were not proposed for a clear application area, and researchers have simply proposed various schemes based on different energy harvesting mechanisms and explored their energy harvesting performance. However, the proposed human motion-based energy harvesters have potential to operate as a power supply. As long as the output power of the harvesters is larger than the required operating power, they have potential to be used to power electronics. If the output power is smaller than the operating power, the energy generated from the harvesters can be used as a supplement for batteries so that they are be recharged or used for a longer period of time. One important potential application case, from the viewpoint of the authors, is self-powered outdoor rescue devices [110] such as the headlight/hand lamp, compass, global positioning system (GPS) locator, portable batteries and rescue signal transmitter. Hence, all the proposed devices provide energy options of the low-power electronics in the future. It is clear that a high output power, small size, lightweight, highly integrate, flexible and durable energy harvesters are favourable for these electronics.

5.1.4. Application challenges. Human motion-based energy harvesters can be used in a range of applications, whose performance is decided by the structure, size, output power, flexibility, and biocompatibility. In the literature, some specific devices are designed to power themselves, such as implantable medical devices, while other devices only show their potential in powering any low-power electronics by only quantifying the energy harvesting capability. It can be seen the area of human motion-based self-powered devices is at an early research stage and low technology readiness (TRL) level. The main application challenges of human motion-based self-powered devices are :

(1) The output power is a key index to evaluate the performance of human motion-based self-powered devices. It can be seen from Table 7 that most harvesters have a relatively low output power level (mW or μW level). There are reports that the output power is larger than the power consumption or power requirement of some low-powered electronics [127, 265], so has the potential to act as a power supply for these electronics. However, in practical applications, the generated electrical energy may be dissipated through the external circuit and energy storage system. Hence, the output power of current harvesters should be improved to ensure their reliability in operation of power supply.

(2) In small-scale applications, such as powering implantable medical devices, the devices have strict dimensional restrictions. Hence, the power density of existing harvesters, see Table 7, should be further improved so that the harvesters can supply sufficient energy with a reasonable size.

(3) As shown in Table 7, the energy conversion efficiency of human motion-based energy harvesters have not been fully studied, and the reported efficiencies are relatively low. Although most harvesters scavenge energy from the wasted energy of human motions, the conversion efficiency is less well studied. However, enhancing the energy conversion efficiency could be beneficial to improving the output power of a harvester under a certain operation environment, thereby improving overall performance.

(4) Human motion-based energy harvesters can convert human motion into electricity, but before it can be used by the terminal electronics, an extrenal management circuit or energy storage system [68, 255, 265] are

necessary. As introduced previously (Section X), electromagnetic and piezoelectric generaters usually produce an AC voltage under human motion, while wireless sensors and portable devices often use a DC voltage. Therefore, an electrical interface between the harvesters and terminal electronics is essential. However, the external circuit may consume energy, thus reducing the available energy of the whole system. This is a particularly important restriction for small-scale human motion-based harvesters with a low output power/power density, which must be taken into account in future applications. Moreover, the electrical interface or the external circuit may have influence the dynamic response of the harvester, which impedes effective optimization design and application of the harvesters.

(5) In some applications, the output power generated from the human motion-based harvesters is not necessary to power a terminal electronic directly. Instead, it can be stored in an energy storage device, such as advanced batteries and supercapacitors. Thus, human motion-based energy harvesters and energy storage devices can be integrated into self-charging power systems (SCPSs) [349], which can storage the generated power effectively and supply power when needed. While there some reports have demonstrated that the power generated from a human motion-based energy harvester can be used to charge a capacitor [68, 107, 255], more work is needed on self-charging power systems . For example, the energy density of the energy storage devices can be improved [350, 351], and the potential flexibility and wearability of energy storage devices should be considered [352]. These progresses have been summarized in other review papers [353-355]. Moreover, the total efficiency of a self-charging power system is determined by the energy conversion efficiency, the circuit efficiency and the storage efficiency. These factors along with their combined influences should be fully studied facing the pratical applications.

5.2. Human motion-based self-sensing devices

The development of advanced energy harvesters has an important role in the development of wireless sensors. On one hand, harvesters can provide energy for low-powered wireless sensors so that they can act only as a power supply. Wireless sensors have broad applications in many wireless environments and are useful in our daily life. For example, wireless sensor networks can be applied in condition monitoring of engineering structures [356] and in the railway industry [357]; wearable sensors can be used for human health monitoring [358] and activity monitoring [359], and sensors inside a human body can be used to monitor important physiological indexes such as heart rate [360], arterial pulse [361] and blood pressure [362]; sensors installed outdoor can be used to measure the temperature, wind speed, and collect data [363-365]; wireless sensor networks are the core element of the Internet of Things [366, 367]. On the other hand, some energy harvesters can behave as sensors, without any sensor incorporation based on their unique material properties, thereby removing the restriction of using additional sensors. In these cases, the devices can be termed *self-sensing devices*, which have attracted significant attention in the research community. In this section, the state-of-the-art human motion-based self-sensing devices will be fully reviewed.

For most human motion-based self-sensing devices, the measured physical quantities are reflected by the electrical signal generated from the energy harvester. Hence, the accuracy of the electrical signal is a key factor of energy harvesters, but not the generated output power. Moreover, the materials for energy harvesters should be sensitive to excitations, such as the pressure-induced strain. Therefore, according to the energy conversion mechanisms of the pre-mentioned energy harvesters (Section 3), most human motion-based self-sensing devices are based on a flexible piezoelectric or triboelectric energy harvester, which can be mounted on the human body and generate electrical signals according to different strains, angles and pressures.

In the following of this section, human motion-based self-sensing devices, which can generate electricity from human motions and act as a sensor for human activity monitoring, healthcare monitoring, and human-machine interactions and other bio-signals, are comprehensively reviewed.

5.2.1. Human activity recognition. Considering that human motion-based energy harvesters are installed upon the human body, the energy harvesters with sensing properties can be used to recognize human activities. Examples of such self-sensing devices can be found in Fig. 17**.**

Human motion-based energy harvesters can be used to recognize the macroscopic limb movements of a human, such as finger tapping, leg contact-separation movements, and the upper limb swing. For example, the human body constituted TENG [106] introduced in Fig. 14(c) can act as a high-performance, self-powered body motion sensor, as shown in Fig. 17(a). When the TENG is packed on a trouser, it can work in a vertical contact mode with the open-circuit voltage being proportional to the size of the TENG or the pressure applied onto the TENG. Thus, when the harvester is subjected to finger tapping with the pressure being relatively unchanged, its open-circuit voltage has a linear relationship with the contact area, which can be simply represented by the number of fingers. This device can be used to sense the adding/removing of the hand, and the friction between the skin and the polytetrafluoroethylene (PTFE) film from hand sliding. Based on a similar mechanism, a flexible and self-powered e-skin based on an extra-stretchable TENG [368] can generate energy from finger pressure, and sense the strength and the motion trajectory of mechanical stimulations, as shown in Fig. 17(b). Other self-powered e-skins with tactile sensing characteristics can be found in Refs. [368, 369]. Another similar self-sensing device that can recognize the contact-separation movement of a leg or other body movement was proposed by Tian *et al*. [296]. A flexible nanocomposite-based piezoelectric nanogenerator proposed by Choudhry *et al*. [280] can act as a strain sensor to recognize the bending and relaxing states of the finger, wrist and elbow. The yarn-based TENG proposed by Dong et al. [93] has many applications in human activity recognition, as shown in Fig. 17(c). A skipping rope with two yarn-based TENGs can be used for self-counting by analyzing the generated electrical signal that reflects the contact-separation motion between the bottom touch-down section and the ground; a self-powered smart gesture-recognizing glove, which is simply assembled by pasting five TENG yarns on the dorsal of a regular glove, has been designed to detect and recognize the finger gestures; a real-time golf scoring system based on this TENG can be used to recognize eight golf swing steps through the corresponding output voltage curve, as shown in Fig. 17(c).

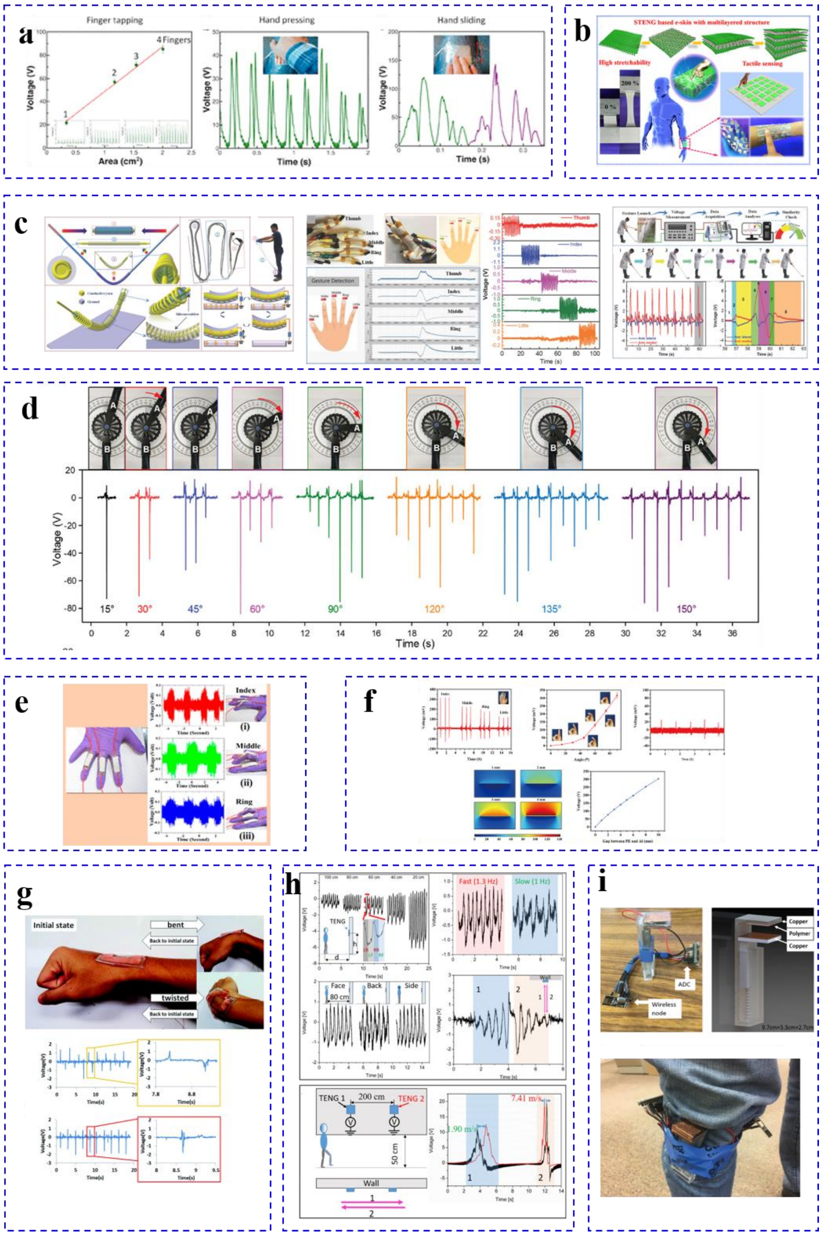

Fig. 17 Human motion-based self-sensing devices for human activity recognition. (a) Human body constituted TENG which can act as an active sensor to recognize the finger pressure [106]; (b) a flexible and self-powered e-skin based on an extra-stretchable TENG that can sense the strength and the motion trajectory of mechanical stimulations [368]; (c) versatile core-heath yarn used in

a self-counting skipping rope, a self-powered gesture-recognizing glove, and a real-time golf scoring system [93]; (d) digitalized outputs of a ratchet-based TENG that can match the rotation angles to the pulse numbers [304]; (e) health-data glove with three e-skin sensors integrated to index, middle and ring fingers [107]; (f) flexible and dual-mode TENG as a self-powered sensor to detect the phalanges' movement of fingers and even the bending angles [370]; (g) Performance of highly flexible power generator as an active sensor under the skin and operated by human motion movement when attached to the wrist joint [250]; (h) noncontact TENG, whose output voltage signals can reflect the walking gait cycle (leg raising and falling), moving direction, walking or running speed and moving path directly and clearly [371]; (i) wireless TE motion sensor node which can recognize the common physical activities including sitting and standing, walking, climbing upstairs and downstairs, and running [293].

Micro motions and their accuracy in terms of displacement or angle can be recognized by human motion-based energy harvesters, especially the finger and wrist motion. For example, Gao *et al*. proposed a motion capturing and energy harvesting hybridized lower-limb system [304], which consisted of a sliding block-rail piezoelectric generator that can harvest low-frequency biomechanical energy, and a ratchet-based TENG (R-TENG) that can sense the lower-limb. It was reported that the digitalized output of the R-TENG matched the rotation angles to the pulse numbers, as shown in Fig. 17(d), making it useful for demonstrative rehabilitation, virtual reality and sports monitoring. The same research group proposed the use of a triboelectric bidirectional sensor as a universal and cost-effective solution for developing a customized exoskeleton for monitoring the movable joints of the human upper limbs with low power consumption [372]. Its potential application for supporting the manipulation in both real and virtual worlds, including robotic automation, healthcare, and training applications were demonstrated. A stretchable and shape-adaptable liquid-based single-electrode TENG [108] can generate electrical signals that directly respond to external mechanical actions. When the TENG is installed on the finger joint, it can monitor the angle of finger bending since the peak value of the electrical output varies with the bending angle. Hence, this TENG can act as a wearable active sensor to monitor human motions by extracting information from electrical signals. Some other human motion sensors that can recognize the fingers and bending angle include a fabricated piezoelectric nanogenerator based on SiO_2/PVDF nanocomposites [107] shown in Fig. 17(e) and a human motion sensor based on flexible dual-mode nanogenerator [370] shown in Fig. 17(f). A highly stretchable all-rubber-based thread-shaped TENG [95] can quantitatively recognize the state of finger motion using the similar operating mechanism, as shown in Fig. 13(b). In addition, Fig. 17(g) presents a nano/micro fiber (NMF) based on an all-direction energy harvester [250] that can recognize a bending wrist and the torsion of a wrist when operated by human motion.

Another important human activity that can be recognized by self-powered sensors is a standing/walking posture. For example, a noncontact paper-based TENG [371], shown in Fig. 17(h), has demonstrated its potential in monitoring the walking gait cycle (leg raising and falling), moving direction, walking or running speed and moving path. This device consists of a printed paper with a metal electrode as one part of the TENG, and the human body as the other part. The rise and fall of the leg during the motion cycle can be reflected by the output voltage simultaneously, and the moving direction can also be recognized. Moreover, by simply fixing two paper-based TENGs on the wall, the walking or running speed of a person can be calculated through the voltage peak values of these two TENGs with passing time. By fixing two individual TENGs on two orthogonal walls, the moving path of a person can be derived based on the measured output voltages. The human activity recognition from kinetic energy harvester (HARKE) is realized through a simple piezoelectric cantilevered beam system [275]. Results show that the HARKE can detect daily activities such as standing, walking, running, ascending stairs and descending stairs with 80% to 96% accuracy depending on the activities and the placement (location) of the wearable device on the human body (hand or wrist). A simple wireless triboelectric motion sensor node [293] shown in Fig. 17(i) can recognize common physical activities including sitting and standing, walking, climbing upstairs and downstairs, and running. A similar function can be realized through a wearable TENG with polytetrafluoroethylene (PTFE) film and cotton film [373], which can measure the human walking state when it is located on the sole of shoes. Another interesting example is a pedometer without batteries, which is an energy harvesting shoe [285]. The proposed simple activity monitoring system based on a piezoelectric harvesting platform can record the step number according to the output voltage with the median accuracy of 10.8%. The hybridized electromagnetic-triboelectric nanogenerator designed by Liu *et al*. [249] can be also used to recognize squatting and standing up actions of, lifting of the leg up and down (when mounted on the thigh and foot) and to record motions of forward and unexpected falling (when equipped on the walking aid).

We have seen that some human motion-based energy harvesters can act as self-sensing devices to recognize human activities, and in some cases, they can even measure physical quantities, such as the joint bending angle, and walking speed. However, it should be noted that the relationships between these physical quantities and outputs (voltage or current, in most cases) are relatively poor, therefore, their performance as sensors for obtaining accurate physical quantities should be further improved by developing high-performance self-sensing devices. This is an important development direction for human motion-based self-sensing devices for human activity recognition.

5.2.2. Human health monitoring. Human health monitoring is another promising application for human motion-based self-sensing devices. For example, the fabricated piezoelectric nanogenerator [107] shown in Fig. 17(c) can recognize the movements of different fingers, and the signal patterns can provide information for healthcare monitoring for bead-ridden patients [374-377]. The walking gesture can provide rich human health information, which corresponds to diverse physical states. A human body-based electrode-free TENG [118] (Fig. 15(c)) can realize health monitoring and disease diagnosis based on the generated signal during human walking, as shown in Fig. 18(a). This energy harvester will generate a positive pulse voltage when the left foot departs from the floor and a negative pulse voltage when the left foot falls on the floor. Similarly, a pair of opposite pulse voltages will arise when the right foot lifts and lands. The abnormity of either foot (such as being injured) will result in different walking gestures and output voltage compared to those in a normal way. The second plot in Fig. 18(a) shows the output voltage of an able-bodied person and a disabled person. One can see a clear distinction between the output voltages, thereby determining the possible physical condition of a person. The weight of a person can also be recognized from the output voltages. As shown in the third plot of Fig. 18(a) and the inset, the amplitude of the output voltage shows an approximately linear increase as the weight increases, indicating that the TENG has a potential application in weight-bearing training and weight monitoring. In addition, this TENG can be used to recognize the height of a person's vertical leap, as shown in Fig. 18(a), which indicates a linear relationship between the jumping height and the amplitude of the output voltage. This can be explained that the vertical separation velocity between two triboelectric materials reflects the take-off velocity of a person, and further decides the amplitude of the output voltage. The results further demonstrate that the TENG has potential in physical training and physiological monitoring. Another interesting self-sensing device for health monitoring are the self-powered sensors for coughing action [271, 274], as shown in Fig. 18(b, c). When the cellular polypropylene flexible piezoelectric generator [271] shown in Fig. 18(b) is fastened on the neck of a healthy person, coughing, which leads to vocal cords vibration, will produce a current signal. The normalized power spectrum density can reflect the coughing action better. Hence, some coughing-based diseases can be monitored. This device can be also used to detect the arterial pulses of a person when it is fastened on the wrist, thereby monitoring a person's health condition. The mechanism and function of the flexible (1−x)Pb(Mg,Nb)O_3-xPbTiO_3 (PMN-PT) ribbon-based piezoelectric-pyroelectric hybrid generator for coughing action recognition (Fig. 18(c)) is similar to this device. The flexible nanocomposite-based piezoelectric generator [280] is stated to be a suitable candidate in various medical diagnostic applications, but the authors did not provide an in-depth elaboration.

Most human motion-based self-sensing devices for human health monitoring are *in vitro* and mounted outside of human body, and the human health status can be monitored by the generated signal resulting from finger touching, walking, jumping, and coughing. Hence, the human health status is recognized indirectly. If the self-sensing devices can measure the biomedical signals, such as blood pressure, pulse, blood sugar level, and heart rate, the human health status can be recognized directly, and the results can be more informative. Hence, one important development direction of human motion-based self-sensing devices for human health monitoring is *in vivo* self-sensing devices. These devices should be able to harvest energy from human motions, and are sensitive to biomedical excitations. Moreover, they should have good biocompatibility and durability. The development of advanced materials may promote the improvement of such devices.

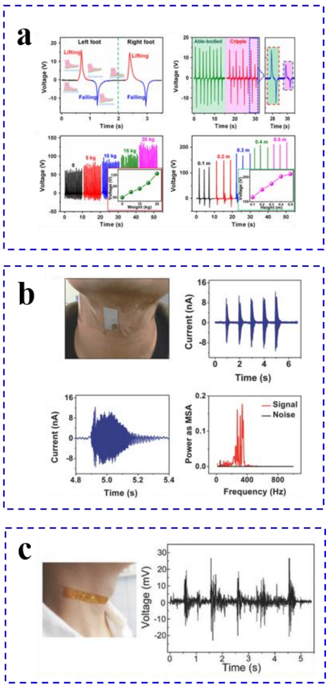

Fig. 18 Human motion-based self-sensing devices for human health monitoring. (a) electrode-free TENG, through the output voltages of which the gait of an able-bodied person and a person with disability and different weights and jumping heights can be recognized [118]; (b) human body biological signals detecting sensor to measure the coughing action, along with the electrical outputs caused by coughing [271]; (c) device attached on a neck and the voltage output waveform for the sensor caused by coughing [274].

5.2.3. Human-machine interactions. In some cases, human motion-based self-sensing devices cannot measure the physical quantities precisely, but the obtained electrical signal can be used as a trigger signal to enable human-machine interaction systems. These devices do not act strictly act as sensors, but their sensitivity to human motion has wide ranging innovative applications. Hence, these devices will be introduced in this subsection, and typical devices are presented in Fig. 19.

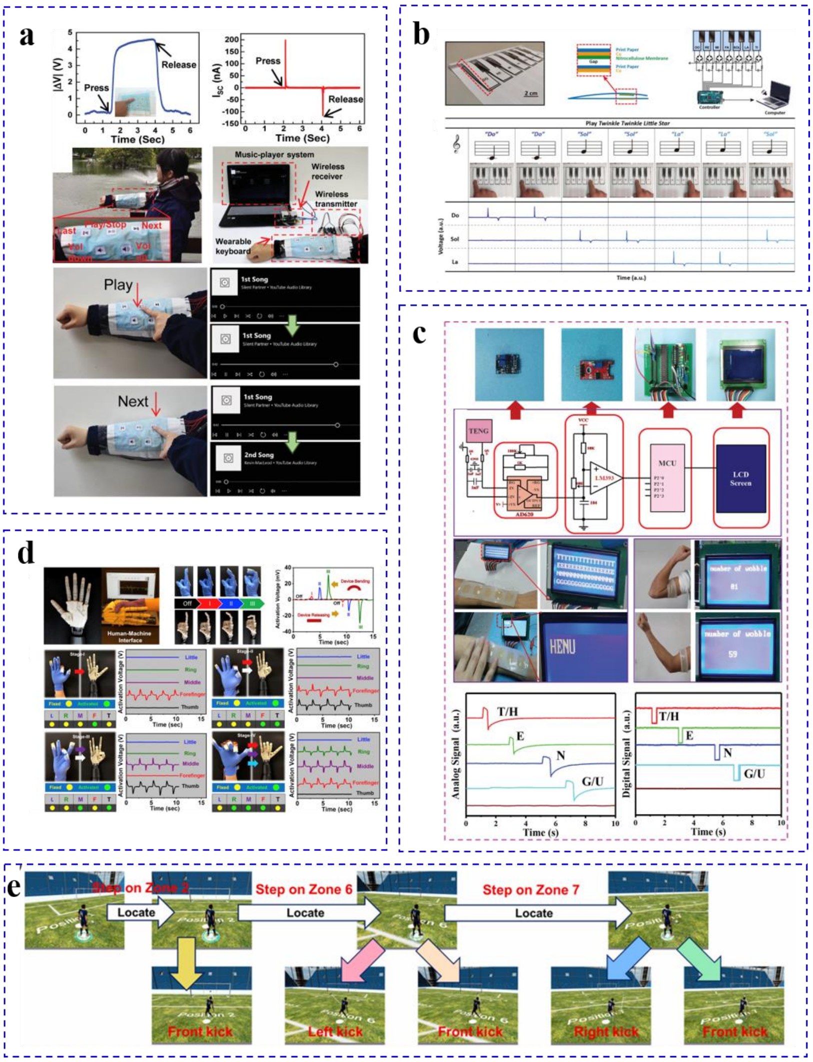

Fig. 19 Human motion-based self-sensing devices for human-machine interactions. (a) Output voltage and current during finger touching and releasing, which provide a basis for the fabric-based multifunctional TENG (WPF-MTENG) as fabric human-system interface. Photos show the wireless wearable WPF-MTENG-based music-controlling keypad and music-play system [97]; (b) TENG-based paper piano for self-powered human-machine interfacing [105]; (c) human-machine interaction with a self-powered wearable touch panel based on the liquid-based single-electrode triboelectric nanogenerator attached on a person's forearm, and letters can be typed to display by light emitting diode (LED) screen [108]; (d) intelligent human-robotic interface established based on the interaction between human and 3D printing robotic hands. Human forefinger in different bending states can generate the corresponding activation voltages synchronously by the SnS_2 piezoelectric nanogenerator device adhered to the

human forefinger, thus driving a robotic forefinger [100]; (e) a virtual foot game controlled by a magnetic-interaction assisted hybridized triboelectric-electromagnetic nanogenerator [378].

Fig. 19(a) shows a waterproof and fabric-based multifunctional TENG (WPF-MTENG) [97]. Electrical signals can be generated when the two fabrics are in contact with each other during finger touching. Using these responding signals, the WPF-MTENG, which can be simply integrated into a smart cloth, and can act as a self-powered human-system interface. For example, this work proposed a smart cloth with five WPF-MTENGs acting as music-controlled keys, which can control a music player system remotely when they are integrated with a data-processing micro controller and wireless transmitter. Pressing the keys of "Play" and "Next" can remotely play the music and play the next song of the player system, respectively. A similar application can be found in Fig. 19(b), which shows a paper piano with paper-based TENGs (P-ENGs) [105] (Fig. 14(b)). In the proposed self-powered human-machine interactive paper piano, the keyboard is composed of seven P-TENGs. On pressing and releasing the keys (i.e., the P-TENGs) of the keyboard, electrical energy is produced, which is used to charge the related capacitors. Thus, the sound programme can be controlled by the varying voltage through real-time communication. Similarly, a wearable and self-powered touch panel [108] fabricated as an array of lateral sliding TENG (Fig. 16(d)) units as touch-sensing components has demonstrated its application as a self-powered interactive device, as shown in Fig. 19(c). Moreover, the disulphide piezoelectric generator with strain sensing and self-powered functionalities [100] in Fig. 13(h) can act as a human-robot interaction system to synchronize human-robot motion, as shown in Fig. 19(d). This figure presents the platform of a fully 3D printed robotic hand, which is connected to a control program. Flexible piezoelectric nanogenerator devices adhered to the fingers, whose bending and stretching will y produce signals, can be used to drive the robot hand simultaneously with a series of signal generation, processing and recognition. Researchers have shown that the movements of a robotic forefinger can be precisely controlled by a human forefinger through the activation voltage generated at different bending states (off, I, II and III), thereby demonstrating its application in real-time imitation of human gesture. To apply this platform for a future human-machine interaction (HMI) system, the real-time performance of a smart sign language system is further demonstrated. Liu *et al.* proposed a magnetic-interaction assisted hybridized triboelectric-electromagnetic (MAHN) device [378] , which can harvest energy from various sources and realize human-machine interfaces. It was demonstrated that the MAHN can be applied as a self-sensing device in transferring direction commands, which can be applied in the orientation control in a game of Snake, real-time operation of a PowerPoint presentation, and a virtual football game, as shown in Fig. 19(e).

The concept that the generated electrical signal acting as a trigger signal opens a new world for the application of human motion-based self-sensing devices. If the electrical signal is sufficient to reflect the actions from human body, it can be used to transmit a signal or trigger a machine, even though the energy density of the device is small. This is helpful for the design of a rescue signal generator, a remote controller, or a complex human-machine interaction system for remote or dangerous work. It should be noted that for establishing a human-machine interaction system, data-processing micro-controller/ signal processing circuit and the wireless transmitter for remote control are necessary, which often needs an external power supply.

5.2.4. Application challenges. Human motion-based self-sensing devices have been comprehensively reviewed and introduced from the perspective of their applications. It should be noted that some harvesters can harvest energy not only from human motion, but also from other energy sources, and they can act as self-powered sensors to measure specific physical quantities such as velocity [294], pressure [107, 299], weight [297, 302], sound and temperature [274]. However, these devices are not introduced in this review paper since they do not harvest energy from human motions. Moreover, self-powered e-skin [379] is a form of self-sensing device, which can harvest energy from light, heat, movement and biochemical elements [380]. Among these energy sources, human motion is a type of suitable energy source for the self-powered e-skins, where more details on self-powered e-skins can be found in Ref. [[381]].

For self-sensing devices, the accuracy of the electrical signal is highly important, but not the generated output power. Based on the accuracy of the device in reflecting the measured physical quantities, the applications of the generalized human motion-based self-sensing devices can be divided into two groups, namely *sensing* and *identification*. To date, human motion-based self-sensing devices which can recognize human activities and monitor human health only have limited accuracy, which is a key challenge to develop high-performance self-sensing devices. The generalized self-sensing devices, which utilize the obtained electrical signal as a trigger signal for human-machine interaction systems, have shown their potential in the design of rescue signal generators, remote controllers, and complex human-machine interaction systems for remote or hazardous work. The challenges for such devices include integration with the rest system, and the stability and reliable of generated electrical signal.

6. Conclusions and prospects

The utilization of advanced energies, including wind energy, wave energy, tidal energy, hydropower, solar energy, nuclear energy, vibrational energy, and human body-related energy provides an important solution for sustainable development and environmental protection. Among these available sources, energy from the human body can provide a promising opportunity to generate energy from ourselves, with a reduced reliance on an external energy source. Hence, human motion energy is highly suitable for active or passive small-scale energy harvesters. Although their generated power is significantly lower than that from large-power grid, they are stable and abundant, and have unique applications as an energy supply for low-powered electronic devices. This includes consumer electronics, wireless sensors, structural health monitoring devices, human healthcare devices, and in the design of rescue devices, self-sensing devices, human-machine interactions, and in biology, military, or transportation. Therefore, human body-related energy harvesters have attracted increasing attention in recent decades.

The human body-related energy sources include temperature difference, heat dissipation, blood pressure, human sweat, and human motion, among which human motion has attracted attention. Moreover, human body-related energy can be transformed into both non-electrical energy (e.g., the mechanical energy to drive a mechanical watch) and electrical energy, and the electricity-oriented energy harvesters are popular since they have wide application potential. Therefore, the development of human motion-based energy harvesters is a rapidly developing area.

In this paper, the state-of-the-art advances of the human motion-based energy harvesters and their applications in self-powered and self-sensing devices are comprehensively reviewed. Firstly, the available human motion sources are re-classified into three categories based on how they operate as excitation sources for human motion-based energy harvesters, including human motion operating as an external base excitation (Category I), human body movement operating as a direct form of excitation by deformation (Category II), and a slowly varying pressure or small displacement motion (Category III). Four commonly used electromechanical energy conversion mechanisms, by which the human motion energies can be converted into electricity, are further introduced along with the relevant materials. The human motion-based energy harvesters can be further used for self-powered and self-sensing devices.

In reviewing the current literature, inspiration can be obtained for the future research direction of human motion-based self-powered and self-sensing devices, and the challenges that should be addressed. These include:

(1) The performance of the human motion-based self-powered and self-sensing devices highly depends on the nature of the material. Hence, the future development of advanced functional or energy materials can be exploited in novel human motion-based devices.

(2) It is of importance to improve the power density by increasing the output power, optimizing the device structure, and reducing the weight of vitro human motion-based energy harvesters. An additional challenge is to ensure consideration to the comfort of the carrier.

(3) For the use of *in vivo* energy harvesters to power implantable medical devices, the most important factors which should be taken into account include its light weight nature, small size, anti-infection property, stability, durability, biocompatibility and comfort.

(4) For practical applications of the human motion-based energy harvesters, since the output power is typically low, designers should enhance the power of harvesters by both improving their energy harvesting performance and designing high-efficiency interface circuits. The inherent irregularity and inhomogeneity of the human motions should be also considered in the design of future energy harvesters.

(5) Another approach to enhance the electrical output of harvesters is to design multi-source harvesters which can simultaneously harvest heat energy, chemical energy, fluid-solid coupling and self-excited vibration energy. This is of interest for the development of the intestinal and vascular self-powered micro-robots by improving their function in human health monitoring and microsurgery.

(6) For human motion-based self-sensing devices, the sensing accuracy and reliability should be further improved, and the multi-functional self-sensing devices are of interest.

(7) Other important potential applications for the human motion-based self-sensing devices include gait monitoring, motion capture and human-machine interaction. By combining energy harvesting with information and sensing technologies, they can provide a basis for the future high-accuracy multi-functional devices.

(8) Human motion-based self-powered and self-sensing devices have potential to acquire data from human body or ambient environment, which has significant potential when combined with Artificial Intelligence and Machine Learning approaches.

In summary, human motion is a type of promising energy sources for small-scale self-powered and self-sensing devices. These devices have shown their wide applications in human's daily life ranging from daily energy supply to delicate human health monitoring, and can be applied in more and more scenarios by solving their application challenges in the future.

Conflicts of interest

There are no conflicts to declare.

Acknowledgements

This work was supported by the National Natural Science Foundation of China (Grant nos. 51905349, U2013603, 12072267), the Natural Science Foundation of Guangdong Province (Grant nos. 2020A1515011509, 2022A1515010126), the Science, Technology and Innovation Commission of Shenzhen Municipality (Grant no. JCYJ20190806153615091), the Natural Science Foundation of Shenzhen University (Grant no. 860-000002110264), and the 111 Project (Grant no. BP0719007).

References

_ENREF_11. V. Kashyap, S. Sakunkaewkasem, P. Jafari, M. Nazari, B. Eslami, S. Nazifi, P. Irajizad, M. D. Marquez, T. R. Lee and H. Ghasemi, *Joule*, 2019, **3**, 3100-3111.
2. L. Yang, D. K. Nandakumar, L. Q. Miao, L. Suresh, D. W. Zhang, T. Xiong, J. V. Vaghasiya, K. C. Kwon and S. C. Tan, *Joule*, 2020, **4**, 176-188.
3. Z. Chen, L. X. Zhu, W. Li and S. H. Fan, *Joule*, 2019, **3**, 101-110.
4. S. Y. Chang, P. Cheng, G. Li and Y. Yang, *Joule*, 2018, **2**, 1039-1054.
5. Z. H. Liu, N. Sato, W. H. Gao, K. Yubuta, N. Kawamoto, M. Mitome, K. Kurashima, Y. Owada, K. Nagase, C. H. Lee, J. Yi, K. Tsuchiya and T. Mori, *Joule*, 2021, **5**, 1196-1208.
6. F. K. Shaikh and S. Zeadally, *Renewable & Sustainable Energy Reviews*, 2016, **55**, 1041-1054.
7. H. L. Zhou, Y. Zhang, Y. Qiu, H. P. Wu, W. Y. Qin, Y. B. Liao, Q. M. Yu and H. Y. Cheng, *Biosensors & Bioelectronics*, 2020, **168**.
8. J. T. Xue, Y. Zou, Y. L. Deng and Z. Li, *Ecomat*, 2022, DOI: 10.1002/eom2.12209.

9. N. S. Hudak and G. G. Amatucci, *Journal of Applied Physics*, 2008, **103**, 101301.
10. D. Guyomar and M. Lallart, *Micromachines*, 2011, **2**, 274-294.
11. L. Zhao and Y. Yang, *Shock and Vibration*, 2017, **2017**, 3585972.
12. P. K. Sharma and P. V. Baredar, *Journal of King Saud University Science*, 2019, **31**, 869-877.
13. P. S. Kumar, J. Sundaramurthy, S. Sundarrajan, V. J. Babu, G. Singh, S. I. Allakhverdiev and S. Ramakrishna, *Energy & Environmental Science*, 2014, **7**, 3192-3222.
14. L. Liu, X. Guo and C. Lee, *Nano Energy*, 2021, **88**.
15. J. M. Donelan, Q. Li, V. Naing, J. A. Hoffer, D. J. Weber and A. D. Kuo, *Science*, 2008, **319**, 807-810.
16. Y. Qi and M. C. McAlpine, *Energy & Environmental Science*, 2010, **3**, 1275.
17. C.-Y. Sue and N.-C. Tsai, *Applied Energy*, 2012, **93**, 390-403.
18. M. Gao, P. Wang, L. Jiang, B. Wang, Y. Yao, S. Liu, D. Chu, W. Cheng and Y. Lu, *Energy & Environmental Science*, 2021, **14**, 2114-2157.
19. S. Wu, P. C. K. Luk, C. Li, X. Zhao, Z. Jiao and Y. Shang, *Applied Energy*, 2017, **197**, 364-374.
20. P. V, M. K. Rajendran, S. Kansal, G. Chowdary and A. Dutta, *IEEE Internet of Things Journal*, 2018, **5**, 4989-5001.
21. H. K. Cho, D. H. Kim, H. S. Sin, C.-H. Cho and S. Han, *Journal of the Korean Ceramic Society*, 2017, **54**, 518-524.
22. Z. Lu, H. Zhang, C. Mao and C. M. Li, *Applied Energy*, 2016, **164**, 57-63.
23. T. Ghomian, O. Kizilkaya and J.-W. Choi, *Applied Energy*, 2018, **230**, 761-768.
24. M.-S. Kim, S.-E. Jo, H.-R. Ahn and Y.-J. Kim, *Smart Materials and Structures*, 2015, **24**, 065032.
25. A. Nanda and M. A. Karami, *Journal of Applied Physics*, 2017, **121**, 124506.
26. A. J. Bandodkar, J.-M. You, N.-H. Kim, Y. Gu, R. Kumar, A. M. V. Mohan, J. Kurniawan, S. Imani, T. Nakagawa, B. Parish, M. Parthasarathy, P. P. Mercier, S. Xu and J. Wang, *Energy & Environmental Science*, 2017, **10**, 1581.
27. J. Lv, I. Jeerapan, F. Tehrani, L. Yin, C. A. Silva-Lopez, J.-H. Jang, D. Joshuia, R. Shah, Y. Liang, L. Xie, F. Soto, C. Chen, E. Karshalev, C. Kong, Z. Yang and J. Wang, *Energy & Environmental Science*, 2018, **11**, 3431-3442.
28. P. D. Mitcheson, E. M. Yeatman, G. K. Rao, A. S. Holmes and T. C. Green, *Proceedings of the IEEE*, 2008, **96**, 1457-1486.
29. X. Guo, T. He, Z. Zhang, A. Luo, F. Wang, E. J. Ng, Y. Zhu, H. Liu and C. Lee, *Acs Nano*, 2021, **15**, 19054-19069.
30. M.-S. Kim, M.-K. Kim, K. Kim and Y.-J. Kim, *Smart Materials and Structures*, 2017, **26**, 095046.
31. V. Leonov, *IEEE SENSORS JOURNAL*, 2013, **13**, 2284-2291.
32. A. P. Straub, N. Y. Yip, S. Lin, J. Lee and M. Elimelech, *Nature Energy*, 2016, **1**, 16090.
33. A. Waske, D. Dzekan, K. Sellschopp, D. Berger, A. Stork, K. Nielsch and S. Fähler, *Nature Energy*, 2019, **4**, 68-74.
34. A. Sultana, M. M. Alam, T. R. Middya and D. Mandal, *Applied Energy*, 2018, **221**, 299-307.
35. C. R. Bowen, J. Taylor, E. LeBoulbar, D. Zabek, A. Chauhan and R. Vaish, *Energy & Environmental Science*, 2014, **7**, 3836-3856.
36. Y. Zhang, P. T. T. Phuong, E. Roake, H. Khanbareh, Y. Q. Wang, S. Dunn and C. Bowen, *Joule*, 2020, **4**, 301-309.
37. N. A. Shepelin, A. M. Glushenkov, V. C. Lussini, P. J. Fox, G. W. Dicinoski, J. G. Shapter and A. V. Ellis, *Energy & Environmental Science*, 2019, **12**, 1143-1176.
38. H. Shi, S. Luo, J. Xu and X. Mei, *Energy Conversion and Management*, 2021, **229**, 113790.
39. X. Zhou, G. Liu, B. Han, L. Wu and H. Li, *Energy Technology*, 2020, **9**, 2000726.
40. X. Zhou, G. Liu, B. Han and X. Liu, *International Journal of Energy Research*, 2021, **45**, 4841-4870.
41. H. Zhang, X. Cui, S. Cao, Q. Zhang, S. Sang and W. Zhang, *Energy Technology*, 2018, **6**, 2053-2057.

42. H. Ouyang, Z. Li, M. Gu, Y. Hu, L. Xu, D. Jiang, S. Cheng, Y. Zou, Y. Deng, B. Shi, W. Hua, Y. Fan, Z. Li and Z. Wang, *Advanced materials*, 2021, **33**, 2102302.
43. Z. Liu, Y. Ma, H. Ouyang, B. Shi, N. Li, D. Jiang, F. Xie, D. Qu, Y. Zou, Y. Huang, H. Li, C. Zhao, P. Tan, M. Yu, Y. Fan, H. Zhang, Z. L. Wang and Z. Li, *Advanced Functional Materials*, 2019, **29**, 1807560.
44. Z. C. Yu, J. H. Xu, H. X. Gong, Y. X. Li, L. Li, Q. H. Wei and D. A. P. Tang, *ACS applied materials & interfaces*, 2022, **14**, 5101-5111.
45. Z. Zhang, L. Wang, H. Yu, F. Zhang, L. Tang, Y. Feng and W. Feng, *ACS applied materials & interfaces*, 2020, **12**, 15657-15666.
46. self-powered, https://www.merriam-webster.com/dictionary/self-powered, (accessed 4 Jan, 2022).
47. H. L. Fu, X. T. Mei, D. Yurchenko, S. X. Zhou, S. Theodossiades, K. Nakano and E. M. Yeatman, *Joule*, 2021, **5**, 1074-1118.
48. D. D. L. Chung, *International Journal of Smart and Nano Materials*, 2021, **12**, 1-19.
49. D. I. Cho and T. J. Lee, *Sensors and Materials*, 2015, **27**, 447-463.
50. M. Qin, M. Sun, M. T. Hua and X. M. He, *Current Opinion in Solid State & Materials Science*, 2019, **23**, 13-27.
51. D. Zhang and X. J. Zhang, *Small*, 2021, **17**.
52. G. Zhang, M. Li, H. Li, Q. Wang and S. Jiang, *Energy Technology*, 2018, **8**, 791-812.
53. A. Proto, M. Penhaker, S. Conforto and M. Schmid, *Trends in biotechnology*, 2017, **35**, 610-624.
54. L. Huang, S. Lin, Z. Xu, H. Zhou, J. Duan, B. Hu and J. Zhou, *Advanced materials*, 2020, **32**, e1902034.
55. Y. Zou, L. Bo and Z. Li, *Fundamental Research*, 2021, **1**, 364-382.
56. H. Shi, Z. Liu and X. Mei, *Energies*, 2019, **13**, 86.
57. S. Khalid, I. Raouf, A. Khan, N. Kim and H. S. Kim, *International Journal of Precision Engineering and Manufacturing-Green Technology*, 2019, **6**, 821-851.
58. C. Dagdeviren, Z. Li and Z. L. Wang, *Annual Review of Biomedical Engineering*, 2017, **19**, 85-108.
59. F. Invernizzi, S. Dulio, M. Patrini, G. Guizzetti and P. Mustarelli, *Chemical Society reviews*, 2016, **45**, 5455-5473.
60. M. Cai, Z. Yang, J. Cao and W.-H. Liao, *Energy Technology*, 2020, **8**, 2000533.
61. L. Huang, R. Wang, Z. Yang and L. Xie, *Electronics*, 2020, **9**, 1061.
62. M. Liu, C. Hughes-Oliver, R. Queen and L. Zuo, *Renewable Energy*, 2021, **170**, 525-538.
63. R. Shukla and A. J. Bell, *Sensors and Actuators A: Physical*, 2015, **222**, 39-47.
64. L. C. Rome, L. Flynn, E. M. Goldman and T. D. Yoo, *Science*, 2005, **309**, 1725-1728.
65. K. Xia, Z. Zhu, H. Zhang, C. Du, Z. Xu and R. Wang, *Nano Energy*, 2018, **50**, 571-580.
66. K. Fan, Y. Zhang, H. Liu, M. Cai and Q. Tan, *Renewable Energy*, 2019, **138**, 292-302.
67. K. Fan, H. Qu, Y. Wu, T. Wen and F. Wang, *Renewable Energy*, 2020, **156**, 1028-1039.
68. P. Maharjan, T. Bhatta, M. Salauddin Rasel, M. Salauddin, M. Toyabur Rahman and J. Y. Park, *Applied Energy*, 2019, **256**, 113987.
69. H. Lee and J.-S. Roh, *Textile Research Journal*, 2018, **89**, 2532-2541.
70. D. Jia, J. Liu and Y. Zhou, *Physics Letters A*, 2009, **373**, 1305-1309.
71. M. A. Halim, M. H. Kabir, H. Cho and J. Y. Park, *Micromachines*, 2019, **10**, 701.
72. D. Dai and J. Liu, *Frontiers in Energy*, 2014, **8**, 173-181.
73. W. Wang, J. Cao, N. Zhang, J. Lin and W.-H. Liao, *Energy Conversion and Management*, 2017, **132**, 189-197.
74. K. Fan, B. Yu, Y. Zhu, Z. Liu and L. Wang, *International Journal of Modern Physics B*, 2017, **31**, 1741011.
75. K. Ylli, D. Hoffmann, A. Willmann, B. Folkmer and Y. Manoli, *Smart Materials and Structures*, 2016, **25**, 095014.

76. S. Wei, H. Hu and S. He, *Smart Materials and Structures*, 2013, **22**, 105020.
77. K. Ylli, D. Hoffmann, A. Willmann, P. Becker, B. Folkmer and Y. Manoli, *Smart Materials and Structures*, 2015, **24**, 025029.
78. Z. L. Kangqi Fan, Haiyan Liu, Liansong Wang, Yingmin Zhu, and Bo Yu, *Applied Physics Letters*, 2017, **110**, 143902.
79. Y. Kuang, T. Ruan, Z. J. Chew and M. Zhu, *Sensors and Actuators A: Physical*, 2017, **254**, 69-77.
80. M. A. Halim and J. Y. Park, *Microsystem Technologies*, 2017, **24**, 2099-2107.
81. P. Pillatsch, E. M. Yeatman and A. S. Holmes, *Smart Materials and Structures*, 2012, **21**, 115018.
82. B. Yang and C. Lee, *Microsystem Technologies*, 2010, **16**, 961-966.
83. C. R. Saha, T. O'Donnell, N. Wang and P. McCloskey, *Sensors and Actuators A: Physical*, 2008, **147**, 248-253.
84. B. J. Bowers and D. P. Arnold, *Journal of Micromechanics and Microengineering*, 2009, **19**, 094008.
85. K. Ashraf, M. H. Md Khir, J. O. Dennis and Z. Baharudin, *Smart Materials and Structures*, 2013, **22**, 025018.
86. K. Ashraf, M. H. Md Khir, J. O. Dennis and Z. Baharudin, *Sensors and Actuators A: Physical*, 2013, **195**, 123-132.
87. T. Galchev, H. Kim and K. Najafi, *Journal of Microelectromechanical Systems*, 2011, **20**, 852-866.
88. S. Ju, S. H. Chae, Y. Choi, S. Lee, H. W. Lee and C.-H. Ji, *Smart Materials and Structures*, 2013, **22**, 115037.
89. X. Zhao, J. Cai, Y. Guo, C. Li, J. Wang and H. Zheng, *Smart Materials and Structures*, 2018, **27**, 085008.
90. M. Salauddin, R. M. Toyabur, P. Maharjan and J. Y. Park, *Nano Energy*, 2018, **45**, 236-246.
91. P. Maharjan, H. Cho, M. S. Rasel, M. Salauddin and J. Y. Park, *Nano Energy*, 2018, **53**, 213-224.
92. M. Amin Karami and D. J. Inman, *Applied Physics Letters*, 2012, **100**, 042901.
93. K. Dong, J. Deng, W. Ding, A. C. Wang, P. Wang, C. Cheng, Y.-C. Wang, L. Jin, B. Gu, B. Sun and Z. L. Wang, *Advanced Energy Materials*, 2018, **8**, 1801114.
94. K. Li, Q. He, J. Wang, Z. Zhou and X. Li, *Microsystems & nanoengineering*, 2018, **4**, 24.
95. J. Zhu, X. Wang, Y. Xing and J. Li, *Nanoscale research letters*, 2019, **14**, 247.
96. X. Hou, J. Zhu, J. Qian, X. Niu, J. He, J. Mu, W. Geng, C. Xue and X. Chou, *ACS applied materials & interfaces*, 2018, **10**, 43661-43668.
97. Y. C. Lai, Y. C. Hsiao, H. M. Wu and Z. L. Wang, *Advanced science*, 2019, **6**, 1801883.
98. M. B. Khan, D. H. Kim, J. H. Han, H. Saif, H. Lee, Y. Lee, M. Kim, E. Jang, S. K. Hong, D. J. Joe, T.-I. Lee, T.-S. Kim, K. J. Lee and Y. Lee, *Nano Energy*, 2019, **58**, 211-219.
99. S. Mondal, T. Paul, S. Maiti, B. K. Das and K. K. Chattopadhyay, *Nano Energy*, 2020, **74**, 104870.
100. P.-K. Yang, S.-A. Chou, C.-H. Hsu, R. J. Mathew, K.-H. Chiang, J.-Y. Yang and Y.-T. Chen, *Nano Energy*, 2020, **75**, 104879.
101. C. Jean-Mistral, T. Vu Cong and A. Sylvestre, *Applied Physics Letters*, 2012, **101**, 162901.
102. H. Abdi, N. Mohajer and S. Nahavandi, *Journal of Intelligent Material Systems and Structures*, 2013, **25**, 923-936.
103. Y. Zhang, Y. Chen, B. Lu, C. Lü and X. Feng, *Journal of Applied Mechanics*, 2016, **83**, 061007.
104. A. R. Mule, B. Dudem, S. A. Graham and J. S. Yu, *Advanced Functional Materials*, 2019, **29**, 1807779.
105. S. Chen, J. Jiang, F. Xu and S. Gong, *Nano Energy*, 2019, **61**, 69-77.
106. R. Zhang, M. Hummelgård, J. Örtegren, M. Olsen, H. Andersson, Y. Yang and H. Olin, *ACS Applied Energy Materials*, 2018, **1**, 2955-2960.
107. B. Dutta, E. Kar, N. Bose and S. Mukherjee, *ACS Sustainable Chemistry & Engineering*, 2018, **6**, 10505-10516.
108. L. Wang, W. Liu, Z. Yan, F. Wang and X. Wang, *Advanced Functional Materials*, 2020, **31**, 2007221.
109. L. Xie and M. Cai, *IEEE/ASME Transactions on Mechatronics*, 2015, **20**, 3264-3268.

110. D. W. Lee, D. G. Jeong, J. H. Kim, H. S. Kim, G. Murillo, G.-H. Lee, H.-C. Song and J. H. Jung, *Nano Energy*, 2020, **76**, 105066.
111. V. Goudar, Z. Ren, P. Brochu, M. Potkonjak and Q. Pei, *IEEE Sensors Journal*, 2014, **14**, 2084-2091.
112. C. L. Zhang, Z. H. Lai, X. X. Rao, J. W. Zhang and D. Yurchenko, *Energy Conversion and Management*, 2020, **205**, 112351.
113. G. Thomson, Z. H. Lai, D. V. Val and D. Yurchenko, *Journal of Sound and Vibration*, 2019, **442**, 167-182.
114. P. Bai, G. Zhu, Z.-H. Lin, Q. Jing, J. Chen, G. Zhang, J. Ma and Z. L. Wang, *ACS NANO*, 2013, **7**, 3713-3719.
115. F. Deng, Y. Cai, X. Fan, P. Gui and J. Chen, *Energy*, 2019, **171**, 785-794.
116. L. Mateu and F. Moll, *Journal of Intelligent Material Systems and Structures*, 2016, **16**, 835-845.
117. H. J. Oh, J. H. Bae, Y. K. Park, J. Song, D. K. Kim, W. Lee, M. Kim, K. J. Heo, Y. Kim, S. H. Kim, B. J. Yeang and S. J. Lim, *Polymers*, 2020, **12**, 1044.
118. X. Cui, S. Cao, Z. Yuan, G. Xie, J. Ding, S. Sang and H. Zhang, *Energy Technology*, 2019, **7**, 1800931.
119. Z. Zhang, Y. Chen and J. Guo, *Physica E: Low-dimensional Systems and Nanostructures*, 2019, **105**, 212-218.
120. J. Fu, K. Xia and Z. Xu, *Microelectronic Engineering*, 2020, **232**, 111408.
121. M. S. U. Rasel and J.-Y. Park, *Applied Energy*, 2017, **206**, 150-158.
122. H. Li, Y. N. Sun, Y. J. Su, R. H. Li, H. W. Jiang, Y. X. Xie, X. R. Ding, X. Y. Wu and Y. Tang, *Nano Energy*, 2021, **89**, 106423.
123. D. CARDWELL, *ANNALS OF SCIENCE*, 1992, **49**, 479-487.
124. C. Cepnik, R. Lausecker and U. Wallrabe, *Micromachines*, 2013, **4**, 168-196.
125. L. Lamprecht, R. Ehrenpfordt, T. Zoller and A. Zimmermann, *IET Wireless Sensor Systems*, 2019, **9**, 53-60.
126. P. Gui, F. Deng, Z. Liang, Y. Cai and J. Chen, *Energy*, 2018, **154**, 365-373.
127. V. Nico and J. Punch, *The European Physical Journal Special Topics*, 2019, **228**, 1647-1657.
128. E. M. Nia, N. A. W. A. Zawawi and B. S. M. Singh, *Materialwissenschaft Und Werkstofftechnik*, 2019, **50**, 320-328.
129. G. Lippmann, *J. Phys. Theor. Appl.*, 1881, **10**, 381-394.
130. S. P. Beeby, M. J. Tudor and N. M. White, *Measurement Science and Technology*, 2006, **17**, R175-R195.
131. R. Calio, U. B. Rongala, D. Camboni, M. Milazzo, C. Stefanini, G. de Petris and C. M. Oddo, *Sensors*, 2014, **14**, 4755-4790.
132. H. Li, C. Tian and Z. D. Deng, *Applied Physics Reviews*, 2014, **1**, 041301.
133. S. Mishra, L. Unnikrishnan, S. K. Nayak and S. Mohanty, *Macromolecular Materials and Engineering*, 2019, **304**, 1800463.
134. S. Priya, H.-C. Song, Y. Zhou, R. Varghese, A. Chopra, S.-G. Kim, I. Kanno, L. Wu, D. S. Ha, J. Ryu and R. G. Polcawich, *Energy Harvesting and Systems*, 2017, **4**, 3-39.
135. Q. Zhou, K. H. Lam, H. Zheng, W. Qiu and K. K. Shung, *Progress in Materials Science*, 2014, **66**, 87-111.
136. H. Chen, R. Panda and Ieee, Rotterdam, Netherlands, 2005.
137. C. Jin, N. Hao, Z. Xu, I. Trase, Y. Nie, L. Dong, A. Closson, Z. Chen and J. X. J. Zhang, *Sensors and Actuators A: Physical*, 2020, **305**, 111912.
138. A. Khan, Z. Abas, H. S. Kim and I.-K. Oh, *Smart Materials and Structures*, 2016, **25**, 053002.
139. R. Caliò, U. B. Rongala, D. Camboni, M. Milazzo, C. Stefanini, G. De Petris and C. M. Oddo, 2014, **14**, 4755-4790.
140. S. Zhang, F. Li, X. Jiang, J. Kim, J. Luo and X. Geng, *Progress in Materials Science*, 2015, **68**, 1-66.
141. Z. Yang, S. Zhou, J. Zu and D. Inman, *Joule*, 2018, **2**, 642-697.
142. C. Covaci and A. Gontean, *Sensors*, 2020, **20**, 3512.

143. S. Roundy and P. K. Wright, *Smart Materials & Structures*, 2004, **13**, 1131-1142.
144. C. R. Bowen, H. A. Kim, P. M. Weaver and S. Dunn, *Energy & Environmental Science*, 2014, **7**, 25-44.
145. A. Toprak and O. Tigli, *Applied Physics Reviews*, 2014, **1**, 031104.
146. Y. Lu, F. Cottone, S. Boisseau, F. Marty, D. Galayko and P. Basset, *Applied Physics Letters*, 2015, **107**, 253902.
147. F. U. Khan and M. U. Qadir, *Journal of Micromechanics and Microengineering*, 2016, **26**, 103001.
148. R. Pelrine, R. Kornbluh, J. Eckerle, P. Jeuck, S. J. Oh, Q. B. Pei and S. Stanford, 2001.
149. Y. Guo, L. Liu, Y. Liu and J. Leng, *Advanced Intelligent Systems*, 2021, **3**, 2000282.
150. A. Bruschi, D. M. Donati, P. Choong, E. Lucarelli and G. Wallace, *Advanced Healthcare Materials*, 2021, **10**, 2100041.
151. Y. Zhao, L.-J. Yin, S.-L. Zhong, J.-W. Zha and Z.-M. Dang, *Iet Nanodielectrics*, 2020, **3**, 99-106.
152. M. Panahi-Sarmad, B. Zahiri and M. Noroozi, *Sensors and Actuators a-Physical*, 2019, **293**, 222-241.
153. Z. Li, C. Gao, S. Fan, J. Zou, G. Gu, M. Dong and J. Song, *Nano-Micro Letters*, 2019, **11**, 98.
154. U. Gupta, L. Qin, Y. Wang, H. Godaba and J. Zhu, *Smart Materials and Structures*, 2019, **28**, 103002.
155. G. Li, X. Chen, F. Zhou, Y. Liang, Y. Xiao, X. Cao, Z. Zhang, M. Zhang, B. Wu, S. Yin, Y. Xu, H. Fan, Z. Chen, W. Song, W. Yang, B. Pan, J. Hou, W. Zou, S. He, X. Yang, G. Mao, Z. Jia, H. Zhou, T. Li, S. Qu, Z. Xu, Z. Huang, Y. Luo, T. Xie, J. Gu, S. Zhu and W. Yang, *Nature*, 2021, **591**, 66-+.
156. A. York, J. Dunn and S. Seelecke, *Smart Materials and Structures*, 2013, **22**, 094015.
157. R. Kaltseis, C. Keplinger, S. J. A. Koh, R. Baumgartner, Y. F. Goh, W. H. Ng, A. Kogler, A. Troels, C. C. Foo, Z. Suo and S. Bauer, *Rsc Advances*, 2014, **4**, 27905-27913.
158. S. Shian, J. S. Huang, S. J. Zhu and D. R. Clarke, *Advanced Materials*, 2014, **26**, 6617-6621.
159. H. Fu and E. M. Yeatman, *Energy Technology*, 2018, **6**, 2220-2231.
160. F. Carpi, I. Anderson, S. Bauer, G. Frediani, G. Gallone, M. Gei, C. Graaf, C. Jean-Mistral, W. Kaal, G. Kofod, M. Kollosche, R. Kornbluh, B. Lassen, M. Matysek, S. Michel, S. Nowak, B. O'Brien, Q. Pei, R. Pelrine, B. Rechenbach, S. Rosset and H. Shea, *Smart Materials and Structures*, 2015, **24**, 105025.
161. C. Graf, J. Maas and D. Schapeler, San Diego, CA, 2010.
162. T. Hoffstadt, C. Graf and J. Maas, *Smart Materials and Structures*, 2013, **22**, 094028.
163. , !!! INVALID CITATION !!! 160-163.
164. D. Yurchenko, Z. H. Lai, G. Thomson, D. V. Val and R. V. Bobryk, *Applied Energy*, 2017, **208**, 456-470.
165. Z. Suo, X. Zhao and W. H. Greene, *Journal of the Mechanics and Physics of Solids*, 2008, **56**, 467-486.
166. J. Y. Zhou, L. Y. Jiang and R. Khayat, *Epl*, 2016, **115**, 27003.
167. J. Y. Zhou, L. Y. Jiang and R. E. Khayat, *Journal of Applied Physics*, 2017, **121**, 184102.
168. S. J. A. Koh, X. H. Zhao and Z. G. Suo, *Applied Physics Letters*, 2009, **94**, 262902.
169. T. McKay, B. O'Brien, E. Calius and I. Anderson, *Applied Physics Letters*, 2010, **97**, 062911.
170. T. McKay, B. O'Brien, E. Calius and I. Anderson, *Smart Materials & Structures*, 2010, **19**, 055025.
171. T. McKay, B. O'Brien, E. Calius and I. Anderson, in *Electroactive Polymer Actuators and Devices*, ed. Y. BarCohen, 2010, vol. 7642.
172. P. Illenberger, K. Takagi, H. Kojima, U. K. Madawala and I. A. Anderson, *IEEE Trans. Power Electron.*, 2017, **32**, 6904-6912.
173. P. K. Illenberger, K. E. Wilson, E. F. M. Henke, U. K. Madawala and I. A. Anderson, in *Electroactive Polymer Actuators and Devices*, ed. Y. BarCohen, Spie-Int Soc Optical Engineering, Bellingham, 2017, vol. 10163.
174. H. Wang, Y. Zhu, L. Wang and J. Zhao, *Journal of Intelligent Material Systems and Structures*, 2012, **23**, 885-895.

175. R. Kaltseis, C. Keplinger, R. Baumgartner, M. Kaltenbrunner, T. F. Li, P. Machler, R. Schwodiauer, Z. G. Suo and S. Bauer, *Applied Physics Letters*, 2011, **99**, 162904.
176. G. Moretti, M. Fontana and R. Vertechy, *Journal of Intelligent Material Systems and Structures*, 2015, **26**, 740-751.
177. G. Moretti, M. Righi, R. Vertechy and M. Fontana, *Polymers*, 2017, **9**, 283.
178. Y. J. Lee, P. Caspari, D. M. Opris, F. A. Nuesch, S. Ham, J.-H. Kim, S.-R. Kim, B.-K. Ju and W. K. Choi, *Journal of Materials Chemistry C*, 2019, **7**, 3535-3542.
179. J. Biggs, K. Danielmeier, J. Hitzbleck, J. Krause, T. Kridl, S. Nowak, E. Orselli, X. Quan, D. Schapeler, W. Sutherland and J. Wagner, *Angewandte Chemie-International Edition*, 2013, **52**, 9409-9421.
180. C. Jean-Mistral, G. Jacquet-Richardet and A. Sylvestre, *Polymer Testing*, 2020, **81**, 106198.
181. S. J. A. Koh, C. Keplinger, T. F. Li, S. Bauer and Z. G. Suo, *IEEE-ASME Transactions on Mechatronics*, 2011, **16**, 33-41.
182. Y. Chen, L. Agostini, G. Moretti, M. Fontana and R. Vertechy, *Smart Materials and Structures*, 2019, **28**, 114001.
183. S. Rosset, O. A. Araromi, S. Schlatter and H. R. Shea, *Jove-Journal of Visualized Experiments*, 2016, **108**, e53423.
184. B. Fasolt, M. Hodgins, G. Rizzello and S. Seelecke, *Sensors and Actuators a-Physical*, 2017, **265**, 10-19.
185. F. B. Madsen, A. E. Daugaard, S. Hvilsted and A. L. Skov, *Macromolecular Rapid Communications*, 2016, **37**, 378-413.
186. F. Forster-Zuegel, S. Solano-Arana, F. Klug and H. F. Schlaak, *Smart Materials and Structures*, 2019, **28**, 075042.
187. D. Gatti, H. Haus, M. Matysek, B. Frohnapfel, C. Tropea and H. F. Schlaak, *Applied Physics Letters*, 2014, **104**, 052905.
188. T. Lu, C. Ma and T. Wang, *Extreme Mechanics Letters*, 2020, **38**, 100752.
189. G. Moretti, S. Rosset, R. Vertechy, I. Anderson and M. Fontana, *Advanced Intelligent Systems*, 2020, **2**, 2000125.
190. T. Vu-Cong, C. Jean-Mistral and A. Sylvestre, *Smart Materials and Structures*, 2013, **22**, 025012.
191. H.-Y. Ong, M. Shrestha and G.-K. Lau, *Applied Physics Letters*, 2015, **107**, 132902.
192. J. S. Huang, S. Shian, Z. G. Suo and D. R. Clarke, *Advanced Functional Materials*, 2013, **23**, 5056-5061.
193. Z. Q. Song, K. Ohyama, S. Shian, D. R. Clarke and S. J. Zhu, *Smart Materials and Structures*, 2020, **29**, 015018.
194. Y. Jiang, S. Liu, M. Zhong, L. Zhang, N. Ning and M. Tian, *Nano Energy*, 2020, **71**, 104606.
195. E. Bortot and M. Gei, *Extreme Mechanics Letters*, 2015, **5**, 62-73.
196. J. W. Zhang, Z. H. Lai, X. X. Rao and C. L. Zhang, *Smart Materials and Structures*, 2020, **29**.
197. D. Yurchenko, D. V. Val, Z. H. Lai, G. Gu and G. Thomson, *Smart Materials and Structures*, 2017, **26**, 105001.
198. Z. H. Lai, G. Thomson, D. Yurchenko, D. V. Val and E. Rodgers, *Mechanical Systems and Signal Processing*, 2018, **107**, 105-121.
199. S. Pan and Z. Zhang, *Friction*, 2019, **7**, 2-17.
200. Y. S. Choi, S.-W. Kim and S. Kar-Narayan, 2021, **11**, 2003802.
201. J. Li, N. A. Shepelin, P. C. Sherrell and A. V. Ellis, *Chemistry of Materials*, 2021, **33**, 4304-4327.
202. S. Niu, S. Wang, L. Lin, Y. Liu, Y. S. Zhou, Y. Hu and Z. L. Wang, *Energy & Environmental Science*, 2013, **6**, 3576-3583.
203. B. Yang, W. Zeng, Z.-H. Peng, S.-R. Liu, K. Chen and X.-M. Tao, 2016, **6**, 1600505.
204. F.-R. Fan, Z.-Q. Tian and Z. Lin Wang, *Nano Energy*, 2012, **1**, 328-334.
205. Y. A. Mezenov, A. A. Krasilin, V. P. Dzyuba, A. Nominé and V. A. Milichko, 2019, **6**, 1900506.
206. Z. L. Wang, *Faraday Discussions*, 2014, **176**, 447-458.
207. Z. L. Wang, *ACS Nano*, 2013, **7**, 9533-9557.
208. X. Cao, Y. Jie, N. Wang and Z. L. Wang, *Advanced Energy Materials*, 2016, **6**, 1600665.

209. C. G. Zhang, L. X. He, L. L. Zhou, O. Yang, W. Yuan, X. L. Wei, Y. B. Liu, L. Lu, J. Wang and Z. L. Wang, *Joule*, 2021, **5**, 1613-1623.
210. Z. L. Wang, J. Chen and L. Lin, *Energy & Environmental Science*, 2015, **8**, 2250-2282.
211. J. Chen and Z. L. Wang, *Joule*, 2017, **1**, 480-521.
212. C. Wu, A. C. Wang, W. Ding, H. Guo and Z. L. Wang, 2019, **9**, 1802906.
213. Y. Zi, S. Niu, J. Wang, Z. Wen, W. Tang and Z. L. Wang, *Nature Communications*, 2015, **6**, 8376.
214. G. Khandelwal, A. Chandrasekhar, R. Pandey, N. P. Maria Joseph Raj and S.-J. Kim, *Sensors and Actuators B: Chemical*, 2019, **282**, 590-598.
215. G. Khandelwal, A. Chandrasekhar, N. R. Alluri, V. Vivekananthan, N. P. Maria Joseph Raj and S.-J. Kim, *Applied Energy*, 2018, **219**, 338-349.
216. S. Niu, Y. Liu, S. Wang, L. Lin, Y. S. Zhou, Y. Hu and Z. L. Wang, 2013, **25**, 6184-6193.
217. S. Niu, Y. Liu, S. Wang, L. Lin, Y. S. Zhou, Y. Hu and Z. L. Wang, 2014, **24**, 3332-3340.
218. Y. Li, G. Cheng, Z.-H. Lin, J. Yang, L. Lin and Z. L. Wang, *Nano Energy*, 2015, **11**, 323-332.
219. G. Khandelwal, T. Minocha, S. K. Yadav, A. Chandrasekhar, N. P. Maria Joseph Raj, S. C. Gupta and S.-J. Kim, *Nano Energy*, 2019, **65**, 104016.
220. T. Jiang, X. Chen, C. B. Han, W. Tang and Z. L. Wang, 2015, **25**, 2928-2938.
221. S. Wang, Y. Xie, S. Niu, L. Lin and Z. L. Wang, *Advanced materials*, 2014, **26**, 2818-2824.
222. G. Khandelwal, N. P. M. J. Raj and S.-J. Kim, *Nano Today*, 2020, **33**, 100882.
223. H. Jafari, A. Ghodsi, S. Azizi and M. R. Ghazavi, *Energy*, 2017, **124**, 1-8.
224. J. I. Preimesberger, S. Kang and C. B. Arnold, *Joule*, 2020, **4**, 1893-1906.
225. T.-H. Hsu, J. A. Taylor and T. N. Krupenkin, *Faraday Discussions*, 2017, **199**, 377-392.
226. G. Kim, W. Kim and H. Chun, *Advanced Functional Materials*, 2021, **31**, 2105233.
227. T. Krupenkin and J. A. Taylor, *Nature Communications*, 2011, **2**, 448.
228. H. Yang, S. Hong, B. Koo, D. Lee and Y.-B. Kim, *Nano Energy*, 2017, **31**, 450-455.
229. S. R. Panigrahi, B. P. Bernard, B. F. Feeny, B. P. Mann and A. R. Diaz, *Journal of Sound and Vibration*, 2017, **399**, 216-227.
230. T. Liu, R. St Pierre and C. Livermore, *Smart Materials and Structures*, 2014, **23**, 095045.
231. S.-M. Jung and K.-S. Yun, *Applied Physics Letters*, 2010, **96**, 111906.
232. L. Gu and C. Livermore, *Smart Materials and Structures*, 2011, **20**, 045004.
233. S. Ju and C.-H. Ji, *Applied Energy*, 2018, **214**, 139-151.
234. P. Li, N. Xu and C. H. Gao, *International Journal of Precision Engineering and Manufacturing*, 2020, **21**, 1781-1788.
235. C. Wang, Q. Zhang, W. Wang and J. Feng, *Mechanical Systems and Signal Processing*, 2018, **112**, 305-318.
236. R. M. Toyabur, M. Salauddin, H. Cho and J. Y. Park, *Energy Conversion and Management*, 2018, **168**, 454-466.
237. H. Madinei, H. H. Khodaparast, S. Adhikari, M. I. Friswell and M. Fazeli, *European Physical Journal-Special Topics*, 2015, **224**, 2703-2717.
238. R. M. Alexander, *Journal of Experimental Biology*, 1991, **160**, 55-69.
239. G. A. Cavagna and M. Kaneko, *Journal of Physiology-London*, 1977, **268**, 467-481.
240. S. A. Gard, S. C. Miff and A. D. Kuo, *Human Movement Science*, 2004, **22**, 597-610.
241. A. D. Kuo, *Science*, 2005, **309**, 1686-1687.
242. L. Xie and MingjingCai, *Mechanical Systems and Signal Processing*, 2015, **58-59**, 399-451.

243. Z. H. Hou, J. Y. Cao, G. H. Huang, Y. Zhang and L. Zuo, *Mechanical Systems and Signal Processing*, 2021, **155**, 107621.
244. Y. Yuan, M. Liu, W.-C. Tai and L. Zuo, *Journal of Mechanical Design*, 2018, **140**, 085001.
245. M. Liu, W. Tai and L. Zuo, *Smart Materials and Structures*, 2020, **29**, 025007.
246. J. Feenstra, J. Granstrom and H. Sodano, *Mechanical Systems and Signal Processing*, 2008, **22**, 721-734.
247. D. F. Berdy, D. J. Valentino and D. Peroulis, *Sensors and Actuators A: Physical*, 2015, **222**, 262-271.
248. W. Yang, J. Chen, G. Zhu, J. Yang, P. Bai, Y. Su, Q. Jing, X. Cao and Z. L. Wang, *ACS NANO*, 2013, **7**, 11317-11324.
249. L. Liu, Q. Shi and C. Lee, *Nano Research*, 2021, **14**, 4227-4235.
250. Y.-K. Fuh, P.-C. Chen, H.-C. Ho, Z.-M. Huang and S.-C. Li, *Royal Society of Chemistry*, 2015, **5**, 67787.
251. M. R. Shorten, *Journal of biomechanics*, 1993, **26**, 41-51.
252. S. E. Jo, M. S. Kim and Y. J. Kim, *Electronics Letters*, 2012, **48**, 874.
253. V. Luciano, E. Sardini, M. Serpelloni and G. Baronio, *Measurement Science and Technology*, 2014, **25**, 025702.
254. J. Yeo, M. H. Ryu and Y. Yang, *Sensors*, 2015, **15**, 15853-15867.
255. D. Alghisi, M. Ferrari and V. Ferrari, *IET Circuits, Devices & Systems*, 2015, **9**, 96-104.
256. J. Jun, Y. Shin, S.-J. Cho, Y.-W. Cho, S. H. Lee and J. H. Kim, *Advances in Mechanical Engineering*, 2016, **8**, 168781401664988.
257. J. Seo, J.-S. Kim, U.-C. Jeong, Y.-D. Kim, Y.-C. Kim, H. Lee and J.-E. Oh, *Journal of the Korean Physical Society*, 2016, **68**, 431-442.
258. M. A. Halim, H. Cho, M. Salauddin and J. Y. Park, *Sensors and Actuators A: Physical*, 2016, **249**, 23-31.
259. M. Geisler, S. Boisseau, M. Perez, P. Gasnier, J. Willemin, I. Ait-Ali and S. Perraud, *Smart Materials and Structures*, 2017, **26**, 035028.
260. M. Geisler, S. Boisseau, P. Gasnier, J. Willemin, C. Gobbo, G. Despesse, I. Ait-Ali and S. Perraud, *Smart Materials and Structures*, 2017, **26**, 105035.
261. P. Chen and Z. Zhang, *IETE Journal of Research*, 2017, **64**, 503-513.
262. H. Liu, C. Hou, J. Lin, Y. Li, Q. Shi, T. Chen, L. Sun and Chengkuo, *Applied Physics Letters*, 2018, **113**, 203901.
263. C. Li, S. Wu, P. C. K. Luk, M. Gu and Z. Jiao, *IEEE/ASME Transactions on Mechatronics*, 2019, **24**, 710-717.
264. H.-X. Z. Lin-Chuan Zhao, Qiu-Hua Gao, Ge Yan, Feng-Rui Liu, Ting Tan, Ke-Xiang Wei, and Wen-Ming Zhang, *Applied Physics Letters*, 2019, **115**, 263902.
265. Y. Zhang, A. Luo, Y. Wang, X. Dai, Y. Lu and F. Wang, *Applied Physics Letters*, 2020, **116**, 053902.
266. M. Renaud, P. Fiorini, R. van Schaijk and C. van Hoof, *Smart Materials and Structures*, 2012, **21**, 049501.
267. P. Pillatsch, E. M. Yeatman and A. S. Holmes, *Sensors and Actuators A: Physical*, 2014, **206**, 178-185.
268. M. Wahbah, M. Alhawari, B. Mohammad, H. Saleh and M. Ismail, *IEEE Journal on Emerging and Selected Topics in Circuits and Systems*, 2014, **4**, 354-363.
269. D. Alghisi, S. Dalola, M. Ferrari and V. Ferrari, *Sensors and Actuators A: Physical*, 2015, **233**, 569-581.
270. J. Cao, W. Wang, S. Zhou, D. J. Inman and J. Lin, *Applied Physics Letters*, 2015, **107**, 143904.
271. N. Wu, X. Cheng, Q. Zhong, J. Zhong, W. Li, B. Wang, B. Hu and J. Zhou, *Advanced Functional Materials*, 2015, **25**, 4788-4794.
272. P. Pillatsch, E. M. Yeatman, A. S. Holmes and P. K. Wright, *Sensors and Actuators A: Physical*, 2016, **244**, 77-85.
273. W. Wang, J. Cao, C. R. Bowen, S. Zhou and J. Lin, *Energy*, 2017, **118**, 221-230.
274. Y. Chen, Y. Zhang, F. Yuan, F. Ding and O. G. Schmidt, *Advanced Electronic Materials*, 2017, **3**, 1600540.

275. S. Khalifa, G. Lan, M. Hassan, A. Seneviratne and S. K. Das, *IEEE TRANSACTIONS ON MOBILE COMPUTING*, 2018, **17**, 1353-1368.
276. I. Izadgoshasb, Y. Y. Lim, N. Lake, L. Tang, R. V. Padilla and T. Kashiwao, *Energy Conversion and Management*, 2018, **161**, 66-73.
277. W. Wang, J. Cao, C. R. Bowen, D. J. Inman and J. Lin, *Applied Physics Letters*, 2018, **112**, 213903.
278. I. Izadgoshasb, Y. Y. Lim, L. Tang, R. V. Padilla, Z. S. Tang and M. Sedighi, *Energy Conversion and Management*, 2019, **184**, 559-570.
279. F. Gao, G. Liu, B. L.-H. Chung, H. H.-T. Chan and W.-H. Liao, *Applied Physics Letters*, 2019, **115**, 033901.
280. I. Choudhry, H. R. Khalid and H.-K. Lee, *ACS Applied Electronic Materials*, 2020, **2**, 3346-3357.
281. B. Wang, Z. H. Long, Y. Hong, Q. Q. Pan, W. K. Lin and Z. B. Yang, *Nano Energy*, 2021, **89**, 106385.
282. G. De Pasquale, S.-G. Kim and D. De Pasquale, *IEEE/ASME Transactions on Mechatronics*, 2015, **21**, 565-575.
283. Y. Cha, *Journal of Intelligent Material Systems and Structures*, 2017, **28**, 3006-3015.
284. L. Xie and M. Cai, *Applied Physics Letters*, 2014, **105**, 143901.
285. H. Kalantarian and M. Sarrafzadeh, *IEEE Sensors Journal*, 2016, **16**, 8314-8321.
286. W. Cao, W. Yu and Z. Li, *Industria Textila*, 2018, **69**, 390-393.
287. Z. He, B. Gao, T. Li, J. Liao, B. Liu, X. Liu, C. Wang, Z. Feng and Z. Gu, *ACS Sustainable Chemistry & Engineering*, 2018, **7**, 1745-1752.
288. S. M. Hossain and M. N. Uddin, *International Journal of Ambient Energy*, 2018, **42**, 251-256.
289. F. Qian, T.-B. Xu and L. Zuo, *Energy*, 2019, **189**, 116140.
290. H. Lai and K. Reid, *Journal of rehabilitation and assistive technologies engineering*, 2019, **6**, 31662883.
291. Y. Lu, X. Wang, X. Wu, J. Qin and R. Lu, *Journal of Micromechanics and Microengineering*, 2014, **24**, 065010.
292. J. Chen, Y. Huang, N. Zhang, H. Zou, R. Liu, C. Tao, X. Fan and Z. L. Wang, *Nature Energy*, 2016, **1**, 16138.
293. H. Huang, X. Li, S. Liu, S. Hu and Y. Sun, *IEEE Internet of Things Journal*, 2018, **5**, 4441-4453.
294. H. J. Hwang, Y. Jung, K. Choi, D. Kim, J. Park and D. Choi, *Science and technology of advanced materials*, 2019, **20**, 725-732.
295. H. Ouyang, Z. Liu, N. Li, B. Shi, Y. Zou, F. Xie, Y. Ma, Z. Li, H. Li, Q. Zheng, X. Qu, Y. Fan, Z. L. Wang, H. Zhang and Z. Li, *Nature Communications*, 2019, **10**.
296. Z. Tian, J. He, X. Chen, Z. Zhang, T. Wen, C. Zhai, J. Han, J. Mu, X. Hou, X. Chou and C. Xue, *Nano Energy*, 2017, **39**, 562-570.
297. Y. Kang, B. Wang, S. Dai, G. Liu, Y. Pu and C. Hu, *ACS applied materials & interfaces*, 2015, **7**, 20469-20476.
298. X. Li and Y. Sun, *Sensors*, 2017, **17**, 29149035.
299. Z. Zhang, K. Du, X. Chen, C. Xue and K. Wang, *Nano Energy*, 2018, **53**, 108-115.
300. L. Wang and W. A. Daoud, *Nano Energy*, 2019, **66**, 104080.
301. Khushboo and P. Azad, *Bulletin of Materials Science*, 2019, **42**, 121.
302. J. Fu, K. Xia and Z. Xu, *Sensors and Actuators A: Physical*, 2021, **323**, 112650.
303. C. Hou, T. Chen, Y. Li, M. Huang, Q. Shi, H. Liu, L. Sun and C. Lee, *Nano Energy*, 2019, **63**, 103871.
304. S. Gao, T. He, Z. Zhang, H. Ao, H. Jiang and C. Lee, *Advanced science*, 2021, **8**.
305. S. A. P. Haddad, R. P. M. Houben and W. A. Serdijn, *Ieee Engineering in Medicine and Biology Magazine*, 2006, **25**, 38-48.
306. P. D. Mitcheson, Ph.D., University of London, 2005.
307. Z. Li, G. Zhu, R. Yang, A. C. Wang and Z. L. Wang, *Advanced materials*, 2010, **22**, 2534-2537.

308. M. Irimia-Vladu, P. A. Troshin, M. Reisinger, L. Shmygleva, Y. Kanbur, G. Schwabegger, M. Bodea, R. Schwoediauer, A. Mumyatov, J. W. Fergus, V. F. Razumov, H. Sitter, N. S. Sariciftci and S. Bauer, *Advanced Functional Materials*, 2010, **20**, 4069-4076.
309. Q. Zheng, Y. Zou, Y. Zhang, Z. Liu, B. Shi, X. Wang, Y. Jin, H. Ouyang, Z. Li and Z. L. Wang, *Science Advances*, 2016, **2**.
310. O. J. Ohm and D. Danilovic, *Pace-Pacing and Clinical Electrophysiology*, 1997, **20**, 2-9.
311. *Journal*, 2007, **2**, 10-11.
312. D. J. Jiang, B. J. Shi, H. Ouyang, Y. B. Fan, Z. L. Wang and Z. Li, *Acs Nano*, 2020, **14**, 6436-6448.
313. A Heart-Powered Pacemaker, http://inventorspot.com/articles/heartpowered_pacemaker_8238, (accessed 11 Jan, 2022).
314. Y. Z. Shulong Ye, Peng Yu, in *Titanium for Consumer Applications*, ed. M. Q. Francis Froes, Mitsuo Niinomi, Elsevier, 2019, ch. 14, pp. 269-278.
315. H. Chen, Y. Song, X. Cheng and H. Zhang, *Nano Energy*, 2019, **56**, 252-268.
316. A. Chortos, J. Liu and Z. Bao, *Nature Materials*, 2016, **15**, 937-950.
317. D. H. Ho, Q. Sun, S. Y. Kim, J. T. Han, D. H. Kim and J. H. Cho, *Advanced materials*, 2016, **28**, 2601-+.
318. X. Wang, L. Dong, H. Zhang, R. Yu, C. Pan and Z. L. Wang, *Advanced science*, 2015, **2**, 1500169.
319. K. Ren and J. Yu, *Ocean Engineering*, 2021, **227**, 108862.
320. T.-M. Wang, Y. Tao and H. Liu, *International Journal of Automation and Computing*, 2018, **15**, 525-546.
321. Y. Zhang and M. Lu, *International Journal of Medical Robotics and Computer Assisted Surgery*, 2020, **16**, e2096.
322. V. Amoli, J. S. Kim, S. Y. Kim, J. Koo, Y. S. Chung, H. Choi and D. H. Kim, *Advanced Functional Materials*, 2020, **30**, 1904532.
323. S. Pyo, J. Lee, K. Bae, S. Sim and J. Kim, *Advanced materials*, 2021, **33**, 2005902.
324. S. Goswami, A. d. Santos, S. Nandy, R. Igreja, P. Barquinha, R. Martins and E. Fortunato, *Nano Energy*, 2019, **60**, 794-801.
325. K. Hinde, G. White and N. Armstrong, *Sensors*, 2021, **21**, 1061.
326. H. Shi, H. Zhao, Y. Liu, W. Gao and S.-C. Dou, *Sensors*, 2019, **19**, 2651.
327. D. Kim and Y. Choi, *Applied Sciences-Basel*, 2021, **11**, 4956.
328. F. Lareyre, A. Chaudhuri, C. Adam, M. Carrier, C. Mialhe and J. Raffort, *Annals of Vascular Surgery*, 2021, **75**, 497-512.
329. S. Mitrasinovic, E. Camacho, N. Trivedi, J. Logan, C. Campbell, R. Zilinyi, B. Lieber, E. Bruce, B. Taylor, D. Martineau, E. L. P. Dumont, G. Appelboom and E. S. Connolly, Jr., *Technology and Health Care*, 2015, **23**, 381-401.
330. C. Romare and L. Skar, *Jmir Mhealth and Uhealth*, 2020, **8**, e16055.
331. E. Connor, *Journal of the Medical Library Association*, 2016, **104**, 180-180.
332. A. Linosld, *Journal of Academic Librarianship*, 2016, **42**, 287-287.
333. T.-C. Lu, C.-M. Fu, M. H.-M. Ma, C.-C. Fang and A. M. Turner, *Applied Clinical Informatics*, 2016, **7**, 850-869.
334. F. Michard, *Anesthesiology clinics*, 2021, **39**, 555-564.
335. B. Reeder and A. David, *Journal of Biomedical Informatics*, 2016, **63**, 269-276.
336. F. Z. Tajrishi, M. Chitsazan, M. Chitsazan, F. Shojaei, V. Gunnam and G. Chi, *Critical pathways in cardiology*, 2019, **18**, 176-184.
337. B. Wang and A. Facchetti, *Advanced materials*, 2019, **31**, 1901408.
338. J. C. Yang, J. Mun, S. Y. Kwon, S. Park, Z. Bao and S. Park, *Advanced materials*, 2019, **31**, 1904765.

339. S. J. Benight, C. Wang, J. B. H. Tok and Z. Bao, *Progress in Polymer Science*, 2013, **38**, 1961-1977.
340. D. Chen and Q. Pei, *Chemical Reviews*, 2017, **117**, 11239-11268.
341. A.-C. Bunea, V. Dediu, E. A. Laszlo, F. Pistritu, M. Carp, F. S. Iliescu, O. N. Ionescu and C. Iliescu, *Micromachines*, 2021, **12**, 1091.
342. J. Chen, Y. Zhu, X. Chang, D. Pan, G. Song, Z. Guo and N. Naik, *Advanced Functional Materials*, 2021, **31**, 2104686.
343. U. Pierre Claver and G. Zhao, *Advanced Engineering Materials*, 2021, **23**, 2001187.
344. L. Wang, K. Jiang and G. Shen, *Advanced Materials Technologies*, 2021, **6**, 2100107.
345. H. Guan, D. Lv, T. Zhong, Y. Dai, L. Xing, X. Xue, Y. Zhang and Y. Zhan, *Nano Energy*, 2020, **67**, 104182.
346. Z. Lou, L. Li, L. Wang and G. Shen, *Small*, 2017, **13**, 1701791.
347. L. Wang, S. Chen, W. Li, K. Wang, Z. Lou and G. Shen, *Advanced materials*, 2019, **31**, 1804583.
348. J. Lim, D. S. Choi, G. Y. Lee, H. J. Lee, S. P. Sasikala, K. E. Lee, S. H. Kang and S. O. Kim, *ACS applied materials & interfaces*, 2017, **9**, 41363-41370.
349. X. Pu, W. Hu and Z. L. Wang, *Small*, 2018, **14**.
350. J. B. Goodenough and Y. Kim, *Chemistry of Materials*, 2010, **22**, 587-603.
351. M. Beidaghi and Y. Gogotsi, *Energy & Environmental Science*, 2014, **7**, 867-884.
352. W. Liu, M. S. Song, B. Kong and Y. Cui, *Advanced materials*, 2017, **29**.
353. P. G. Bruce, S. A. Freunberger, L. J. Hardwick and J. M. Tarascon, *Nature Materials*, 2012, **11**, 19-29.
354. S. W. Pan, J. Ren, X. Fang and H. S. Peng, *Advanced Energy Materials*, 2016, **6**.
355. H. Sun, Y. Zhang, J. Zhang, X. M. Sun and H. S. Peng, *Nature Reviews Materials*, 2017, **2**.
356. M. Z. A. Bhuiyan, G. J. Wang, J. Wu, J. N. Cao, X. F. Liu and T. Wang, *Ieee Transactions on Dependable and Secure Computing*, 2017, **14**, 363-376.
357. V. J. Hodge, S. O'Keefe, M. Weeks and A. Moulds, *Ieee Transactions on Intelligent Transportation Systems*, 2015, **16**, 1088-1106.
358. W. Honda, S. Harada, T. Arie, S. Akita and K. Takei, *Advanced Functional Materials*, 2014, **24**, 3299-3304.
359. S. C. Mukhopadhyay, *Ieee Sensors Journal*, 2015, **15**, 1321-1330.
360. Z. M. Lin, J. Chen, X. S. Li, Z. H. Zhou, K. Y. Meng, W. Wei, J. Yang and Z. L. Wang, *Acs Nano*, 2017, **11**, 8830-8837.
361. C. M. Boutry, L. Beker, Y. Kaizawa, C. Vassos, H. Tran, A. C. Hinckley, R. Pfattner, S. Niu, J. Li, J. Claverie, Z. Wang, J. Chang, P. M. Fox and Z. Bao, *Nature Biomedical Engineering*, 2019, **3**, 47-57.
362. L. Y. Chen, B. C. K. Tee, A. L. Chortos, G. Schwartz, V. Tse, D. J. Lipomi, H. S. P. Wong, M. V. McConnell and Z. Bao, *Nature Communications*, 2014, **5**, 5028.
363. X. Y. Liu, Y. M. Zhu, L. H. Kong, C. Liu, Y. Gu, A. V. Vasilakos and M. Y. Wu, *Ieee Transactions on Parallel and Distributed Systems*, 2015, **26**, 2188-2197.
364. Y. J. Yao, Q. Cao and A. V. Vasilakos, *Ieee-Acm Transactions on Networking*, 2015, **23**, 810-823.
365. J. Wang, X. J. Gu, W. Liu, A. K. Sangaiah and H. J. Kim, *Human-Centric Computing and Information Sciences*, 2019, **9**, 18.
366. Z. T. Li, Y. X. Liu, A. F. Liu, S. G. Wang and H. L. Liu, *Ieee Transactions on Emerging Topics in Computing*, 2020, **8**, 797-813.
367. M. L. Zhu, Z. R. Yi, B. Yang and C. Lee, *Nano Today*, 2021, **36**, 101016.
368. K. Zhou, Y. Zhao, X. Sun, Z. Yuan, G. Zheng, K. Dai, L. Mi, C. Pan, C. Liu and C. Shen, *Nano Energy*, 2020, **70**, 104546.

369. X. Pu, M. Liu, X. Chen, J. Sun, C. Du, Y. Zhang, J. Zhai, W. Hu and Z. L. Wang, *Science Advances*, 2017, **3**, e1700015.
370. L. B. Huang, W. Xu, C. Zhao, Y. L. Zhang, K. L. Yung, D. Diao, K. H. Fung and J. Hao, *ACS applied materials & interfaces*, 2020, **12**, 24030-24038.
371. Y. Xi, J. Hua and Y. Shi, *Nano Energy*, 2020, **69**, 104390.
372. M. Zhu, Z. Sun, T. Chen and C. Lee, *Nature Communications*, 2021, **12**.
373. Z. Zhang and J. Cai, *Current Applied Physics*, 2021, **22**, 1-5.
374. Q. Hua, J. Sun, H. Liu, R. Bao, R. Yu, J. Zhai, C. Pan and Z. L. Wang, *Nature Communications*, 2018, **9**, 244.
375. L. Wang, J. A. Jackman, E.-L. Tan, J. H. Park, M. G. Potroz, E. T. Hwang and N.-J. Cho, *Nano Energy*, 2017, **36**, 38-45.
376. Z. Lou, S. Chen, L. Wang, R. Shi, L. Li, K. Jiang, D. Chen and G. Shen, *Nano Energy*, 2017, **38**, 28-35.
377. S. K. Ghosh, P. Adhikary, S. Jana, A. Biswas, V. Sencadas, S. D. Gupta, B. Tudu and D. Mandal, *Nano Energy*, 2017, **36**, 166-175.
378. L. Liu, Q. Shi, Z. Sun and C. Lee, *Nano Energy*, 2021, **86**.
379. J. Rao, Z. Chen, D. Zhao, Y. Yin, X. Wang and F. Yi, *Sensors*, 2019, **19**, 2763.
380. J. Park, Y. Lee, M. Ha, S. Cho and H. Ko, *Journal of Materials Chemistry B*, 2016, **4**, 2999-3018.
381. H. S. Oh, C. H. Lee, N. K. Kim, T. An and G. H. Kim, *Polymers*, 2021, **13**, 2478.